Materials Science & Engineering R 126 (2018) 1–29

Contents lists available at ScienceDirect

Materials Science & Engineering R

journal homepage: www.elsevier.com/locate/mser

MATERIALS SCIENCE & ENGINEERING

R Reports: A Review Journal

Electrically conducting fibres for e-textiles: An open playground for conjugated polymers and carbon nanomaterials

Anja Lund[a,*], Natascha M. van der Velden[b], Nils-Krister Persson[c], Mahiar M. Hamedi[d], Christian Müller[a,*]

[a] *Department of Chemistry and Chemical Engineering, Chalmers University of Technology, 412 96 Göteborg, Sweden*
[b] *Faculty of Industrial Design Engineering, Delft University of Technology, 2600 AA Delft, The Netherlands*
[c] *Smart Textiles and The Swedish School of Textiles, University of Borås, 501 90 Borås, Sweden*
[d] *Fibre and Polymer Technology, KTH Royal Institute of Technology, 100 44 Stockholm, Sweden*

ARTICLE INFO

Keywords:
E-textiles
Nanocomposites
Conjugated polymers
Graphene
Carbon nanotubes
Conducting fibres

ABSTRACT

Conducting fibres and yarns promise to become an essential part of the next generation of wearable electronics that seamlessly integrate electronic function into one of the most versatile and most widely used form of materials: textiles. This review explores the many types of conducting fibres and yarns that can be realised with conjugated polymers and carbon materials, including carbon black, carbon nanotubes and graphene. We discuss how the interplay of materials properties and the chosen processing technique lead to fibres with a wide range of electrical and mechanical properties. Depending on the choice of conjugated polymer, carbon nanotube, graphene, polymer blend, or nanocomposite the electrical conductivity can vary from less than 10^{-3} to more than $10^3\ \mathrm{S\,cm^{-1}}$, accompanied by an increase in Young's modulus from 10 s of MPa to 100 s of GPa. Further, we discuss how conducting fibres can be integrated into electronic textiles (e-textiles) through e.g. weaving and knitting. Then, we provide an overview of some of the envisaged functionalities, such as sensing, data processing and storage, as well as energy harvesting e.g. by using the piezoelectric, thermoelectric, triboelectric or photovoltaic effect. Finally, we critically discuss sustainability aspects such as the supply of materials, their toxicity, the embodied energy of fibre and textile production and recyclability, which currently are not adequately considered but must be taken into account to ready carbon based conducting fibres for truly practical e-textile applications.

1. Introduction

Textiles are ubiquitous; we continuously interact with textiles in some form such as garments, bed linen, towels, furniture upholstery. Moreover, medical textiles – including wipes, bandages, wound dressings – as well as textiles used in construction and the automobile industry are an integral part of our everyday lives. One intriguing avenue that promises to greatly expand the ways in which we use and interact with textiles is the integration of electronic functionalities. Such electronic textiles (e-textiles) will be able to connect to the *Internet*

Abbreviations: APS, ammonium peroxydisulfate; AQSA, anthraquinone-2-sulfonic acid sodium salt; BSA, bovine serum albumin; CNT, carbon nanotube; CSA, camphorsulfonic acid; CTAB, hexadecyltrimethylammonium bromide; DBSA, dodecylbenzenesulfonic acid; DCSS, dicyclohexyl sulfosuccinate sodium salt; DWNT, double-walled carbon nanotubes; ECG, electrocardiography; e-textile, electronic textile; FeTos, Iron (III) tosylate; FWNT, few-walled carbon nanotubes; GO, graphene oxide; HBF_4, tetrafluoroboric acid; HI, hydroiodic acid; IL, ionic liquid; LC, liquid crystalline; LCA, life cycle assessment; LED, light emitting diode; MEMS, microelectromechanical systems; MWNT, multi-walled carbon nanotubes; NDS, sodium naphtalene disulfonate; NDSA, 1,5-naphthalenedisulfonic acid tetrahydrate; NSDA, 1,5 Naphthalenedisulfonic acid sodium salt; NW, nano-wires; oCVD, oxidative chemical vapour deposition; OECT, organic electrochemical transistors; OFET, organic field-effect transistor; PA, polyamide; PA 6, polyamide 6; PAc, polyacetylene; PAN, polyacrylonitrile; PANI, polyaniline; PC, polycarbonate; PDMPV, poly(2,5-dimethoxy-*p*-phenylenevinylene); PDMS, polydimethylsiloxane; PE, polyethylene; PEDOT, poly(3,4-ethylenedioxythiophene); PEDOT-S, poly(4-(2,3-dihydrothieno[3,4-b]-[1,4]dioxin-2-ylmethoxy)-1-butanesulfonic acid, sodium salt); pEGDMA, poly(ethylene glycol dimethacrylate); PEI, poly(ether imide); PEK, poly (ether ketone); PET, poly(ethylene terephthalate); PLGA, poly(lactic-co-glycolic acid); MEH-PPV, poly(metoxy-5-(2-ethylhexyloxy)-1,4-phenylenevinylene); PMMA, poly(methyl methacrylate); PP, polypropylene; PPTA, poly(*p*-phenylene terephthalamide); PPV, poly(*p*-phenylenevinylene); PPy, polypyrrole; PSS, poly(styrenesulfonate); PTT, poly(trimethylene terephthalate); PTV, poly(2,5-Thienylene vinylene); PU, polyurethane; PVA, poly(vinyl alcohol); PVDF, poly(vinylidene fluoride); P3AT, poly(3-alkylthiophene); P3DDT, poly(3-dodecylthiophene-2,5-diyl); P3HT, poly(3-hexylthiophene-2,5-diyl); P3OT, poly(3-octylthiophene-2,5-diyl); rGO, reduced graphene oxide; SA, sulfonic acid; SEM, scanning electron microscopy; SIBS, styrene-isobutylene-styrene block copolymer; SWNT, single-walled carbon nanotubes; TEM, transmission electron microscopy; T_g, glass transition temperature; T_m, crystal melting temperature; UHMWPE, ultra-high molecular weight polyethylene

[*] Corresponding authors.

E-mail addresses: anja.lund@chalmers.se (A. Lund), christian.muller@chalmers.se (C. Müller).

https://doi.org/10.1016/j.mser.2018.03.001
Received 23 January 2018; Accepted 19 March 2018

of Things, i.e. the rapidly growing network of countless tiny devices that surround us. E-textiles will be able to collect, process, store and display information and as such enrich a wide range of application areas from fashion and functional clothing to healthcare and interior design. Textile-based devices have been demonstrated that provide the necessary functionalities: sensors and keyboards collect data [1–6], that are processed by logic circuits [7,8], stored by memory devices [9], and finally relayed by antennas [10] or displays [11]. In addition, to power these devices, energy harvesting textiles are widely explored that utilise the triboelectric [12,13], piezoelectric [14–17], thermoelectric [18–20] or photovoltaic effect [21,22] to turn motion, heat or light into electricity. Moreover, energy storage in the form of textile-based batteries and supercapacitors receives considerable attention [23–26].

One component that is critical as both, a basic building block of many textile-based electronic devices, as well as for interconnections between discrete devices, are fibres and yarns that can conduct electricity (see Sections 2.1 and 2.5 for definitions of fibres and yarns). For instance, a conducting fibre can be used as a *resistor*, two conducting fibres separated by a dielectric medium form a *capacitor*, and two conducting fibres separated by an electrolyte can be used as an electrochemical *transistor* [7,8] (cf. section 4.8). This review will focus on conducting fibres produced from conjugated polymers and/or carbon nanomaterials, and discuss their particular advantages and disadvantages, highlighting areas where further development is necessary. Conducting fibres may consist only of the charge conducting material: (1) conjugated polymers, (2) carbon nanotubes (CNTs), and (3) graphene or graphene oxide (GO). Further, an insulating polymer can be added, leading to fibres made from (4) blends of a conjugated and a matrix polymer, and (5) nanocomposites that comprise a carbon nanomaterial (or carbon black) embedded in a polymer matrix. Alternatively, the conducting material can be applied as (6) a coating to an already existing textile fibre or fabric that acts as a template.

The electrical and mechanical properties of a conducting fibre are dictated by the materials used to produce them, as well as by the method by which they are processed. We have constructed an Ashby plot comparing the electrical conductivity and Young's modulus of different types of fibres and yarns (Fig. 1), and find that across the different types of fibres, the modulus can vary by more than four orders of magnitude, ranging from only 10 s of MPa in case of elastic and therefore pliable fibres, to 100 s of GPa in case of stiff high-modulus fibres. Likewise, the electrical conductivity can vary from poorly conducting fibres with a value of only about 10^{-3} S cm^{-1} (or less if the amount of conducting material is reduced further) to highly conducting fibres that offer more than 10^3 S cm^{-1}. We note that, overall, more conducting fibres also tend to display a higher modulus. This trend arises because both charge transport and the transmission of mechanical force along the long axis of the fibre benefit from alignment of the fibre-forming material (cf. Sections 2 & 3). The most conducting and at the same time stiffest fibres are situated in the top right corner of the Ashby plot shown in Fig. 1: carbon fibres can display values of almost 10^4 S cm^{-1} and 10^3 GPa [27]. Fibres fabricated exclusively of a charge conducting material, i.e. conducting polymers, graphene and in particular CNTs, can offer properties that approach those of carbon fibres, with a conductivity and modulus of more than 10^3 S cm^{-1} and 100 GPa, respectively.

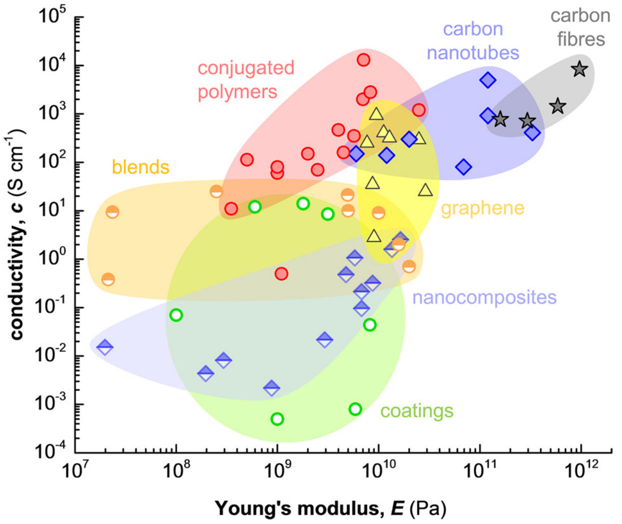

Fig. 1. Ashby plot of the electrical conductivity vs. Young's modulus of fibres based on (grey stars) carbon fibres, (blue diamonds) carbon nanotubes, (yellow triangles) graphene, (red circles) conjugated polymers, (orange/white circles) blends of conjugated and insulating polymers, (blue/white diamonds) nanocomposites of carbon black, carbon nanotubes or graphene embedded in an insulating polymer matrix and (green/white circles) coatings of textile fibres with conjugated polymers, carbon nanotubes or graphene. Data were extracted from the references as indicated in Tables 2–6. (For interpretation of the references to colour in this figure legend, the reader is referred to the web version of this article.)

Polymer blends, coated fibres and nanocomposites make up the lower left corner of the conductivity/modulus Ashby plot and appear to be limited by a maximum conductivity of about 10 S cm^{-1}. This is because a large fraction of the fibre is composed of an insulating polymer, either in the form of a matrix or inner core of the fibre, which reduces the amount of charge conducting material. On the other hand, polymer blends allow to disentangle the mechanical and electrical properties of the fibre: the amount and connectivity of the conjugated polymer determines the electrical conductivity. Instead, the mechanical properties depend on the properties of the matrix polymer and can range from about 20 MPa in case of an elastic polyurethane (PU) matrix [4], to 20 GPa if ultra-high molecular weight polyethylene (UHMWPE) is used as the matrix [28] (cf. Section 3.2). Fibres that are coated with either conjugated polymers or carbon nanomaterials display a similar behaviour, i.e. the modulus depends on the properties of the fibre core, which carries the mechanical load. In case of nanocomposite fibres where the carbon nanomaterial is instead embedded in a polymer matrix, there exists a trade-off between draw ratio and conductivity (cf. Section 3.4) limiting the effective degree of alignment that can be imparted in the fibre. Still, the reinforcing effect of the nanofillers results in mechanical properties comparable to that of fibres with higher draw ratios.

In addition to suitable electrical and mechanical properties, which can be adjusted with regard to the intended application, fibres need to fulfil a number of other criteria. For instance, fibres must be able to handle the different types of mechanical stresses that arise during both textile production and later during use (cf. Sections 2 and 5). Further, fibres must be able to maintain their functionality in different types of environments, including (1) exposure to ambient atmosphere, which is a challenge if volatile dopants are used to adjust the electrical conductivity, (2) exposure to water during washing and use (sweat, rain, etc.), as well as (3) exposure to other chemical agents (e.g. washing powder). These additional requirements may necessitate compromises with regard to the electrical and mechanical performance, as discussed in more detail in Section 3.

In the next chapter of this review we will first introduce the reader to the most important fundamental aspects of fibre technology covering both structure and function. We recommend that readers skilled in the field skip Section 2 and immediately move on to Section 3, where we introduce the main types of conjugated polymer and/or carbon nanomaterial-based fibres. In Section 4 we then discuss the integration of conducting fibres into e-textiles, as well as some of the envisaged applications. Finally, in Section 5, we provide a critical perspective on the – often neglected – sustainability aspects of conducting fibres and e-textiles.

2. From fibre to yarn to textile – the fundamentals

Textiles is a class of hierarchical materials that has been in constant development for several thousand years. This chapter introduces the reader to fundamental concepts and processing techniques related to textiles and their manufacture and is, unless otherwise specified, based on several excellent textbooks on fibre spinning [29,30], polymer processing [31] and textile manufacture, dyeing and finishing [32–35].

2.1. Filaments, staple fibres and yarns

A textile fibre is by definition an entity characterised by flexibility, fineness and a high aspect ratio typically exceeding 1000. Depending on their origin, fibres are classified as either natural or manufactured; manufactured fibres in turn may be fabricated from natural or synthetic polymers. Textile fibres can be in the form of filaments (continuous fibres) or staple fibres (of a discrete length). Staple fibres must be collected and twisted into a yarn to form a continuous structure. Therefore, they should have a length of at least 15 mm, to provide sufficient cohesion for yarn formation, but less than 150 mm as this instead requires specialised yarn spinning machinery. The fibre thickness usually ranges from 10 to 50 μm; thinner fibres tend to be too delicate for yarn spinning, and with fibres exceeding 50 μm in thickness the resulting yarn will be too coarse for comfort. For a fibre to successfully pass the rather unforgiving textile manufacturing processes – including yarn-spinning, dyeing, weaving, knitting, printing and washing – it will need to display a high tenacity and a recoverable extensibility of at least a few percent. In addition, for many applications textile fibres must display an ability to take up colourants, resistance to chemicals (including alkalis such as detergents/laundry liquors and acids through perspiration), heat (textile production can include heat treatments at 200 °C or more) and sunlight.

Typical tensile properties, i.e. the response to a mechanical load applied in a direction parallel to the fibre axis, of selected textile fibres are given in Table 1. The tenacity (ultimate strength) of a fibre is given by the stress at break (Fig. 2). However, for most practical purposes the load at which permanent deformation is introduced, i.e. the yield point, is more relevant. Because the outer diameter of fibres and yarns can be tricky to define, their mechanical properties are often reported as the specific tensile stress in units of Newtons per tex (N/tex) where tex is the linear density or grams per kilometre.

2.2. Tensile deformation of fibres

The mechanical properties of a fibre are related to its micro- and nanostructure, and in particular to the degree of molecular alignment along the fibre axis. Fibres based on flexible polymers can display different degrees of alignment, whereas rigid-rod polymers tend to feature uniaxial alignment. Tensile stress applied to a fibre will be distributed on a molecular level. Initially, only elastic deformation occurs. If unoriented amorphous regions are present, as is the case for poorly aligned flexible-chain fibres, a relatively small stress will lead to considerable deformation and the fibre will display a low Young's modulus. If the stress is released before plastic deformation occurs – i.e. within the elastic region of the fibre (Fig. 2) – inter-chain network points (such as hydrogen bonds, π-stacking, entanglements, crystallites and/or chemical crosslinks) will force the fibre to revert to its original state. A further increase in stress beyond the yield point will result in plastic/irreversible deformation provided that network points can rearrange (e.g. reorientation and shearing of crystals). In contrast, fibres that do not contain unoriented amorphous regions, which is the case for both rigid-rod fibres and highly drawn flexible-chain fibres, display only a minimal elastic deformation once a high stress is applied, resulting in a high Young's modulus. Such stiff fibres have no yield point and display brittle failure at high loads (Fig. 2). The ultimate mechanical strength of high-modulus fibres depends on the number of inter-chain interactions per molecule, which act perpendicular to the fibre axis (cf. Section 3). In the cases where only weak dispersion forces act, then for very strong fibres a very high molecular weight is required. If instead for instance hydrogen bonds and/or π-stacking occur, then very strong fibres can be prepared with lower molecular-weight material.

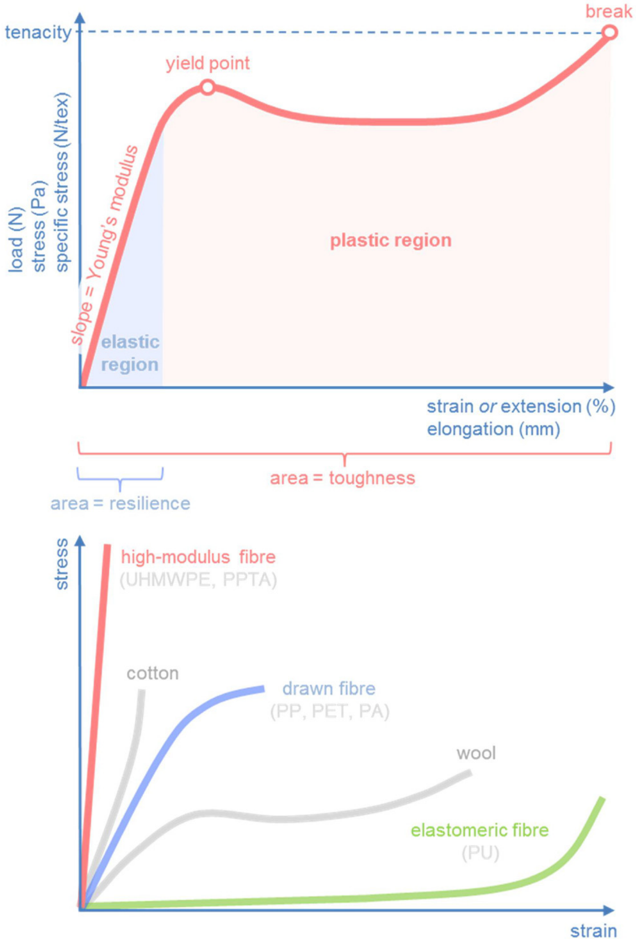

Fig. 2. Illustration of a typical stress-strain curve that is measured during tensile deformation of a semi-crystalline polymer (top), and schematic stress-strain curves of common types of textile fibres (bottom).

Table 1
Typical tensile properties for selected fibres from Refs. [33,35].

fibre	initial modulus (cN/tex)	yield stress (cN/tex)	tenacity (cN/tex)	yield strain (%)	strain at break (%)
cotton	60	[a]	40	[a]	7
wool	23	6	11	5	42
silk	73	16	38	3	23
nylon	26	40	47	16	26
polyester	106	30	47	10	15
viscose	65	7	21	2	16
high modulus fibres (e.g. UHMWPE, PPTA)	2000–35,000	[a]	100–450	[a]	0.5–5

[a] No marked yield point.

2.3. Common natural and synthetic fibre materials

Natural fibres are either cellulose (e.g. cotton and flax) or protein based (e.g. silk, wool and cashmere). The natural fibres tend to have high molecular weights, e.g. the molecular weight of cotton exceeds 1500 kg mol^{-1}, and the molecules are highly oriented along the fibre axis as a result of the natural process of growth. The silk fibre is the only naturally occurring filament, and the silk threads spun by some spider species are among the toughest known fibres, facilitated by a high molecular weight of up to 600 kg mol^{-1}, hydrogen bonds and uniaxial alignment [36].

Manufactured fibres date less than a century back [37] and at present, the most common synthetic fibre materials are poly(ethylene terephthalate) (PET), polyamide (PA), polyacrylonitrile (PAN), and polypropylene (PP). The molecular weight dictates both the spinnability and mechanical properties of the resulting fibre. In case of polyamides, where hydrogen bonding leads to strong intermolecular forces, a molecular weight of about 20 kg mol^{-1} is adequate. Polypropylene instead, must have a molecular weight of at least 60 kg mol^{-1}, since only weak dispersion forces act between polymer chains.

High-modulus fibres can be prepared with both flexible polymers such as UHMWPE, and rigid-rod polymers such as poly(*p*-phenylene terephthalamide) (PPTA or Kevlar™) [38]. Uniaxial alignment and a high molecular weight leads to a large number of weak dispersive interactions in case of UHMWPE fibres. PPTA fibres, instead, can be prepared with lower molecular weights thanks to both hydrogen bonding and π-stacking. Likewise, both carbonaceous nanomaterials (carbon nanotubes, graphene) and conjugated polymers readily permit the fabrication of high-modulus fibres because of stronger π-interactions, which also lead to a high electrical conductivity (cf. Section 3).

2.4. Fibre spinning: melt, dry, wet and air-gap spinning

Fibre spinning is essentially a biomimetic method, inspired by the process that spiders and silkworms use to produce their threads. It involves three steps: (1) preparing a spinnable liquid, (2) extruding the liquid to form a jet, and (3) jet hardening [30]. The liquid may be in the form of a polymer melt or a solution. When spun from solution, the jet hardening can take place in hot air (dry-spinning) or in a coagulant bath (wet spinning), or in a combination of both (air-gap spinning and gel spinning).

Melt spinning is the most common method to prepare fibres with flexible-chain polymers such as polyamide, polyester and polypropylene. A polymer melt is rapidly pumped through a spinneret (die) with one or several small holes. The extruded filament(s) is then cooled and stretched in several steps before being collected on a bobbin (Fig. 3). The first drawing step – melt drawing – occurs before solidification. Alignment of polymer chains in the melt leads to strain-induced crystallisation so that instead of a spherulitic microstructure, which is common for polymers crystallised under quiescent conditions, lamellar or extended chain crystals form, in which polymer chains are oriented in the direction of flow (Fig. 4). The second drawing step occurs after solidification. This so called cold drawing, at a temperature between the glass transition and melting temperature ($T_g < T < T_m$), is critical for achieving a high degree of orientation, which increases the elastic modulus of the fibre [39].

To adjust the viscosity, spinning can be carried out from a solution instead of a melt. A spinning dope is prepared by dissolving the polymer at a high concentration of 10–45%. Solution spinning is then carried out by pumping the dope through a spinneret with typically several hundred, tens-of-micrometre sized holes. To spin fibres with polymers such as cellulose acetate, polyacrylonitrile (PAN) and polyvinyl alcohol (PVA), the filament is spun into hot air to allow for rapid evaporation of the volatile solvent. This process is called *dry spinning*. The spinneret may instead be submerged into a coagulation bath, referred to as *wet spinning* (Fig. 5). The coagulation bath is filled with a liquid that blends with the solvent of the dope, but does not dissolve the polymer. As a result, the extruded jet undergoes gelation and gradually solidifies into a filament. Solution spinning of flexible polymers leads to poorly oriented fibres, since the high molecular mobility in solution results in relaxation of the polymer chains prior to crystallisation. The coagulated filaments are cold drawn during subsequent processing steps to achieve a high degree of orientation.

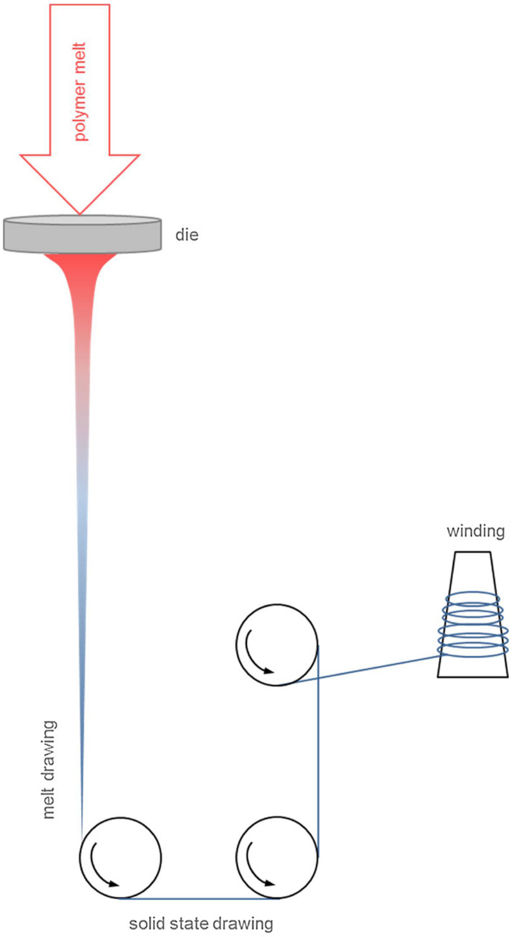

Fig. 3. Illustration of a melt spinning process.

Alternatively, to allow for a significant temperature difference between the spinning dope and coagulation bath, dry and wet spinning can be combined, i.e. an air gap is followed by a coagulation bath, which is called *air-gap* or *dry-jet wet spinning*. A prominent example for an air-gap spinning process is the fibre production of PPTA fibres [40]. A dope of 10–20% PPTA dissolved in concentrated sulfuric acid first enters a short air gap, and then coagulates in an ice bath. The spinning dope is lyotropic and therefore the rigid PPTA chains readily align with the flow direction, leading to a high degree of orientation already during fibre formation [41].

A similar air-gap spinning process is used for the production of UHMWPE fibres, referred to as *gel spinning*. A gel of the polymer dissolved in a few percent of e.g. decalin is extruded through a small air gap into a water bath, followed by slow solidification of the extruded gel fibre in a hot environment, and a cold drawing step to further improve the high degree of orientation [42].

2.5. Yarn formation

Following the extrusion process, fibres may be used as monofilaments (e.g. as fishing lines), but are most commonly spun into yarns. A

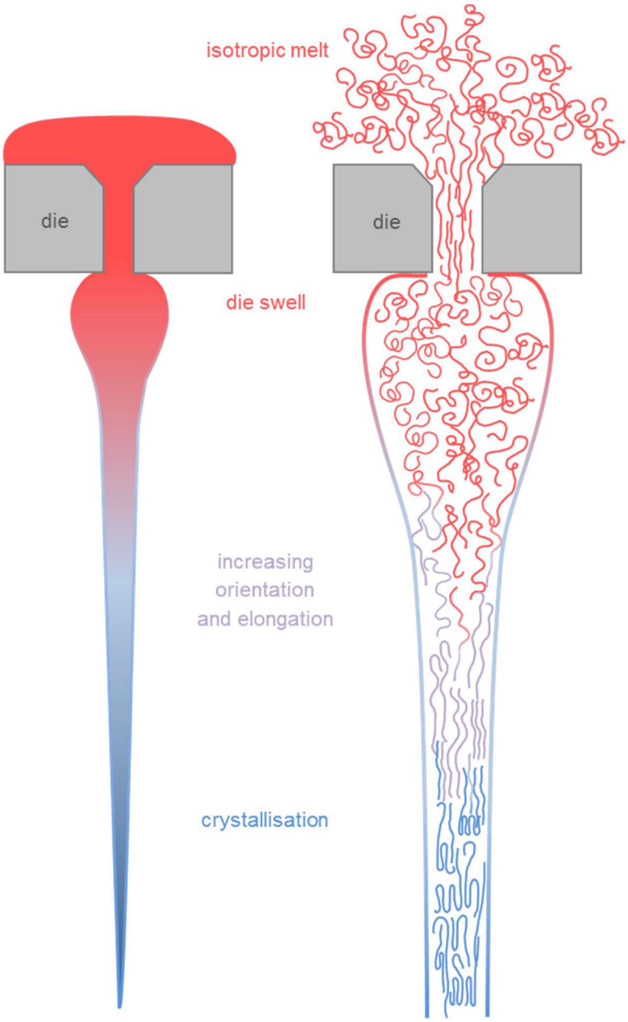

Fig. 4. Illustration of the changes in polymer chain conformation encountered during the initial stage of melt spinning.

yarn is an assembly of staple fibres and/or filaments, usually mechanically twisted to stay together through friction. Sewing threads and ropes are examples of yarns of varying dimensions. For staple fibres, the yarn spinning process involves carding the fibres into a web, twisting the web into a sliver, followed by several steps to further draw and twist the sliver into a yarn. To enhance the tensile strength, several yarns can be twisted together to form a plied yarn.

2.6. Common fabric manufacturing methods: weaving, knitting

'Textile' is the broad term for a material, which consists of fibres – consequently the word textile can denote anything from threads and yarns to pieces of fabric and clothing. The words 'cloth' or 'fabric' denote a coherent, generally two-dimensional, piece of material where the fibres are bound together after a textile process such as knitting, weaving, needle-punching or by means of adhesives. The two latter examples result in *nonwoven* fabrics such as wool felts.

Weaving is carried out in a loom or weaving machine (Fig. 6) by interlacing two sets of yarns – the warp and the weft. The warp yarns, which are suspended along the length of the loom, experience a high tension and a substantial degree of abrasion during weaving, thus a high tenacity yarn is required. During weaving, the warp yarns are lifted in repeated patterns (or individually in a jacquard loom, allowing more intricate patterns), and the weft yarn is inserted orthogonally to the warp direction. The reed then pushes the weft into the forming fabric. The weft yarn can be of lower tenacity compared to the warp yarn, but needs to be mechanically stable and resistant to abrasion.

In *knitting*, a fabric is formed by interlocking loops between yarns. There are two industrial knitting methods: warp knitting and weft knitting (Fig. 6). In warp knitting a number of yarns are fed along the length of the fabric, with latch needles producing a chain of loops in the *wale* direction. This technique can produce lace and – as it can combine yarns with huge variations in dimensions and mechanical properties – is commonly used for technical textiles. In weft knitting, the yarn is fed to form loops in *courses* along the width of the fabric, resulting in the soft and stretchable structure that is commonly used in apparel. Knitting, in contrast to weaving, can be carried out with less tenacious yarns. However, the yarn must be flexible enough to readily form loops. Knitted fabrics can be easily deformed, whereas a woven fabric has an inherent rigidity. This can be exploited e.g. to tailor the performance of electro-active textiles (cf. Section 4).

2.7. Dyeing and finishing: adding colour and function

Filaments, yarns and fabrics can be subjected to a number of dyeing and finishing processes. Washing removes *size* (adhesives) and lubricants that were added during previous processing steps. Dyeing allows to adjust the appearance (colour) and can be used to impart additional functionality, such as electrical conductivity (cf. Section 3.5). The yarn or fabric are placed into a dye bath, either in a continuous or batch process. Dyes can diffuse into the fibre from a (water based) solution or dispersion, which is commonly used to colour e.g. silk and cellulose as well as acetate, nylon and polyester. The adhesion can be improved by using reactive dyes, which covalently bind to the fibre, or acid dyes (common for protein fibres), which bind through electrostatic interactions. Excellent adhesion is important since it imparts resistance

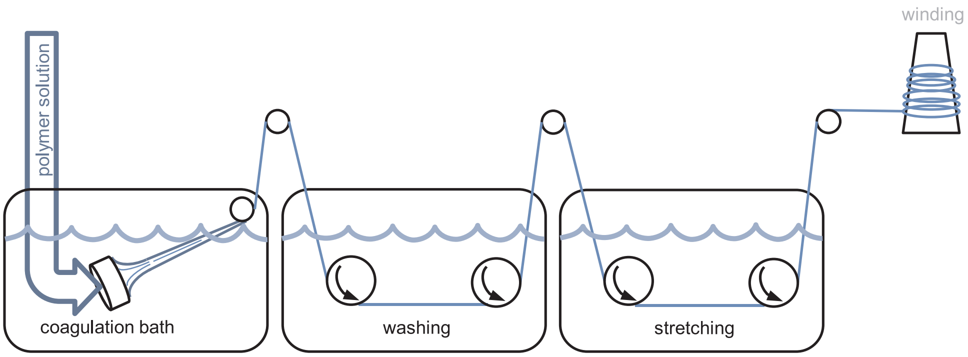

Fig. 5. Illustration of a wet spinning process.

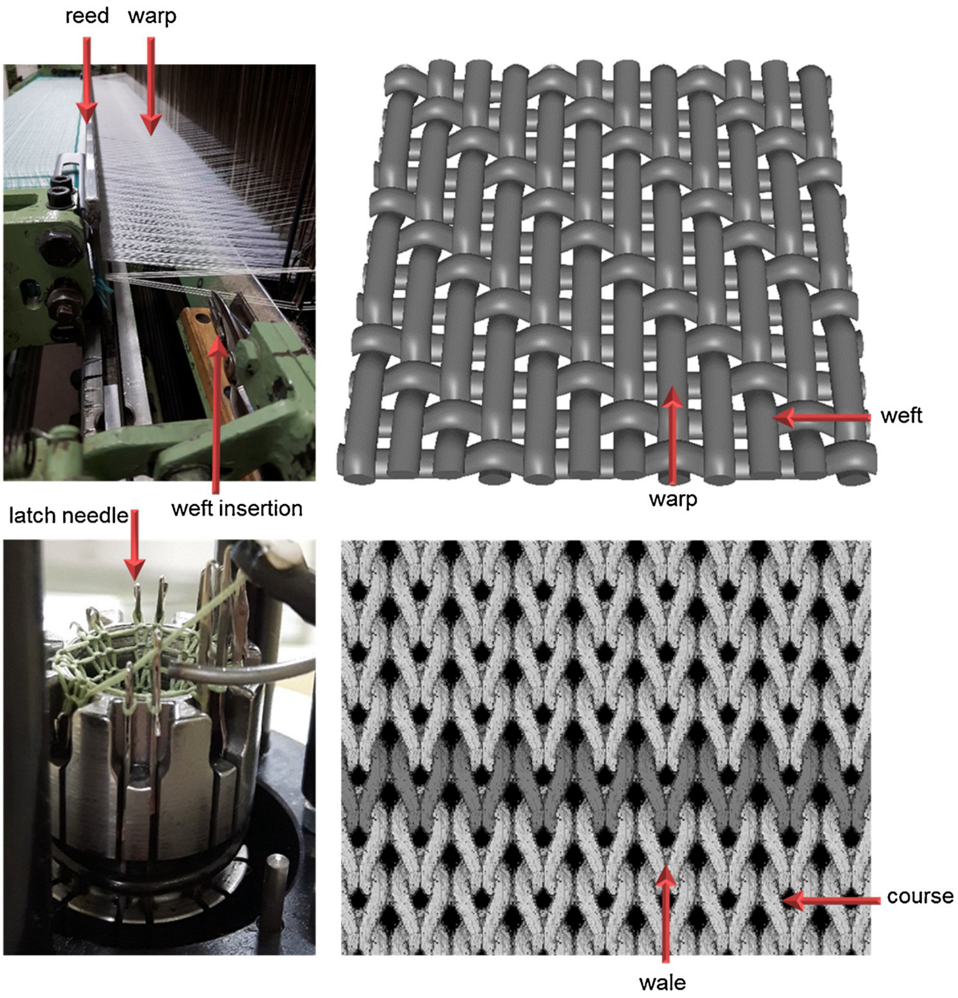

Fig. 6. Photographs of a rapier weaving loom and a circular knitting machine (top and bottom left); illustration of a woven and a knitted textile architecture (top and bottom right). The photos were taken in the workshops of the Swedish School of Textiles, University of Borås, Borås, Sweden.

to abrasion which is necessary for both weaving and knitting (cf. Section 2.6) as well as later during use. Other methods to modify and pattern the fabric include printing and coating (e.g. screen printing, dip or knife coating), which typically require that rheological properties of the ink are adjusted through addition of a suitable binder polymer. Printing and coating of electrically conducting inks readily permits the fabrication of electro-active fabrics (cf. Section 3.5). Regardless of the deposition method, coating is followed by film formation, i.e. the coating is dried and cured so that the solvent is removed and the binder, if applicable, crosslinks.

3. Fabrication of electrically conducting fibres and yarns

A broad range of organic materials can be used to prepare electrically conducting fibres. In this chapter, we introduce the reader to key advances in the field and put emphasis on underlying structure-processing-property relationships. For a comprehensive overview of the current state-of-the-art we refer the reader to recent reviews that cover conducting fibres based on conjugated polymers [43–45], carbon nanotubes [46,47] and graphene [48].

A variety of methods exist to produce electrically conducting fibres and yarns, which can be classified into (1) the functionalisation of an already existing fibre through coating or dyeing, and (2) fibre spinning and drawing with an intrinsically conducting material. In case of the former the structural integrity is provided by the base fibre or yarn. In composite and blend fibres, instead, the mechanical strength is either intrinsic to the conducting material or given by a polymeric matrix. The ultimate mechanical strength of uniaxial aligned, saturated polymers is determined by *weak* van der Waals forces (i.e. dispersion forces, dipole-induced dipole interactions and dipole-dipole interactions) – and in case of e.g. polyamides also strong hydrogen bonds – that act between polymer chains. Neighbouring conjugated polymer chains, carbon nanotubes and graphene sheets display *stronger* π-interactions and therefore can offer superior mechanical properties such as a higher Young's modulus and tensile strength [49–51], provided that the molecular weight of the conjugated polymer and length of the carbon nanomaterial is sufficiently high [52–54].

Up to four ingredients can be used to create electrically conducting fibres with organic materials: (1) conjugated polymers, (2) conducting nanofillers such as carbon black, carbon nanotubes and graphene, (3) dopants and counterions, and (4) insulating matrix or binder polymers [55]. Either conjugated polymers or nanofillers can be used as the primary charge-conducting material. Matrix and binder polymers can be added to adjust the rheological and solid-state mechanical properties. Dopants are needed to select the type of majority charge carriers, i.e. electrons or holes, and to adjust the absolute number of charge carriers. A high number of charge carriers is needed to achieve a high electrical conductivity (cf. Eq. (3)).

The electrical conductivity as well as strength of a conducting fibre are governed by the intrinsic properties of its constituents but also the coupling between individual constituents [56], which can be polymer chains, carbon nanotubes, sheets of graphene, etc. In case of electrical conduction in a material composed of conjugated polymers these processes are referred to as intra- and inter-chain transport. In a scenario where individual components are uniaxially aligned, e.g. along the axis of a conducting fibre, the intrinsic properties of individual components are reached if the sum of all inter-particle interactions outweigh intra-particle properties. For conjugated polymers the following criterion must be fulfilled so that the electrical charge-transport approaches the intrinsic value of individual polymer chains [49]:

$$t_{3D}\cdot\frac{L}{a} \gg t_0 \tag{1}$$

where t_{3D} and t_0 are the inter- and intra-chain π-electron transfer integral, L is the coherence length, i.e. the average length of extended chain segments, and a is the length of a repeat unit. For the mechanical strength a similar relationship holds [49]:

$$E_{3D}\cdot\frac{L}{a} \gg E_0 \tag{2}$$

where E_0 is the energy required to break the covalent main chain, and E_{3D} is the energy of an inter-chain interaction, such as a van der Waals interaction, a hydrogen bond, and/or π-stacking (Fig. 7). For carbon nanoparticles similar criteria apply, with L/a replaced by the number of inter-particle interactions. It is apparent from Eq. (1) that the electrical conductivity $c(L, t_{3D})$ increases with the coherence length of its constituents as well as the degree of electronic coupling. Similarly, the mechanical strength $\sigma_s(L, E_{3D})$ increases with both coherence length and the number and strength of inter-particle interactions (cf. Eq. (2)). Evidently, highly aligned polymer chains or carbon nanoparticles offer a high degree of coherence along the fibre axis. As a result, the electrical conductivity of conjugated polymers and carbon nanoparticles strongly depends on the degree of alignment. A comparison of the Young's modulus and electrical conductivity that have been reported for various highly aligned conjugated polymer and carbon nanotube fibres reveals that the two properties scale with each other (see Fig. 1). Moreover, it should be noted that the mechanical and electrical properties of aligned fibres tend to be highly anisotropic, with higher performance along the fibre axis.

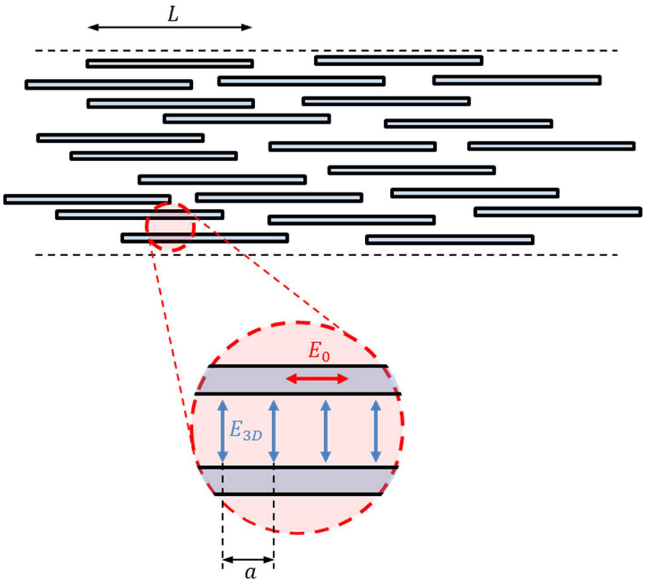

Fig. 7. Illustration of rod-like polymer chain segments or carbon nanotubes with length L aligned along the long axis of a fibre, held together by inter-chain interactions with energy E_{3D} acting per distance a, which must outweigh the energy E_0 needed to break a chain segment.

3.1. Mechanical and electrical properties of aligned conjugated polymers

One prevailing goal of the field of conjugated polymers is the creation of materials that feature both a high electrical conductivity *and* mechanical strength [52]. The electrical conductivity c is given by:

$$c = ne\mu \tag{3}$$

where μ is the charge-carrier mobility, n is the charge carrier density and e is the elementary charge. A high electrical conductivity requires a high charge-carrier mobility, which is facilitated through π-electron delocalisation along the polymer chain (intra-chain transport), as well as π-stacking, which aids hopping of charges between neighbouring chains (inter-chain transport). Moreover, free charge carriers must be introduced into the π-electron system (either electrons or more commonly holes) through either a redox or an acid-base reaction with a dopant molecule in order to achieve a high charge-carrier density [55] (Fig. 8 and Table 2). The dopant molecule remains present as the counterion (cation or anion) to balance the charge on the conjugated polymer. Since each repeat unit represents one redox site, a relatively high number of charge carriers can be realised. However, the introduction of molecular dopants, of which one is needed per redox site, results in volume expansion and reduces interactions between polymer segments. As a result, doping improves the electrical conductivity but tends to decrease the stiffness and strength. For instance, the Young's modulus of tensile drawn polyacetylene (PAc) (draw ratio 15; see Fig. 9 for chemical structure) decreases from almost 50 GPa to 10 GPa upon doping with iodine [57]. At the same time, the electrical conductivity of stretch-aligned, iodine-doped PAc can reach values of up to 60,000 S cm^{-1} [58,59], although the poor environmental stability of the polymer and the tendency of iodine to sublime prevents any practical use. A current trend in the field is the development of larger molecular dopants that do not diffuse as rapidly [60]. However, a larger

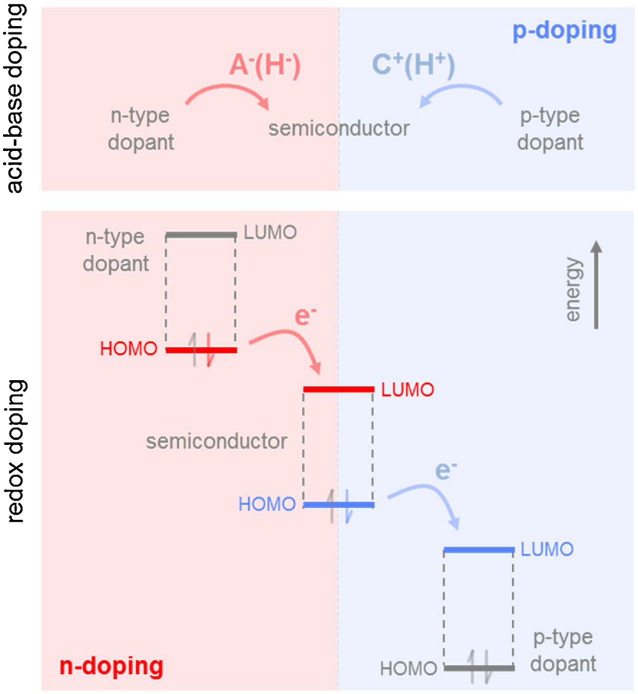

Fig. 8. Basic principle of acid-base doping, which involves the transfer of an anion (A^-, e.g. H^-) or cation (C^+, e.g. H^+) to the semiconductor (top); and redox doping, which involves the transfer of an electron to the LUMO or from the HOMO of the semiconductor in case of n- and p-doping, respectively (bottom).

Reprinted from [55] – Published by The Royal Society of Chemistry.

Table 2
Properties of conducting fibres spun from conjugated polymers; Young's modulus E, tensile strength σ_s, electrical conductivity c.

conjugated polymer	dopant/ counterion	E (GPa)	σ_s (MPa)	c (S cm^{-1})	Ref.
PAc	I_2	7.1	190	13,000	[58]
PTV	I_2	7	450	2000	[64]
PDMPV	I_2	25	700	1200	[65]
MEH-PPV	I_2	2.5	83	70	[69]
PANI	SA	1	20	60	[66]
PANI	DBSA	0.5	20	113	[80]
PEDOT:PSS	PSS	5.7	134	351	[77]
PEDOT:PSS	PSS	4	130	467	[81]
PEDOT:PSS	PSS	8.3	410	2804	[79]
PEDOT:PSS	PSS	1.1	17.2	0.5	[82]
PEDOT:PSS	PSS		80	38	[78]
P3OT	I_2	0.35	29	11	[83]
P3OT	$FeCl_3 \cdot 6H_2O$	2		150	[70]
P3DDT	$FeCl_3 \cdot 6H_2O$	1		80	[70]
P3HT	$FeCl_3 \cdot 6H_2O$	4.5		160	[70]
P3HT	$FeCl_3$			350	[72]

molar mass ultimately reduces the charge that can be obtained per dopant molecule and disrupts the nanostructure of the polymer, leading to a decrease in its final properties.

A number of synthetic routes have been explored to prepare highly aligned conjugated polymers with the aim to maximise both their electrical and mechanical properties. Those include fibre-spinning of (1) soluble precursor polymers, (2) bare conjugated polymers with counter-ion induced solubility, and (3) side-chain functionalised soluble and melt-processable polymers [57,61].

Polymers such as poly(*p*-phenylenevinylene) (PPV) and poly(2,5-Thienylene vinylene) (PTV) can be prepared from water-soluble polyelectrolyte precursors, which carry labile sulfonium or tetrahydrothiophenium side groups that are eliminated to obtain the fully π-conjugated polymer [49,62–64]. For instance, Tokito et al. converted wet-spun precursor fibres to PTV fibres with a Young's modulus of 7 GPa and conductivity of 2000 S cm^{-1} [64]. Another possibility is to use a precursor that is soluble in organic solvents, such as the 1-methoxythylene containing precursor of poly(2,5-dimethoxy-*p*-phenylenevinylene) (PDMPV). Continuous fibres of PDMPV could be spun from chloroform solutions of the precursor polymer, which after conversion at 230 °C and doping with iodine displayed a Young's modulus of 25 GPa and conductivity of 1200 S cm^{-1} along the fibre axis [65] (Fig. 10). X-ray diffraction of PDMPV fibres reveals the (for tensile-drawn polymers typical) high degree of uniaxial orientation, which persists after doping with iodine (Fig. 11; cf. Fig. 4).

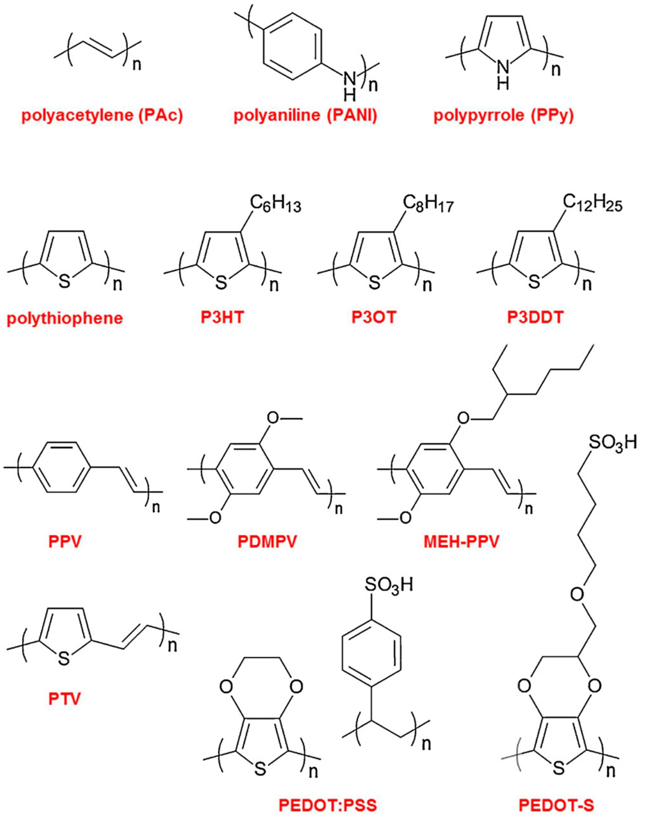

Fig. 9. Chemical structures of the polymers discussed in this review.

Polyaniline (PANI) is fully soluble in strong protonic acids such as concentrated sulphuric acid, which also allow processing of the polymer in its conducting form. Extensive literature exists on spinning of polyaniline fibres [52]. For instance, air-gap wet spinning into water allowed to prepare semi-crystalline PANI fibres, that as-spun can display a conductivity of up to 60 S cm^{-1} [66]. However, because of the low molecular weight of PANI and lack of spin-line drawing, fibres tend

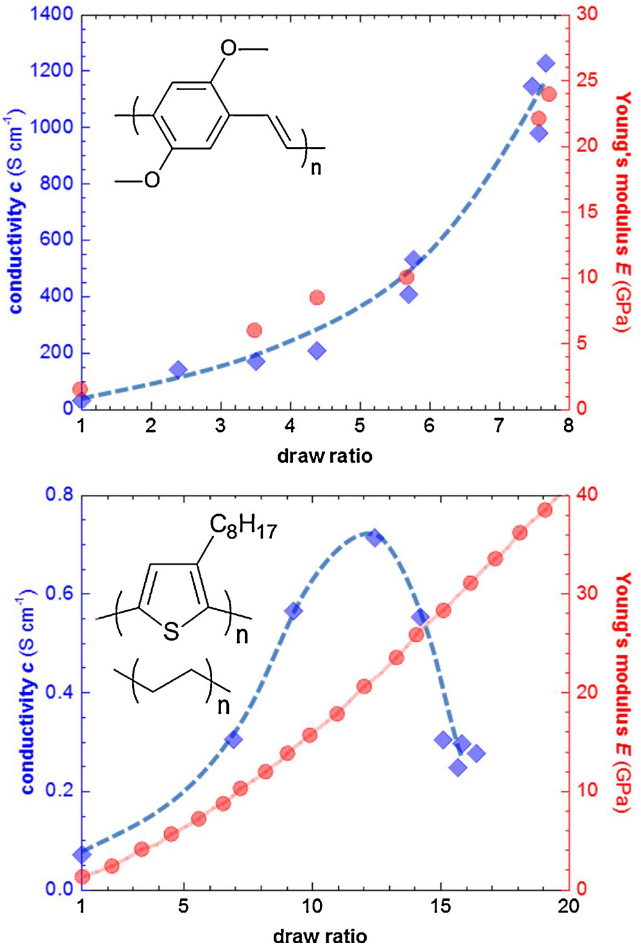

Fig. 10. Conductivity (blue diamonds) and Young's modulus (red circles) vs. draw ratio of iodine-doped fibres produced with the conjugated polymer poly (2,5-dimethoxy-*p*-phenylenevinylene) (PDMPV) (top), and poly(3-octylthiophene) (P3OT) blended with UHMWPE at a stoichiometry of 1:4 (bottom); the modulus of blend fibres was calculated according to $E_{blend} \approx \phi_{PE} E_{PE}$ where ϕ_{PE} is the volume fraction of polyethylene and E_{PE} is the modulus of polyethylene as a function of draw ratio. (For interpretation of the references to colour in this figure legend, the reader is referred to the web version of this article.)
Data for PDMPV and P3OT:UHMWPE from Refs. [28,65], and modulus data for UHMWPE from Ref. [288].

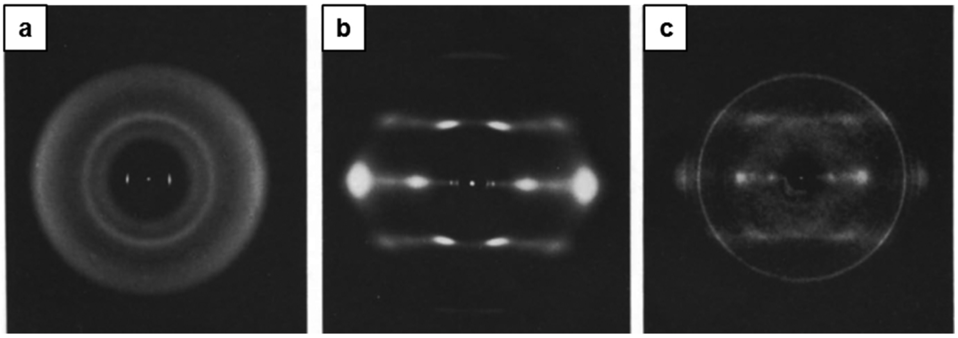

Fig. 11. Transmission X-ray diffraction patterns of (a) unstretched PDMPV, (b) stretched PDMPV, (c) stretched PDMPV doped with iodine.
Reprinted from [65], with permission from Elsevier.

to be brittle. The solubility in concentrated acids opens up the possibility to co-process with high-performance polymers such as polyaramides e.g. PPTA (see Section 3.2).

Counter-ion induced processability is a widely explored route to form complexes of otherwise intractable conjugated polymers with suitable anions. For instance, complexes of PANI and dodecylbenzenesulfonic acid (DBSA) or camphor sulfonic acid (CSA) are soluble in common solvents such as chloroform and m-cresol and when cast into films give rise to an electrical conductivity of more than $100\,\mathrm{S\,cm^{-1}}$ [67]. Moreover, the alkyl chains of the DBSA counter-ion impart compatibility with matrix polymers, which is attractive for the preparation of polymer blends (cf. Section 3.2). Another widely explored example for counter-ion induced solubility is the combination of the otherwise intractable conjugated polymer poly(3,4-ethylenedioxythiophene) (PEDOT) and the polyanion poly(styrenesulfonate) (PSS), which is commercially successful as a water dispersion of swollen particles with a PEDOT rich core surrounded by a PSS rich shell that provides solubility [68].

The decoration of conjugated polymers with alkyl side chains is a widely used tool to reduce the melting and dissolution temperature and hence impart melt and solution processability, which however dilutes the volume fraction of the charge-conducting and load bearing polymer backbone [69,70]. The melting and glass transition temperatures of poly(3-alkylthiophene)s (P3ATs) decrease from $T_m > 300\,°\mathrm{C}$ and $T_g > 100\,°\mathrm{C}$ for unsubstituted polythiophene to e.g. $T_m \sim 220–250\,°\mathrm{C}$ and $T_g \sim 10\,°\mathrm{C}$ for regio-regular poly(3-hexylthiophene) (P3HT) [53,71]. As a result, P3HT can be melt-spun, with fibres reaching an electrical conductivity of $350\,\mathrm{S\,cm^{-1}}$ when subsequently doped with $FeCl_3$ [72]. In case of P3HT a number-average molecular weight $M_n > 25\,\mathrm{kg\,mol^{-1}}$ is needed to facilitate cold drawing beyond the yield point since chain entanglement and tie chain formation only occur for higher molecular weights [53] (Fig. 12). The room-temperature tensile modulus of unoriented P3ATs displays a step-change from more than one 1 GPa to about 0.1 GPa when increasing the side chain length from hexyl to heptyl [73,74], which can be explained with softening of the polymer due to a below ambient T_g.

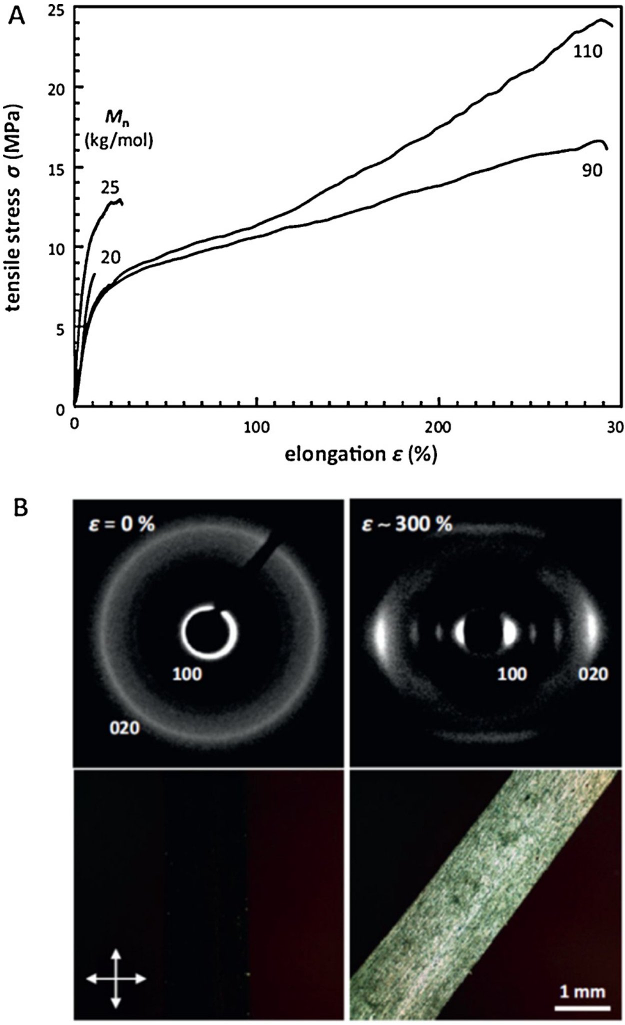

Fig. 12. Stress-strain curves of poly(3-hexylthiophene) (P3HT) tapes with different molecular weights (top), transmission X-ray diffraction patterns and corresponding cross-polarised optical microscopy images of a high-molecular weight P3HT sample before and after stretching to an elongation of 300% (bottom).
Reprinted from [53] with permission from Elsevier.

Moulton and Smith studied the influence of the side chain length, from 6 to 12 carbons, on the electrical and mechanical properties of P3AT fibres, wet-spun from chloroform into acetone [70]. In contrast to conjugated polymer fibres prepared through the precursor route, doping with $FeCl_3$ or iodine increased not only the electrical conductivity but also the strength and stiffness. Stretch-aligned P3HT features a Young's modulus of 4 GPa at a draw ratio of 5 and, when doped with $FeCl_3$, an electrical conductivity of up to $160\,\mathrm{S\,cm^{-1}}$, which is a 4-fold increase as compared to undrawn material [70]. The increase in electrical conductivity with draw ratio depends on the side chain length, since the later dilutes the amount of charge-conducting material. Therefore, for the same draw ratio the conductivity decreases with side chain length. Hence, iodine-doped, unsubstituted polythiophene can display values of more than $300\,\mathrm{S\,cm^{-1}}$ [57,70,75]. Here it is important to note that doping increases the brittleness of a conjugated polymer at room temperature [76], likely through an increase in the T_g

through stiffening of the polymer backbone.

PEDOT:PSS can be considered as a blend of the low molecular weight conjugated polymer PEDOT with not more than 20 repeat units [68], and the polyanion PSS which imparts processability from water. Thanks to its high molecular weight of typically about 200 kg mol^{-1}, the polyanion itself can act as a binder. Therefore, wet spinning of PEDOT:PSS without any additional binder can result in fibres with a Young's modulus as high as 8 GPa and electrical conductivity of more than 2000 S cm^{-1} [77–79].

3.2. Blends of organic semiconductors and insulating polymers

One approach to adjust the rheological and mechanical properties of conjugated polymers is the addition of a high(er) molecular weight binder polymer. The choice of binder polymer then decides the mechanical behaviour such as a high tenacity or elasticity, whereas the (doped) conjugated polymer defines the electrical conductivity of the fibre (Table 3). In other words, the use of polymer blends permits to decouple the mechanical and electrical properties of the fibre. Blend fibres with the same conductivity but widely different elastic moduli can be prepared by changing the matrix polymer (cf. Fig. 1). Other advantages of polymer:polymer blends are encapsulation of the more environmentally sensitive doped conjugated polymer and a considerable cost reduction by using a commodity polymer as the binder. Even today, one kilogram of P3HT will cost more than 30,000 € which makes the exploration of bulk processing routes such as fibre spinning prohibitively expensive. Hence, polymer blends are a convenient means to explore the suitability of conjugated polymers for e-textile applications.

In order to facilitate charge conduction, the conducting phase in a blend or composite must percolate. The percolation threshold Φ_p (conducting filler fraction above which conduction occurs) scales with the aspect ratio L/D:

$$\phi_p \propto \left(\frac{D}{L}\right)^2 \tag{4}$$

where L and D are the length and diameter of the conducting phase (or nanofiller in case of e.g. carbon nanotubes) [84].

For instance, Moulton and Smith have shown that gel-spun blends of UHMWPE and (subsequently) iodine-doped poly(3-octylthiophene) (P3OT) largely retain the electrical conductivity of the latter with e.g. 0.1 S cm^{-1} for 20 wt% P3OT, which increased by one order of magnitude to about 0.7 S cm^{-1} upon stretch-alignment to a draw ratio of 12.5 [28] (Fig. 10). Conductivity can be maintained at very low volume fractions of the conjugated polymer, indicating that the conjugated polymer domains have a high aspect ratio (cf. Eq. (4)). The good

Table 3
Properties of conducting fibres spun from polymer blends; Young's modulus *E*, tensile strength σ_s, electrical conductivity *c*.

blend	wt% conjugated polymer	dopant/counterion	*E* (GPa)	σ_s (MPa)	c (S cm^{-1})	Ref.
P3OT:UHMWPE	20	I_2	20		0.7	[28]
P3OT:UHMWPE	40	I_2	10	0.5	9	[28]
PANI:PPTA	60[a]	HCl			10	[49]
PANI:PPTA	60		5		10	[85]
PANI:PMMA	9	CSA			10	[67]
PANI:UHMWPE	40	DBSA	15.8	930	2	[80]
P3HT:SIBS	12	HBF_4	0.021	11	0.4	[87]
PEDOT:PSS:PU	25	PSS	0.25	10	25	[88]
PEDOT:PSS:PU	13	PSS	0.024	23	9	[4]
PEDOT:PSS:PVA	4.8	PSS	5	145	21	[89]

[a] Refers to vol%.

Table 4
Properties of conducting fibres spun from nanomaterials; Young's modulus *E*, tensile strength σ_s, electrical conductivity *c*.

nanomaterial	spinning technique	*E* (GPa)	σ_s (MPa)	c (S cm^{-1})	Ref.
carbon fibres	carbonised from *meso*-phase pitch	965		8300	[27]
carbon fibres	carbonised from PAN	588		1400	[27]
SWNT	wet spinning	120	116	5000	[92]
SWNT	wet spinning, PEI coagulant	6[a]	85[a]	150	[108]
SWNT	wet spinning	12[a]	65[a]	140	[109]
MWNT	yarn spinning/draw twisting	20	460	300	[102]
MWNT	yarn spinning/draw twisting	330	1910	410	[103]
MWNT	wet spinning from LC[b] state	69	150	80	[100]
MWNT	draw twisting, infiltration with PVA	120	2000	920	[104]
DWNT	draw twisting	195	1900		[54]
rGO[c]	NaOH coagulation	9	115	2.8	[95]
rGO	GO coagulated by $CaCl_2$ and reduced by HI	11	501	410	[93]
rGO	wet spun LC-GO, then reduction	7.7	140	250	[99]
rGO	wet spun LC-GO, then reduction	29		25	[97]
rGO + Ag NW	solution spun GO + Ag nanowires then reduced	9.5	300	930	[110]
rGO	coagulated in CTAB solution and reduced in HI acid	8.7	182	35	[111]
rGO	large GO coagulated in NaOH ethanol solution and reduced with HI	12.8	360	320	[112]
rGO	wet spun from LC water dispersion then thermal reduction	25 (20 N/tex)	173 (0.13 N/tex)	294	[107]

[a] The reported values are normalised with respect to density.
[b] LC = liquid crystalline.
[c] rGO = reduced graphene oxide.

solubility of PANI in concentrated sulphuric acid has been exploited to prepare blends with PPTA, which is commercially processed into fibres with the same solvent (cf. Section 2). At a stoichiometry of 6:4 PANI:PPTA fibres with a Young's modulus of about 5 GPa and 10 S cm^{-1} could be prepared [85]. The choice of protonic acid (e.g. CSA and DBSA) permits to tune the solubility of the conducting PANI:counterion complex in both polar and apolar organic solvents, such as m-cresol and xylene. Cao et al. used this approach to prepare blends of PANI with e.g. poly(methyl methacrylate) (PMMA) and polyethylene (PE), reaching a conductivity of up to 10 S cm^{-1} [67]. Even a low loading of only 2 wt% of the PANI:CSA complex in PMMA and PE resulted in a conductivity of 1 S cm^{-1}, which suggests a co-continuous network [86].

A recent trend is the fabrication of electrically conducting elastomers through blending of a conducting polymer such as HBF_4-doped P3HT or PEDOT:PSS with a rubber phase composed of a styrene-isobutylene-styrene (SIBS) triblock copolymer or a PU [4,87,88]. For instance, Seyedin et al. prepared elastic fibres with PEDOT:PSS and a PU binder *via* wet spinning, which at 13% filler content displayed a low Young's modulus of about 20 MPa and an elongation at break of over 200% as well as an initial (i.e. before stretching) conductivity of about 10 S cm^{-1} [88]. It should be noted that the filler considerably decreased the elastic recovery to only about 65% at 50% strain. The here discussed conducting polymer blends comprising PU or PPTA represent the full spectrum of mechanical properties that can be achieved, i.e. the Young's modulus can be varied from 10 MPa to 5 GPa, while maintaining a ceiling electrical conductivity of about 10 S cm^{-1} (see Ashby plot in Fig. 1).

3.3. Fibre spinning of graphene and carbon nanotubes

CNTs display outstanding intrinsic properties such as a high tensile modulus and strength of up to 1 TPa and 63 GPa, respectively [90], as well as a charge carrier mobility as high as 10,000 $cm^2 V^{-1} s^{-1}$ [91]. Even higher numbers have been reported for graphene [48]. It has proven difficult to translate the exceptional intrinsic properties of individual CNTs or graphene sheets to macroscopic fibres. Carbon fibres, with their graphene nanoribbon structure, can display a very high Young's modulus and electrical conductivity of up to 8000 S cm^{-1} [27]. Fibres based on CNTs or graphene today reach similar values of more than 1000 S cm^{-1} [92,93]. Similar to conjugated polymer fibres, the Young's modulus and conductivity of CNT and carbon fibres show a positive correlation (see Ashby plot in Fig. 1). Macroscopic fibres have been prepared (1) solely with CNTs or graphene, (2) a majority fraction of the carbon material together with a minor component of a polymeric adhesive, and (3) nanocomposites where the CNTs or graphene are embedded in a polymer matrix (Table 4). According to Eqs. (1) and (2) high-performance fibres require the use of a nanomaterial with a high aspect ratio that must be well aligned along the fibre direction. For instance, Zhang et al. prepared fibres through pulling from CNT arrays that varied in height (= CNT length) and found that the tensile strength increases from 0.3 to 1.9 GPa when increasing the CNT length from 0.3 to 1 mm [54]. In addition, a strong lateral coupling between oriented CNTs is required as well as sufficient overlap so that electronic charge (and mechanical force) can easily pass between adjacent building blocks. CNTs have a round cross-section, which excludes close contact of aligned nanotubes over a large area. Motta et al. have argued that a flattened cross-section offers a larger contact area between neighbouring carbon nanotubes [94] (Fig. 13a). In contrast, sheets of graphene or graphene-oxide naturally offer a high contact area [95] (Fig. 13b,c).

A number of recent reviews summarise efforts to prepare conducting fibres with carbon nanomaterials [46–48]. Liu et al. pointed out that despite impressive recent progress, the considerable spread in mechanical and electrical properties continues to limit the practical scope of CNT fibres [46]. Zu et al. used Weibull statistics to analyse the tensile strength and Young's modulus of one type of CNT fibres and found less scatter than reported for e.g. commercial carbon and glass fibres [96]. Evidently, reproducible production of CNT fibres is feasible.

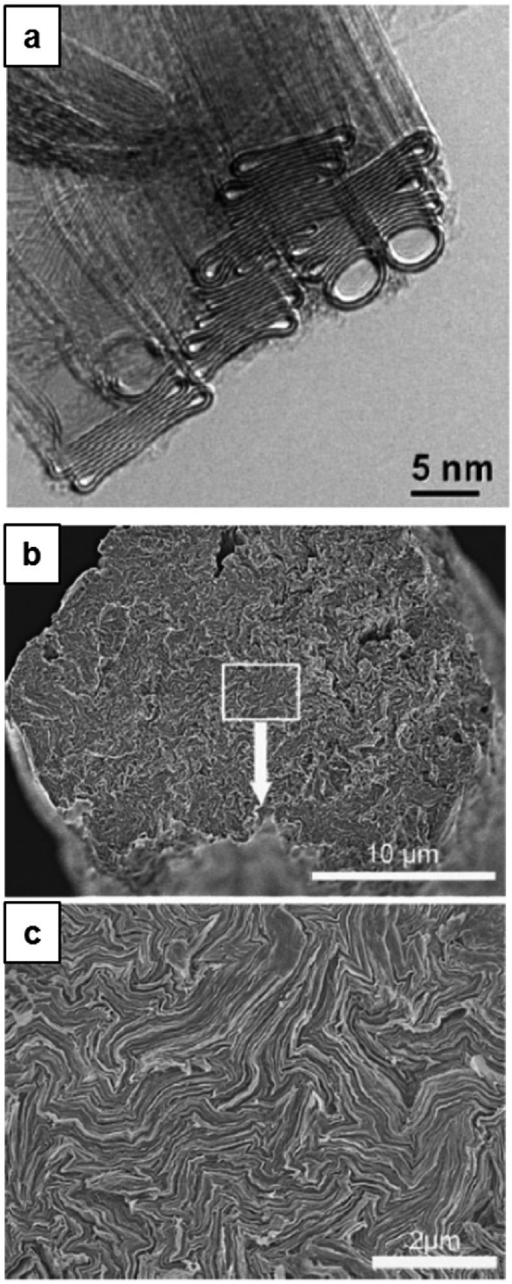

Fig. 13. (a) TEM image of the cross-section of a bundle of collapsed carbon nanotubes recorded close to the fibre fracture surface [94], (b, c) SEM images of the cross-section of a wet-spun GO fibre [95].
Reproduced with permission from Wiley.

As-synthesised powders of carbon materials are largely intractable because of the poor solubility and absence of a melt phase and, in the case of CNTs, a high degree of entanglement. While melt spinning is unfeasible (unless a polymeric binder is added; cf. Section 3.4), wet spinning has been accomplished. Ericson et al. demonstrated that a dispersion of single-walled carbon nanotubes (SWNTs) in a *superacid* of 102% sulfonic acid can be extruded into a water coagulation bath to produce continuous fibres with a Young's modulus of 120 GPa and electrical conductivity of 5000 S cm^{-1} [92]. The key to reaching a high degree of alignment through wet spinning is processing from a liquid-crystalline state, which facilitates a high degree of orientation of CNT bundles or graphene sheets [95,97–100]. For instance, Zhang et al.

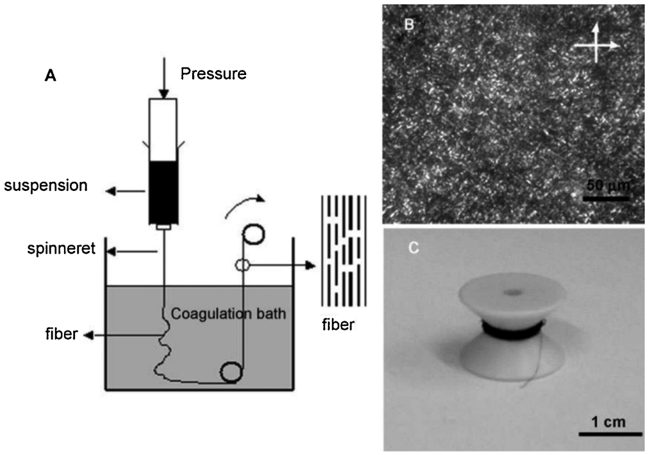

Fig. 14. (a) Schematic of the process used by Zhang et al. to spin fibres from liquid-crystalline solutions of multi-walled carbon nanotubes in ethylene glycol; (b) cross-polarised optical microscopy image of a liquid-crystalline solution, and (c) photograph of a three metre long fibre [100].
Reproduced with permission from Wiley.

were able to wet spin fibres from liquid-crystalline solutions of both multi-walled carbon nanotubes (MWNTs) and nitrogen-doped MWNTs in ethylene glycol (Fig. 14), reaching an electrical conductivity of 300 and 80 S cm^{-1}, respectively [100]. Spinning of CNTs can be carried out in the dry state by pulling fibres from free-standing, aligned arrays of CNTs [101,102] (Fig. 15). The work by Baughman et al. introduced a further concept to the literature of CNT fibres: twisting of the fibre to improve inter-tube mechanical coupling, which prevents slippage of nanotubes but does not affect the electrical conductivity [102,103]. This approach is conceptually similar to twisting of staple fibres to form a yarn (cf. Section 2.5).

The overlap of the nanofiller is critical for the formation of a continuous network that is able to transmit mechanical load. Electronic charge carriers travel fast along individual carbon nanotubes or graphene sheets but must jump to an adjacent nanofiller in order to continue their journey along the direction of the fibre without being trapped. Therefore, both the coupling strength and degree of overlap are critical for both a high degree of mechanical strength and electrical conductivity. The mechanical load transfer between CNTs can be enhanced through infiltration with a polymer [104,105]. Liu et al. have demonstrated that twisted yarns spun from aligned CNT arrays can be infiltrated with PVA, which yields a Young's modulus of more than 120 GPa while maintaining an electrical conductivity of 920 S cm^{-1} [104].

Notably, the yarn-like structure of CNT-fibres results in an outstanding 100% knot efficiency, i.e. the ratio of the tensile strength of a fibre with an overhand knot tied into it, to that of an unknotted fibre [106]. Polymer fibres in general display knot efficiencies below 100% and for carbon fibres the value is close to zero, making them challenging to use in textiles and textile processes. The high knot efficiency in CNT-fibres is presumably due to the low bending moduli of its constituents in combination with their high aspect ratio; a 100% knot efficiency is also observed for fibres spun from large-flake GO [107].

3.4. Polymer nanocomposite fibres

Polymer nanocomposites are an effective way to combine the superior electrical properties of conducting nanofillers with the attractive mechanical properties and ease of processing offered by commodity polymers. As a result, a large number of studies exist on CNT- and graphene-based nanocomposites, which aim to improve the electrical or thermal conductivity, achieve a reinforcement effect or modify the barrier properties of the matrix polymer [113–115]. Conducting composites find widespread commercial use, for instance carbon black is commonly used for plastic articles where antistatic properties are required [116]. Further, polymer/carbon black compounds are widely used for high-voltage applications such as power cables and cable joints [117]. Here graphene nanocomposites are increasingly considered [118].

The development of electrically conducting nanocomposite fibres is typically carried out with a top-down approach, in the sense that nanoparticles are added to otherwise familiar fibre spinning processes and materials (see Table 5). In the present literature, CNT is the preferred filler (Fig. 16), presumably because their 1D format (and related liquid-crystalline behaviour) makes them highly compatible with both the fibre shape and fibre processing (Figs. 14 and 15). Carbon black is also explored, and graphene to a lesser extent. The final macroscale properties of composite fibres will be dictated by a complex relationship of filler-matrix interactions, dispersion and distribution of the filler particles and the degree of orientation of both filler and polymer. Since carbon fillers have a strong reinforcing effect on any polymer matrix, the Young's modulus of nanocomposite fibres is typically found to be in excess of 1 GPa (see Ashby plot in Fig. 1). The electrical conductivity, however, can vary strongly because of the complex internal structure of nanocomposites, with highest values reaching 2.4 S cm^{-1} [119].

The large surface area of carbon nanoparticles gives rise to a high degree of attraction based on van der Waals forces and π-interactions (cf. Eq. (1)). This is an attractive feature for the fabrication of nanoparticle fibres, however in a composite it results in an unwanted tendency to form agglomerates. For a thermoplastic polymer matrix, melt compounding is the most commonly used mixing method as it is both fast and scalable. Here, the shear forces that arise during compounding will aid the dispersion and break up agglomerates [120]. To improve interactions with a polymer matrix, the chemically inert surface of carbon allotropes may be chemically modified by covalent or non-covalent functionalisation routes. The former method entails

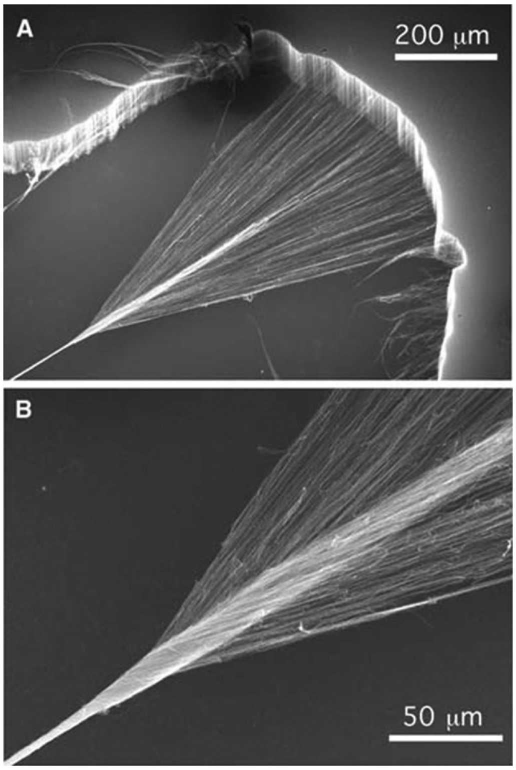

Fig. 15. SEM images, at two different magnifications, of a carbon nanotube yarn in the process of being simultaneously drawn and twisted during spinning from a nanotube forest.
From [102]. Reprinted with permission from AAAS.

introducing surface defects, and the latter may be realised by polymer wrapping i.e. adding a thin insulating polymer layer on the carbon surface. Both routes are likely to reduce the conductivity [121]. In a promising development, conjugated polymers display surfactant-like properties that aid dispersion of the nanofiller and can at the same time act as binder for the insulating polymer matrix [122–124]. As an example of covalent functionalisation towards conducting fibres, Jain et al. grafted poly(ether ketone) (PEK) onto CNTs by in-situ polymerisation, and manufactured composite fibres with up to 20 wt% CNT in a PEK matrix via air-gap wet-spinning [119]. The resulting fibres displayed a conductivity of up to 2.4 S cm^{-1} and an impressive tensile strength of 120 MPa.

For polymer nanocomposites, a percolation threshold as low as 0.1 wt % has been reported [113], corresponding to an aspect ratio of 100 [84] (cf. Eq. (4)). The relationship between filler geometry and conducting network formation in fibres has been studied by Seyedin et al., who prepared stretchable composite fibres by mixing nanofiller/solvent dispersions with a PU solution, followed by wet-spinning [125]. The percolation threshold was found to be about 2 wt% for CNTs, 10 wt% for graphene, and 17 wt% for carbon black. The tendency of the filler to form a network will also result in rheological percolation, which is accompanied by a transition from liquid-like to solid-like behaviour. This generally has a negative influence on the spinnability of the compound as the melt or solution will resist flow, and the accompanying loss of plasticity in the extruded jet hinders drawing. Rheological percolation is particularly well-studied for CNT-polymer compounds. Du et al. have shown that a relatively large inter-particle distance (equivalent to the diameter of a random coil) is sufficient to restrain large-scale polymer relaxation [126]. Hence, the onset of rheological percolation occurs at concentrations below that required for electrical percolation [113,120,126] (Fig. 17). As a practical consequence of this phenomenon, the filler content for melt spun fibres is generally below 10% (Fig. 16) whereas higher concentrations are achieved only in bicomponent systems [127,128]. Not surprisingly, the rheological percolation onset is highly dependent on the filler type; the spinnability of CNT compounds deteriorates at much lower loadings compared to graphene and carbon black based compounds [125,129]. Whether the spinning fluid is a melt or a solution, the loss in spinnability can to some extent be remedied by careful adjustment of the extrusion parameters. A low extrusion rate in combination with a long extrusion channel allows for molecular relaxation prior to extrusion, resulting in an increased draw-down ratio as well as an improvement in the final conductivity by up to two orders of magnitude [129–131]. An advantage of fibre spinning from solution instead of a melt, is that the final filler concentration may be an order of magnitude higher than the concentration in the spinning dope, making it possible to e.g. produce carbon black/cellulose fibres with a 50 wt% filler content by wet spinning [132]. The resulting conductivity of 0.6 S cm^{-1} was facilitated by effective wrapping of carbon black particles

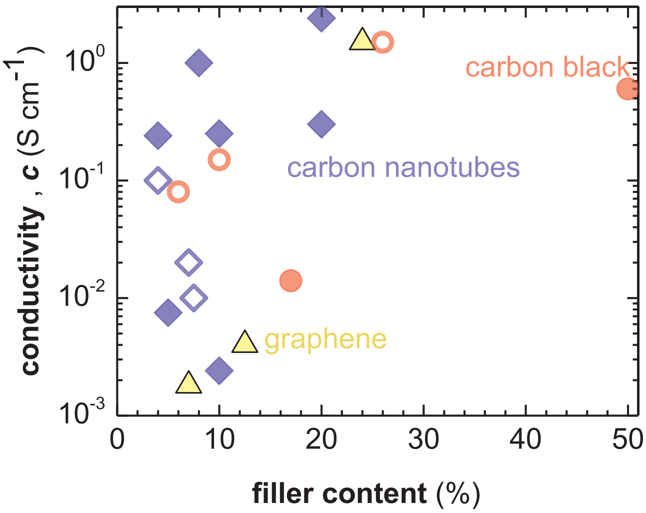

Fig. 16. Conductivity as a function of filler content reported for nanocomposites based on graphene (yellow triangles), carbon nanotubes (blue diamonds) and carbon black (red circles); fibres produced by melt or solution spinning (open and closed symbols); data from Refs. listed in Table 5. (For interpretation of the references to colour in this figure legend, the reader is referred to the web version of this article.)

Table 5
Properties of conducting fibres spun from carbon nanocomposites; Young's modulus *E*, tensile strength σ_s, electrical conductivity *c*.

filler	wt% filler	matrix, processing method	*E* (GPa)	σ_s (MPa)	c (S cm^{-1})	Ref.
FWNT	20	PEK, dry-jet wet-spun	17	122	2.4	[119]
FWNT	10	PEK, dry-jet wet-spun	7	190	0.25	[119]
SWNT	5	PU, wet spun	0.3	30	0.0075	[125]
carbon black	17	PU, wet spun	0.02	25	0.014	[125]
graphene	12.5	PU, wet spun	0.2	30	0.004	[125]
carbon black	26	PE, melt spun core/sheath fibre, annealed	130[b]	24[b]	1.5	[128]
carbon black	6	PP, melt spun			0.08	[129]
MWNT	4	PE, melt spun			0.1	[129]
carbon black	50	cellulose, wet spun	300[b]	8[b]	0.6	[132]
MWNT	3	cellulose, wet spun multifilament	7	117	0.09	[133]
MWNT	8	cellulose, wet spun monofilament	6	78	1	[133]
MWNT	10	cellulose, wet spun			0.0024	[131]
carbon black	10	PE, melt spun core/sheath fibre, annealed	180[b]	25[b]	0.15	[127]
CNT	7	PE/PP 60/40, melt extruded, drawn and annealed films	3	174	0.02	[138]
MWNT	20	PAN, wet spun & annealed	9	130	0.3	[140]
MWNT	7.5	PANI/PP 20/80, melt spun			0.01	[141]
MWNT	4	regenerated silk, wet spun			0.24	[142]
carbon black	9	PA 6, composite coating		30[b]	0.03	[143]
carbon black	10	PA 6, composite coating, washed 50 cycles		40[b]	0.1	[144]
rGO	7	PU, wet spun, annealed/thermally reduced	0.9	30	0.002	[145]
graphene	24	PLGA, wet spun	14	103	1.5	[146]
carbon fibres	15[a]	PP, melt spun	4.9	56	0.45	[147]
carbon fibres	10[a]	PP, melt spun	4.2	54	0.015	[147]

[a] Refers to vol%.

[b] Unit: cN/tex.

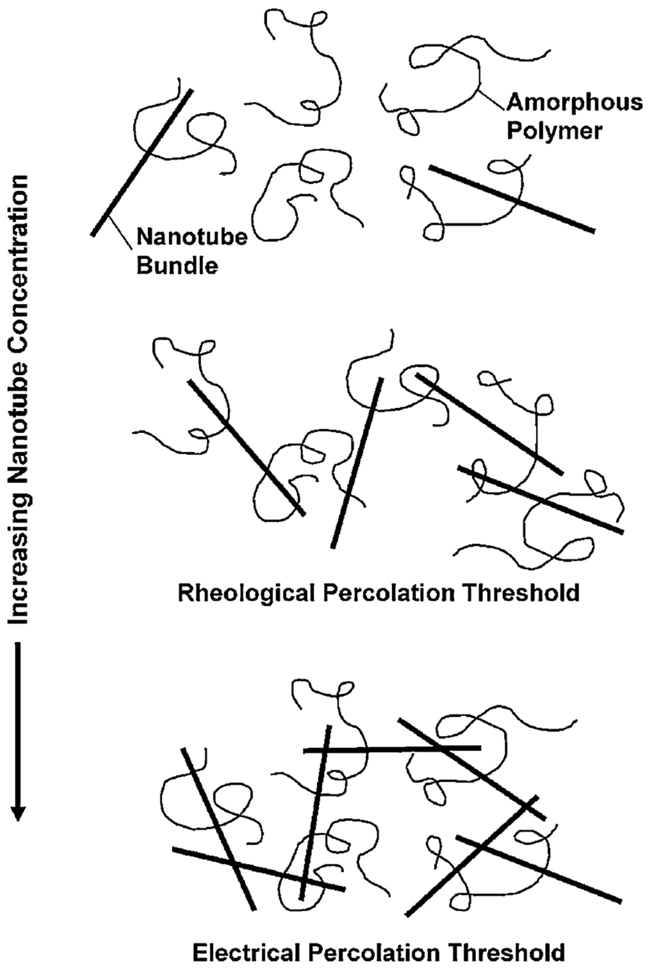

Fig. 17. Illustration of the rheological and electrical percolation threshold in a nanocomposite that consists of carbon nanotubes isotropically dispersed in a polymer matrix.
Reprinted with permission from [126]. Copyright (2004) American Chemical Society.

by the cellulose material during the spinning process. The use of a different solvent system allowed wet spinning of CNT/cellulose fibres with a final conductivity of 1 S cm^{-1} at 8 wt% CNT [133].

Drawing, both in the melt and in the solid state, is a crucial step in any fibre formation process. It is also detrimental to the conductivity in filled polymer fibres, especially at low filler loadings (Fig. 18a). Pötschke et al. have reported that a composite prepared with 2 wt% MWNTs in a polycarbonate (PC) matrix, which after melt mixing had a conductivity of 10^{-3} S cm^{-1}, displayed no measureable conductivity after melt spinning [134]. Electron microscopy revealed that the degree of CNT alignment parallel to the fibre axis increased with the take-up velocity, which disrupted the conducting network (Fig. 18b). The percolation threshold increases with nanoparticle alignment, and CNTs seem to be more sensitive to alignment compared to carbon black [129,134,135].

Annealing, i.e. reheating of the final composite fibre to a temperature exceeding T_m of the polymer matrix, has been found to increase the conductivity by up to several orders of magnitude [136,137]. Heating induces dynamic percolation as it relaxes the polymer chains, reduces their anisotropy and provides the filler particles with sufficient mobility to redistribute and, to a degree, re-aggregate into a conducting network [138,139]. In order to re-melt a fibre while maintaining structural integrity a bi-constituent structure, with at least one component that does not melt, is required. This can be realised through e.g. co-extrusion of core-sheath fibres (Fig. 19) or a polymer blend where the nanoparticles are confined to one of the phases (Fig. 20). The latter entails adding a

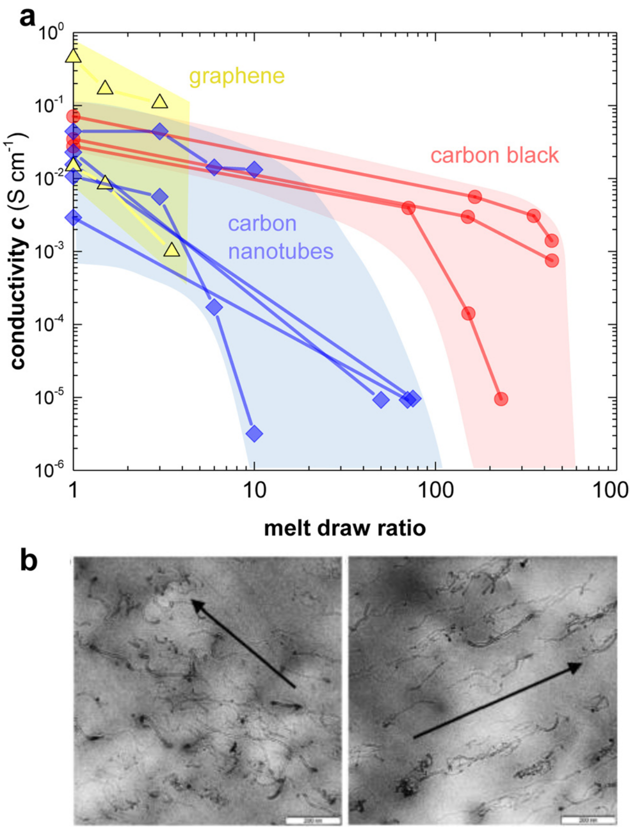

Fig. 18. (a) Conductivity as a function of melt draw ratio reported for nanocomposite fibres based on graphene (yellow triangles), carbon nanotubes (blue diamonds) and carbon black (red circles); data from Refs. [129,138,147]; (b) TEM images of a 2 wt% MWNT/PC composite after melt spinning at melt draw ratios of 8 (left) and 63 (right). Scale bar is 200 nm. (For interpretation of the references to colour in this figure legend, the reader is referred to the web version of this article.)
Reprinted from [134] with permission from Elsevier.

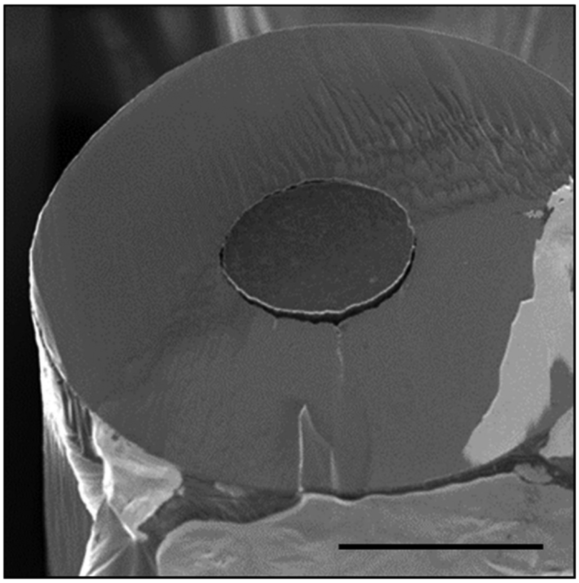

Fig. 19. SEM image of a core-shell bicomponent fibre with a conducting core of carbon black in a PE matrix, and an outer shell of the piezoelectric polymer PVDF. Scale bar is 20 μm.
Reprinted from [14] – Published by Springer Nature.

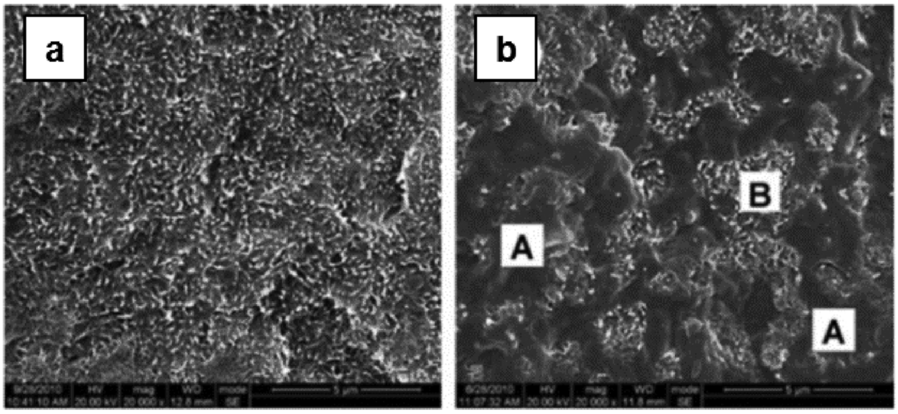

Fig. 20. SEM images of (a) a 7 wt% MWNT/PE composite and (b) the same composite forming a double percolated blend with PP at 50/50 PE/PP. Scale bar is 5 μm. Reproduced from [138] with permission of The Royal Society of Chemistry.

conductive filler to an immiscible polymer blend, and tailoring the composition to preferably locate the filler particles in one of the two polymers or at their interface. Consequently, to achieve sufficient electrical conductivity in the final composite, double percolation is required. Gao et al. studied a blend of PP and PE, with 3–7 wt% CNT located in the PE-phase, and observed a higher conductivity compared to the CNT/PE compound with the same overall CNT content [138]. After drawing, annealing close to the T_m of PE could restore the conductivity to 0.02 S cm^{-1}, similar to its pre-drawing value. The authors proposed a model for dynamic percolation, where time-dependence of the aggregate volume is combined with classical percolation theory.

3.5. Coating and dyeing of textile fibres and fabrics

The mechanical properties of a fibre can be guaranteed by using a

Table 6
Properties of conducting fibres and fabrics with functional coatings; Young's modulus E, sheet resistance R_s, electrical conductivity c.

conducting component/substrate, method	dopant/counterion	***E*** (GPa)	R_s (Ω/square)	c (S cm^{-1})	Ref.
CNT/spider silk, manual coating		0.6		12	[174]
PEDOT-S/silk fibre, dip-coating	-SO$_3$H group on side chain	8.2		0.044	[8]
PEDOT-S/spider silk fibre, dip-coating	-SO$_3$H group on side chain	5.9		0.0008	[149]
PEDOT:PSS/silk fibre, dip-coating	PSS	1.8		14	[20]
PEDOT:PSS/silk fibre, dip-coating	PSS	3.15		8.5	[175]
PEDOT:PSS/PA66 fabric, dip-coating	PSS	0.1		0.07	[150]
rGO/silk fibre, dip-coating				36	[151]
rGO/silk fabric, dip-coating		0.15	1500		[151]
SWNT/cotton fabric, dip-coating		1		0.0004	[176]
PEDOT:PSS/PET-PU fabric, dip-coating	PSS			2	[177]
PPy/PA fabric, in-situ polymerisation[a]	FeCl$_3$ + NSDA		117		[158]
PEDOT/PTT fabric, in-situ polymerisation	FeTos			0.36	[153]
PEDOT/silk fibre, in-situ polymerisation	APS			0.005	[154]
PPy/PET fabric, in-situ polymerisation	AQSA		1000		[178]
PPy/silk fibre, in-situ polymerisation	FeCl$_3$			0.4	[154]
PPy/PET fabric, in-situ polymerisation	AQSA		40		[163]
PPy/Lycra fabric, in-situ polymerisation	FeCl$_3$ + NDSA		600		[179]
PPy/PET fabric, in-situ polymerisation	AQSA		140	0.7[b]	[161]
PPy/wool fabric, in-situ polymerisation	AQSA		200		[161]
PPy/wool fibre, in-situ polymerisation	NDS		350		[159]
PPy/cotton fabric, in-situ polymerisation	DCSS		700	0.1[b]	[160]
PANI + PPy/PET fabric, in-situ polymerisation	AQSA		20	5[b]	[162]
PANI/silk fibre, in-situ polymerisation	APS			0.01	[154]
rGO + PANI/cotton fabric, in-situ polymerisation	APS/HCl			0.02	[164]
PEDOT/fabric from pineapple fibre, oCVD	FeCl$_3$		200	0.5[b]	[167]
PEDOT/viscose fibre, oCVD	FeCl$_3$			14	[165]
PEDOT/cotton fabric, oCVD	FeCl$_3$		370	32	[166]
PEDOT:PSS/PET fabric, direct coating	PSS		740		[169]
PEDOT:PSS/PET fabric, direct coating	PSS		13	8[b]	[170]
PEDOT:PSS/PVDF and PET fabrics, direct coating	PSS		57		[171]
PEDOT:PSS/PET fabric, direct coating	PSS		1.6		[172]
PEDOT:PSS/PET fabric, inkjet printing	PSS		3200	0.01[b]	[172]
PPy/PAN fabric, reactive inkjet printing	APS/HCl		80		[173]
PANI/fabric, reactive inkjet printing	APS/HCl		15	7[b]	[173]
PEDOT:PSS/PA fibre, *die*-coating	PSS		17		[180]

[a] In this table, "in-situ polymerisation" denotes chemical oxidative polymerisation carried out in solution. Reactive inkjet printing and oCVD are other methods for in-situ polymerisation.

[b] Assuming a 100 μm thick fabric.

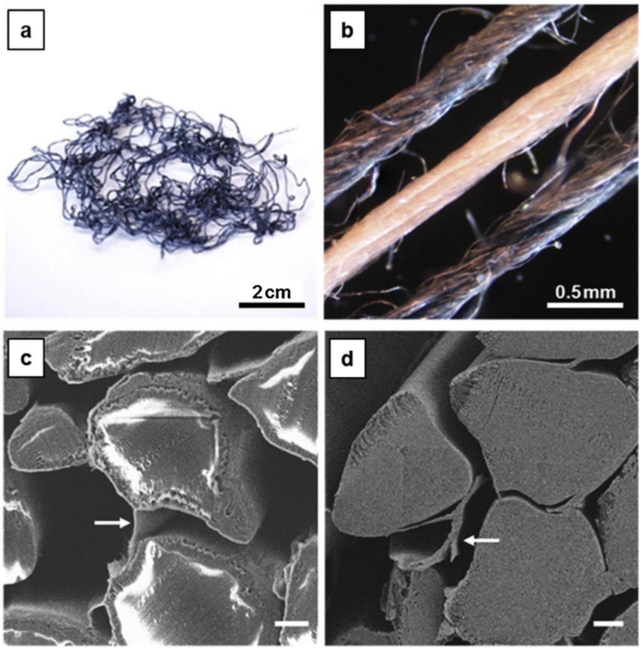

Fig. 21. (a) Bundle of a PEDOT:PSS dyed silk yarn and (b) optical microscopy image of neat and PEDOT:PSS dyed silk yarns; SEM images of freeze-fractured PEDOT:PSS dyed silk yarns recorded (c) before and (d) after sputtering yarns with gold; scale bars = 2 μm.
Reproduced from [20] − Published by the American Chemical Society.

mechanically robust, load-bearing core that is coated or dyed with an electrically conducting material. A commercial example are yarns with metal or carbon particles in the surface layer [148], but insulating fibres and fabrics can also be coated with a conducting polymer. A comparison of literature values indicates that coating and dyeing of commodity fibres results in conducting fibres that display a similar behaviour to those composed of polymer blends; in essence the mechanical and electrical properties are again decoupled (Table 6). As a result, coated or dyed fibres and yarns feature a wide spread in Young's modulus, whereas the conductivity again appears to be limited to a ceiling value of about 10 S cm^{-1} (see Ashby plot in Fig. 1).

The unpredictable, extensively textured surfaces of fabrics and yarns, displaying both pores and protrusions, make them challenging substrates. As with any textile meant for daily use, their functional coating is required to be stable against abrasion and repeated bending as well as chemical treatments. Dip-coating of fibres or textiles with conducting polymers − i.e. soaking the substrate in a polymer solution − is a common approach that can be carried out at virtually any scale and without specialised equipment[44]. Conjugated polymers can bind to natural fibres, which improves the adhesion. Examples include binding of the self-doped conjugated polyelectrolyte PEDOT-S (Fig. 9), or PEDOT:PSS to silk from the silkworm Bombyx mori or recombinant spider silk [8,20,149]. Strong electrostatic interactions, confirmed by the dependency on the pH of the dyeing bath (which changes the net charge of the protein fibre) of the dyeing efficiency, are reminiscent of commonly used acid dyes (see Section 2.7). The use of PEDOT:PSS formulation as a 'conducting acid dye' permits the fabrication of wash and wear resistant silk threads with a bulk electrical conductivity of up to 14 S cm^{-1} [20] (Fig. 21). For polyamides instead, adhesion may be improved by plasma-treatment prior to coating, resulting in conducting textiles that can function as heating elements [150]. In a different approach, Lu et al. dip-coated silk fibres with a graphene oxide solution, following a pre-treatment with bovine serum albumin (BSA) to introduce positive charges to the fibre surface. After hydrazine vapour reduction of the graphene oxide, the textiles retained their conductivity of up to 36 S cm^{-1} during bending and twisting [151].

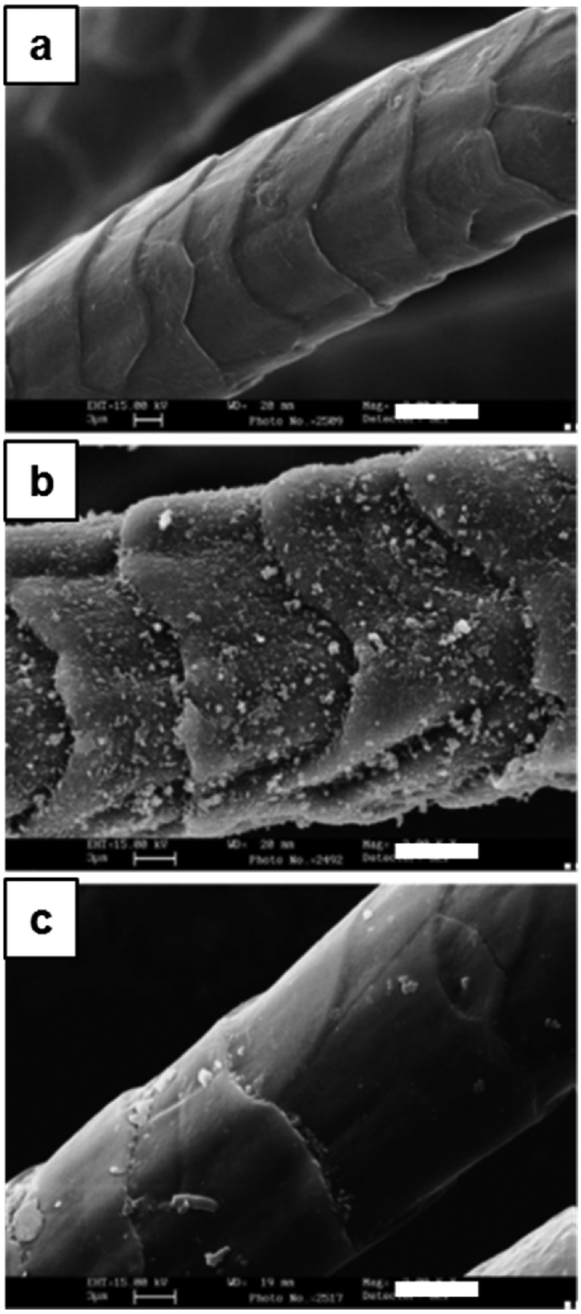

Fig. 22. SEM images of (a) a wool fibre; (b) a wool fibre coated with PPy by in-situ polymerization; (c) a PPy-coated fibre after yarn spinning and knitting processes. Scale bar is 6 μm.
Reprinted from [159] with permission from Elsevier.

Insulating fibres can also be functionalised with an intractable polymer such as PEDOT [152,153] or polypyrrole [154] through in-situ polymerisation on the surface of the fibre, as first demonstrated by Kuhn et al. [155,156]. A common method is chemical oxidative polymerisation where the fibre or fabric is soaked in a solution containing monomer (dominantly pyrrole), dopant and oxidant. Already in the early 1990's, polypyrrole coated polyester fabrics were produced commercially by this method [157,158]. The combination of polymer synthesis and deposition can result in the formation of aggregates and therefore a non-uniform coating (Fig. 22a,b). The aggregates consisting of excess polymer can be readily removed by rubbing or washing, leaving a thin, conformal and conducting coating [159] (Fig. 22c). This method requires interactions between all the components in the

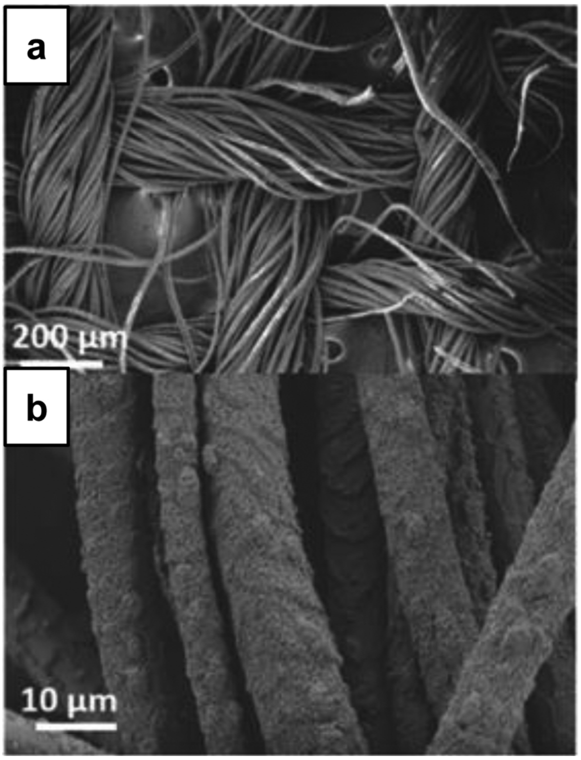

Fig. 23. SEM images after oCVD coating with PEDOT of (a) a wool fabric and (b) wool fibres.
Reprinted from [167] with permission from Wiley.

solution and for example the doping agent, most commonly organic sulphates, will not only act as a dopant/counterion but is also instrumental to the synthesis and deposition on the substrate. Varesano et al. compared the efficacy of 11 compounds to dope polypyrrole polymerised on a cotton fabric, and showed that dicyclohexyl sulfosuccinate sodium salt (DCSS) resulted in a fabric with the lowest sheet resistance below 1 kΩ/square (i.e. 0.1 S cm^{-1} assuming a 100 µm thick fabric), whereas several other dopants prevented film formation altogether [160]. Generally, using synthetic fibre substrates (PET or PA fabrics) with this method has resulted in lower sheet resistances of between 20 and 140 Ω/square [158,161–163] (i.e. 0.7–5 S cm^{-1} assuming a 100 µm thick fabric). Natural fibres present other advantages though, for example degummed silk is biocompatible and therefore attractive as a base fibre for conducting biomaterials. Xia and Lu compared in-situ polymerisation of PPy, PANI and PEDOT on silk fibres, and found that the PPy-coated fibres had the highest conductivity of 0.4 S cm^{-1} as well as the highest rubbing fastness, presumably as a result of hydrogen bonds and electrostatic interactions. The fibres could be washed in water 20 times with only a 10% decrease in conductivity [154]. In a novel approach, Tang et al. deposited graphene oxide nanosheets on a cotton fabric prior to in-situ polymerisation of aniline on the fibre surface [164]. The resulting fibres had a conductivity of 0.02 S cm^{-1}. By comparison, PANI functionalised cotton without graphene oxide had a conductivity of less than 10^{-3} S cm^{-1}.

In case of oxidative chemical vapour deposition (oCVD), a vapour that carries the monomer and oxidant are directed to mix in a reaction zone along the surface of the substrate. This results in a conformal coating that preserves the original surface over multiple length scales (Fig. 23). Polymerisation of PEDOT from the vapour phase has been demonstrated on viscose fibres [165], as well as on a range of commercial fabrics from both synthetic and natural fibres resulting in conducting fabrics with a surface resistivity down to 200 Ω/square [166–168] (i.e. 0.5 S cm^{-1} assuming a 100 µm thick fabric). This method can result in durable coatings that can withstand stretching, abrasion and manual laundry [166,167]. The fact that oCVD is readily combined with masks/stencils − Kovacik et al. [166] went on to print a conducting pattern on a T-shirt − promises interesting developments towards textile based electronic circuitry.

A common industrial method for applying coatings and patterns to fabrics is direct coating, wherein a coating paste is poured directly onto the fabric to be spread evenly by a knife or blade. Direct coating can be combined with a stencil or masked screen in order to print patterns [34]. This method requires strict control over the viscosity of the coating paste, which may well result in a trade-off with other properties such as conductivity. Åkerfeldt et al. used a blend of a PEDOT:PSS water dispersion, ethylene glycol and a PU-based binder, and studied a broad range of compositions with 1–3% PEDOT:PSS required for electrical percolation [169]. Aside from adding conductivity – down to 13 Ω/square (i.e. 8 S cm^{-1} assuming a 100 µm thick fabric) – the relatively thick coating will have an impact on both the appearance (Fig. 24) and the mechanical properties (rigidity) of the fabric [170]. Although, the addition of ethylene glycol has a positive effect on the mechanical properties since it acts as a plasticiser. This formulation was successfully used for screen-printing of a stretchable and washable conducting pattern on a knitted glove [171].

A recent development with regard to dyeing and finishing of fabrics is the use of ink-jet printing, which may be used to functionalise large

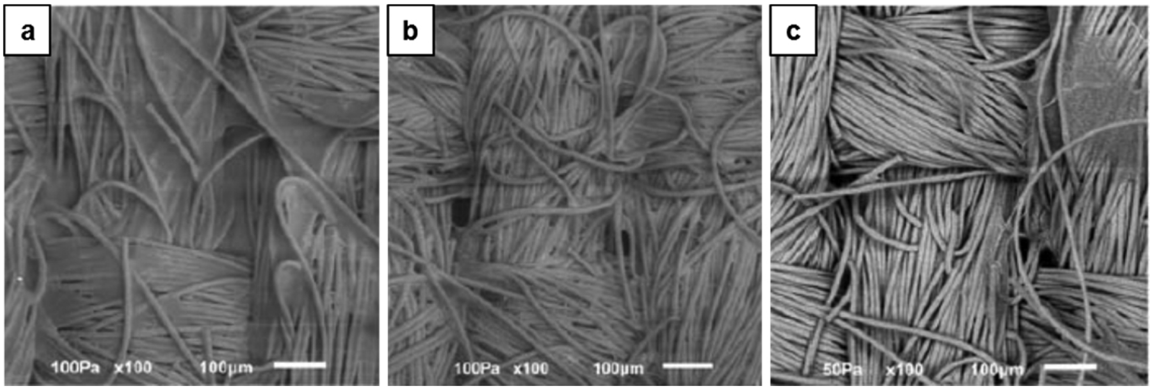

Fig. 24. SEM images of a PET fabric direct-coated with a PU-based blend containing (a) 40 wt% PEDOT:PSS, resistance 44 kΩ/square; (b) 60 wt% PEDOT:PSS, resistance 130 Ω/square; (c) 80 wt% PEDOT:PSS, resistance 13 Ω/square.
From [170], copyright (2013) by Åkerfeldt, Strååt and Walkenström. Reprinted by Permission of SAGE Publications, Ltd.

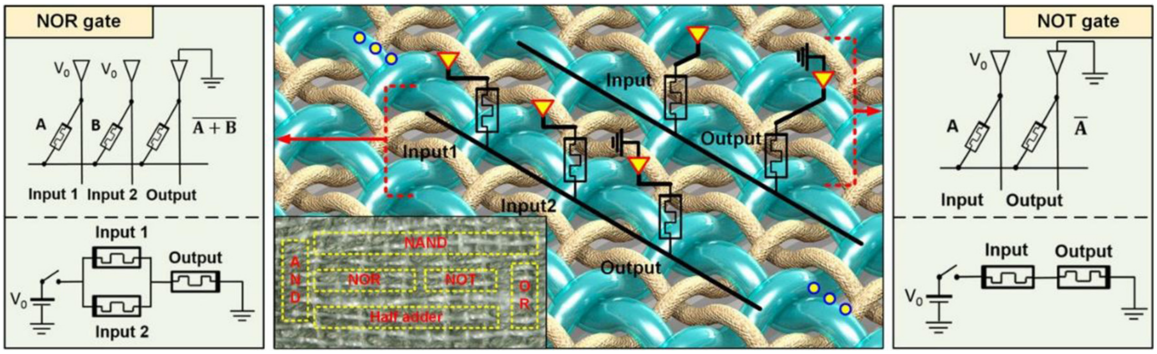

Fig. 25. A woven logic device and its circuit schematic.
Reprinted with permission from [193]. Copyright (2017) American Chemical Society.

surfaces as well as for printing of intricate patterns. This method minimises the amount of material required, as functional or colouring inks are applied in tiny amounts at exact positions on the fabric surface. PEDOT:PSS and diethylene glycol, diluted by ethanol, can be ink-jet printed to form a conducting coating with a sheet resistance of 3.2 kΩ/sq [172] (i.e. about 10^{-2} S cm^{-1} assuming a 100 μm thick fabric). The same ink was used to produce a conducting pattern by a simple sponge stencil method, which lowered the sheet resistance by three orders of magnitude. The difference was attributed to the difficulty in depositing (ink-jet printing) a thin yet continuous film on the textile substrate. Nonetheless, Stempien et al. were able to ink-jet print a conducting layer on a fabric with a surface resistivity as low as 15 Ω/sq (i.e. 7 S cm^{-1} assuming a 100 μm thick fabric), using an innovative "reactive ink-jet printing" method wherein aqueous solutions of monomer and oxidant where printed in parallel from two separate printheads [173].

3.6. Multilayer coatings of fibres and fabrics

Many electronic devices from solar cells and light emitting diodes (LEDs) to transistors consist of multi-layer stacks of insulating, semiconducting and conducting materials. A key paradigm within the field of organic electronics is the deposition of these layers from solution or vapour onto typically flat substrates, which combined with patterning tools can give rise to intricate arrays of electronic devices and circuits. In its simplest form textiles, possibly passivated with a smoothing layer to provide a flat surface, can be used as substrates for the full plethora of organic opto-electronic devices, based on both organic semiconductors and carbon materials (CNTs and graphene). The printing and coating techniques discussed in Section 3.5 can be readily used as patterning tools. In a similar fashion, a fibre can be regarded as a cylindrical substrate where multiple concentric layers of insulators, semiconductors and conductors can be stacked on top of each other to form complete electronic devices (see Section 4). A continuous multilayer coating can then be regarded as one elongated device (suitable for e.g. solar cells and LEDs), whereas patterns such as periodic and interrupted coatings can be introduced to build more than one device on the same fibre (see Section 4). Multilayer coatings can be applied via the techniques discussed in Section 3.5.

Another possibility are multimaterial fibres fabricated by thermal drawing of macroscale cylinders, composed of concentric stacks of functional materials. As pioneered by Fink et al. [181] this fabrication method, originally developed for optical fibres, has evolved into a versatile method that allows for a combination of (inorganic) semiconductor, polymer insulator and metal in one preform resulting in e.g. a micrometer-thick optoelectronic fibre [182]. The technology has since been applied to piezoelectric polymer fibres [183], graphite/polymer composite-based neural probes [184] and pressure-sensing micro-electromechanical systems- (MEMS-) fibres with a carbon black/polymer composite as its active component [185].

4. Architectures of electronic textiles

Conducting fibres and yarns, which are the focus of this review, can be used to construct simple building blocks. They can be incorporated as a warp or weft line in a weave (Fig. 6), as a wale or a course in a knitted fabric (Fig. 6), or by embroidery or other types of stitching into a base fabric. Conducting lines can then be used as interconnects to shuttle electrical energy or electrical communication signals within a circuit. Based on a variety of geometries, they can constitute passive circuit elements i.e. *resistors*, *capacitors* and *inductors* in an electronic circuit. If combined with a thin "active layer" such as a dielectric, an electrolyte, a semiconductor, conducting fibres and yarns can also be used to build advanced components such as capacitors and supercapacitors, batteries, diodes (e.g. solar cells, LEDs), transistors, actuators, valves for microfluidics etc. There are many ways to create this layered architecture in textiles: (1) at the yarn level by working with core-shell fibres where an inner core and outer shell sandwich an intermediate active layer, (2) at the yarn level by intertwining fibres and filaments, (3) at the fabric level by combining several neighbouring woven or knitted fibrous elements, and (4) at the garment level by laminating or printing several layers on a fabric or by placing textile swatches on top of each other.

The aim of this chapter is to outline some of the unique architectures that can be realised by integrating conducting fibres into textiles, which we illustrate with selected examples. We do not intend to provide a comprehensive overview of the e-textile literature, and instead refer the reader to a series of excellent reviews that have been written on the topic, covering areas such as energy storage and harvesting, medical applications, sensing and more [3,11,24,186–190].

4.1. Integration of conducting fibres on vs. in textiles

Electrical functionality can be added to textiles in two ways: i) *integration on*, and ii) *integration in* [191]. *Integration on* means that the functional components are physically placed on the textile – which is typically in the form of a fabric – that then functions as a carrier substrate or platform. Such top-down integration can be achieved for example through embroidery of conventional cables, electronic components and entire circuit boards onto the textile. As a result, the electronic functionality is merely an add-on to the textile, which provides the mechanical integrity. The *integration on* approach can be advantageous as means to incorporate delicate and inherently stiff components into wearable and flexible devices. Another benefit is the relative ease by which components can be separated after use, providing a feasible recycling strategy for e-textiles (cf. Section 5).

Integration in, on the other hand, means that new electronic functions and systems are achieved by combining electrically or electronically active fibres or yarns in a textile *architecture* [192]. The *integration in* approach can be thought of as a means to produce electronics by additive manufacturing. One by one a thread is added to another, which then collectively form a textile architecture with electronic circuit functionality. One example is a distributed network of woven conducting yarns combined with dielectric-coated conductors (Fig. 25), used as a two-dimensional resistive memory where each junction is individually addressable [193]. The remainder of this chapter will focus on the *integration in* approach, which we argue opens up the possibility to create unique, and highly complex circuitry.

4.2. Comparison of woven and knitted architectures

We recognise from Section 2 that the two major fabric forming methods of weaving and knitting present different opportunities but also shortcomings. For weaving, each yarn both in the warp and weft direction can be unique. Consequently, every crossing or junction can be addressed uniquely through one yarn in weft and one yarn in the warp direction. This creates a basis for an active or passive matrix electronic architecture. The junctions can be designed to either be in physical electrical contact or to be separated and insulating, depending on the structure of the weave and/or choice of yarn and any potential insulating shell on these. Aside from the *crimp* (i.e. the yarns form or bend around one another at the intersections) the weaving process as such does not introduce strong bending in the yarns, and relatively stiff fibres can be used to form highly conducting fabrics. Even the stiff and brittle carbon fibres can be woven, although this is preferably carried out with the fibres in preformed bands to further minimise the degree of crimp. According to Fig. 1, highly conducting fibres also display a high inherent stiffness – these fibres can be readily incorporated in woven textiles. A potential shortcoming with woven architectures of stiff fibres is that the resulting textile is non-stretchable, unless an elastic yarn is added.

Instead, for knitted textiles stretchability is an inherent characteristic, which stems from the movement of the yarns and loops relative to each other rather than from the stretchability of the fibres themselves. Both, a uniaxial and biaxial stretching response is possible. This enables a tight fit to the human body in case of knits for garments. In a knit the stiff, and therefore more conductive, fibres and yarns (cf. Fig. 1) can be combined together with standard textile yarns to achieve an overall pliable fabric. Most high-performance fibres as well as pure metal fibres can be machine-knitted, after adjustment of the processing parameters. Knitting of carbon fibres, which are inherently sensitive to bending (cf. Section 3.3), is also doable using specialty yarns [194].

The difference in inherent rigidity in these two types of fabric can be exploited e.g. to tailor the performance of textile muscles or "textuators" [195]. The great mobility of the knitted architecture results in an amplified strain in the fabric compared to the strain produced by the individual fibres. The woven architecture instead, displays a large number of straight fibres running in parallel resulting in an amplified force compared to that exerted by the individual fibres (Fig. 26).

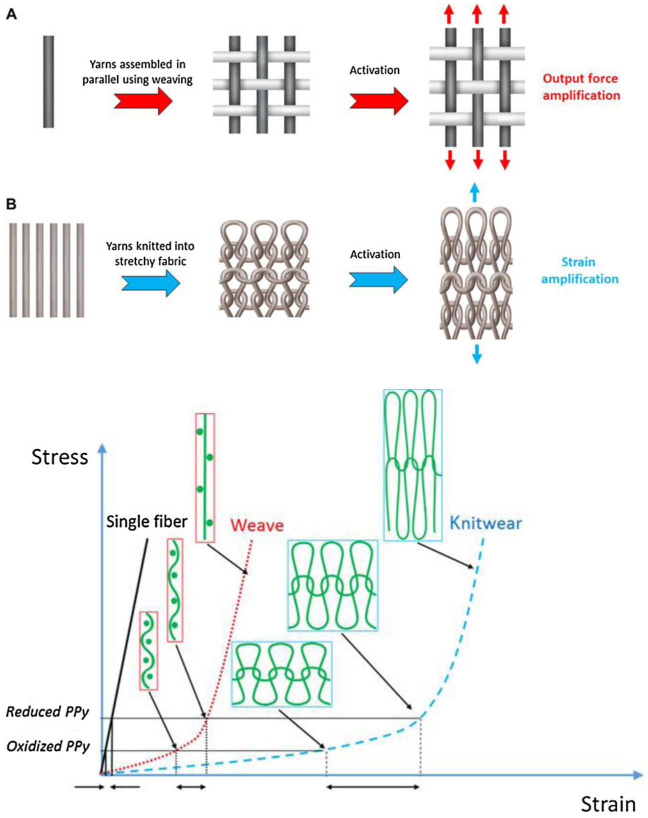

Fig. 26. Top: Schematic of artificial muscles, "textuators", produced by (a) weaving and (b) knitting of PPy-coated fibres. Bottom: Schematic stress-strain curves of textuator fibres and of fabrics woven and knitted thereof.
Reprinted from [195] – Published by AAAS.

4.3. Static and dynamic mode

E-textiles obtain their functionality through the combination of conducting and non-conducting yarns, which can be arranged in a number of basic building blocks outlined below combined to realise more complex designs [192,196]. Any building block can be used in a fixed position and with a fixed dimension, which we refer to as *static* mode. As an example, PEDOT:PSS-dyed silk fibres can be used as interconnects, which also constitute current-limiting resistors between a battery and an LED [20] (Fig. 27a). Conversely, the inherent pliability of textiles can be exploited to produce devices where the position and/or geometry of the building blocks is allowed to change, which we refer to as *dynamic* mode; for instance, Seyedin et al. demonstrated knitted strain sensors from PEDOT:PSS/PU blend fibres [4] (Fig. 27b).

4.4. The resistor and resistive sensing

Conducting fibres and yarns can be regarded as a *resistor* in an electronic circuit, but also as a sensor-type device. Sensing functionality can then be achieved in the *dynamic mode* by measuring changes in the resistance R:

$$R = \rho\frac{l}{A} \tag{5}$$

where $\rho = c^{-1}$ is the resistivity, l the length of the element, and A its cross-sectional area. The resistance variation as a result of dimensional change, sometimes termed *piezoresistivity*, is widely characterised in conducting fibres and yarns as it points to potential applications as strain gauges [87,88,125,133,144,197–199] or pressure sensors [200]. The effect may be enhanced by the fabrication of highly stretchable knitted textiles, where the change in resistance due to deformation (cf. Eq. (5)) is amplified by a change in contact resistance between fibres [4,201–203]. In a further development, garment based computer-human interfaces are presented where, in combination with non-trivial data management, the wearer's movements can be monitored. For instance, Tognetti et al. used a conducting textile coating to realise a stretchable conducting circuit comprising both strain sensors (narrow printed lines) and conducting interconnections (wide printed lines) [204] (Fig. 28a). Eom et al. used PEDOT-coated polyester yarns as strain sensors in a glove, to communicate with a computer software [152] (Fig. 28b).

For some applications, it is necessary to render selected larger areas of a fabric conducting, resulting in a conducting panel type architecture. Conducting panels can be produced by selectively coating or dyeing parts of a pre-formed fabric, or by tightly weaving/knitting several conducting threads so that they are in close electrical contact [205]. The latter leads to a porous conducting textile, which enables breathability for wearables, and provides a large surface area. The panel architecture is particularly useful to realise electrodes – or

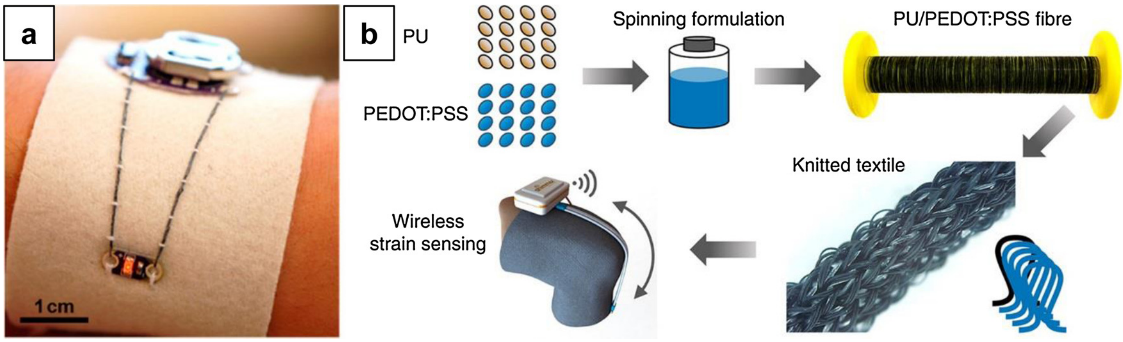

Fig. 27. Examples of static and dynamic mode e-textiles: (a) a wearable LED powered *via* conducting PEDOT:PSS-dyed silk threads. Reproduced from [20] − Published by the American Chemical Society. (b) A strain sensor knitted from blend fibres comprising PEDOT:PSS in a PU matrix. Reprinted with permission from [4]. Copyright (2015) American Chemical Society.

textrodes – e.g. for electrocardiography (ECG) [206–211] (Fig. 29). Conducting panels can also be used as heating elements [140]. The heating rate is given by the power P that is generated due to Joule heating:

$$P = RI^2 \tag{6}$$

where I is the current running through the conductor of resistance R. Such heating elements can be used in climate control elements, e.g. in car seats but also in garments [150,212–214] or in combination with thermochromic inks for visual effects [215,216] (Fig. 30).

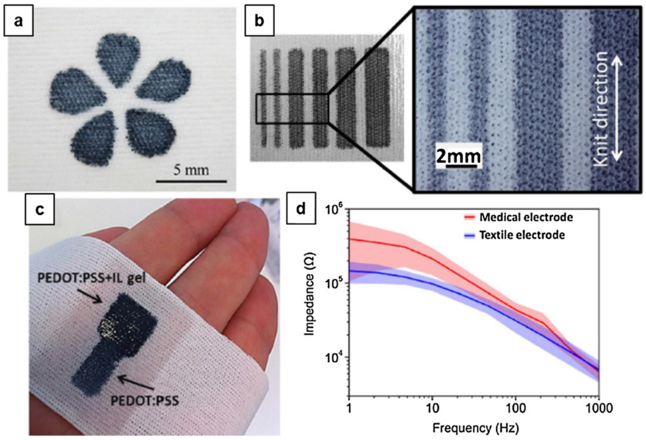

Fig. 29. (a) A stencil print of PEDOT:PSS onto a knitted fabric provides (b) a pattern which is stretchable in the knit direction. (c) With a second layer of ionic liquid (IL) gel, the print functions as a textile ECG-electrode with (d) an impedance spectra comparable to or lower than that of a standard medical electrode.
Reproduced from [210] − Published by Springer Nature.

4.5. *The capacitor and capacitive sensing*

Capacitors are fundamental building blocks of electronic circuitry, consisting of two electrodes that sandwich an insulating dielectric. In a general sense, two conductive elements placed adjacent to each other form a capacitor-type architecture. For a parallel plate capacitor, the capacitance C is given by:

$$C = \varepsilon_r \varepsilon_0 \frac{A}{d} \tag{7}$$

where d is the distance between electrodes of area A, ε_r is the relative permittivity of the dielectric, and ε_0 is the permittivity of vacuum. Capacitors introduce time-dependence and oscillatory electrical behaviour. In the *dynamic mode*, a change in geometry induces a measureable change in capacitance, which can be used for sensing. As can be deduced from Eq. (7), at least four sensor modes are available: (1) the absence/presence of a counter-electrode, e.g. a human finger, (2) an increase or decrease in distance between electrodes, giving rise to a

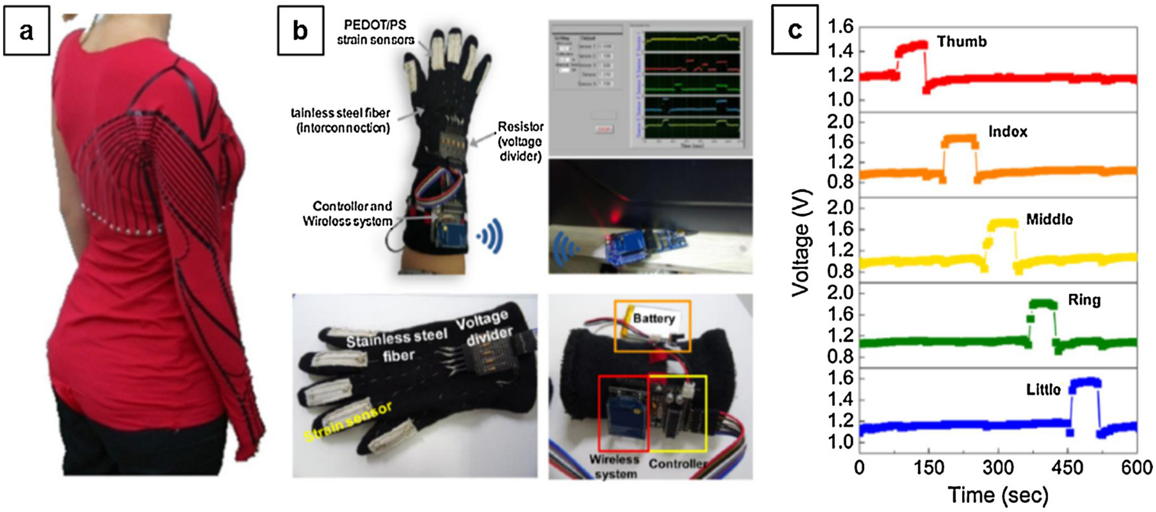

Fig. 28. Garment based computer-human interfaces: (a) a motion sensitive garment with a printed piezoresistive pattern. Reproduced from [204] − Published by BioMed Central Ltd. (b) a glove sensitised by PEDOT-coated fibres providing (c) individual electrical signals from finger movements.
Reprinted with permission from [152]. Copyright (2017) American Chemical Society.

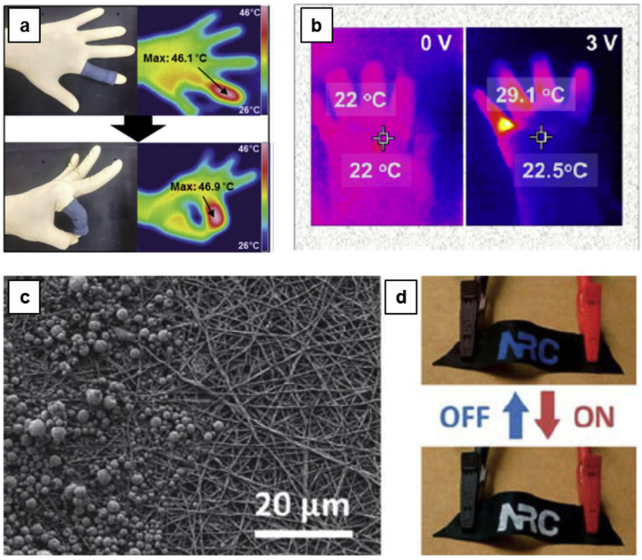

Fig. 30. Joule-heating in (a) a piece of cloth dip-coated in SDS-modified PEDOT:PSS (Reproduced from [213] – Published by the The Royal Society of Chemistry) and (b) a fabric oCVD-coated with PEDOT (Reprinted with permission from [214]. Copyright (2017) American Chemical Society). (c) PEDOT nanofibers combined with thermochromic microcapsules allow to use Joule-heating for (d) dynamic colouring.
Reproduced from [215] with permission of The Royal Society of Chemistry.

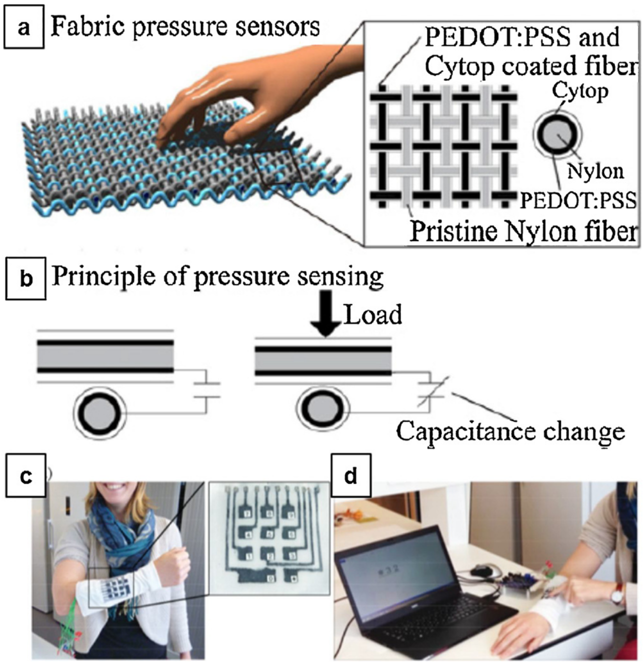

Fig. 31. Capacitive pressure sensors. (a) A woven capacitive pressure sensor comprised of (b) multi-layer (Cytop and PEDOT:PSS) die-coated fibres (Reprinted from [180] with permission from Elsevier). (c,d) A wearable keyboard of a multi-layer (PDMS and PEDOT:PSS) print on a textile.
Reproduced from [2] with permission from Wiley.

stretch or pressure sensor, (3) changes in the overlap and hence area, and (4) changes in relative permittivity. In particular, the first two modes have been explored in the textile format. Many designs are feasible, ranging from two conducting sheets of fabric that form a plate-like capacitor with air as the dielectric medium [217], to fibres with a core-shell architecture where an intermediate insulating layer separates the conducting core and shell [180,218] (Fig. 31a,b). Weaving of such fibres can be used to fabricate pressure-sensitive capacitive sensor arrays with a resolution defined by the distance between the yarns in the weave. By constructing x-y addressable sensors at each crossing, the fabric detects both pressure and its position on the fabric [180]. Weaving may also be employed to produce meter-scale textile capacitive sensors [219]. Using print instead, Takamatsu et al. designed conformal textile keyboards by first creating conducting patterns on a knitted and hence stretchable fabric by selectively coating with PEDOT:PSS, followed by application of a polydimethylsiloxane (PDMS) insulation layer [2] (Fig. 31c). Capacitive sensing with this PEDOT:PSS/PDMS structure is then possible where a human finger is placed on a key to form the counter electrode.

In a related case, the dielectric may be comprised of a ferroelectric and polarised polymer resulting in a piezoelectric textile. After addition of an outer electrode in the form of a conducting coating or conducting yarns, deformation of this type of textile generates a transient voltage signal that can be read out as a sensory signal or be utilised for energy harvesting [14,171,220,221] (cf. Section 4.9).

A curious function that can be realised by combining capacitive functions with textiles is electrowetting. In textile-based electrowetting, a conductive textile is coated with a thin layer of a hydrophobic dielectric. When liquid is placed on top of the hydrophobic textile, it cannot penetrate the pores of the textile. The application of a voltage between the liquid and the conductive core of the textile – which form a dynamic capacitive double layer – allows control of the contact angle between the liquid and the textile. This results in selective penetration of liquids through the textile; the textile functions as an electrical "valve" for liquids. Electrowetting textiles are still very new and unexplored, but may find application areas in Lab on chips or in wearable e-textiles that require control of liquids e.g. sweat [222].

4.6. The induction coil and inductive sensing

To introduce electromagnetic effects such as induction, conducting coils, spirals and helices are needed. Coil shaped elements can be realised over several length scales both as cylindrical structures and as in-plane coils on a textile substrate. This type of architecture enables "contactless electrodes" for signal transfer and wireless charging, where e.g. two separate textiles carry a primary and secondary coil, respectively, that mutually induce a current when placed in close proximity [206]. The inductive coil may also be used for motion sensing, either (1) by detecting the changes in self-inductance due strain-induced variations of coil dimensions, or (2) by detecting changes in the mutual induction between two coils due to their relative displacements. Wijesiriwardana reported a knitted garment with helical inclusions of conductive yarns around the chest and arms. These textile inductors could both detect respiration rate by strain sensing, and detect movement of the arm by displacement monitoring [223] (Fig. 32). Moreover, many antennae designs require complex coil shaped architectures [10,196,224,225] (Fig. 33).

4.7. Data storage

The memristor – sometimes called the fourth passive element – is a device that can be electrically switched between a highly conductive 'on'-state and a low conductive 'off'-state, making it highly useful for non-volatile memory applications [226]. Similar to the pressure sensor array architecture presented in Section 4.5, weaving of multi-layered fibres is a convenient method for producing large scale memory arrays where each junction between functionalised warp and weft yarns can constitute an individually addressable data storage component. Here, the multi-layered fibres are typically comprised of a conducting electrode layer coated by the active – resistive switching – material. Such fibres may be fully carbon-based with an MWNT-fibre core and GO as the active material [227]. Alternatively, washable woven textile memories can be fabricated from cotton fibres coated with aluminium,

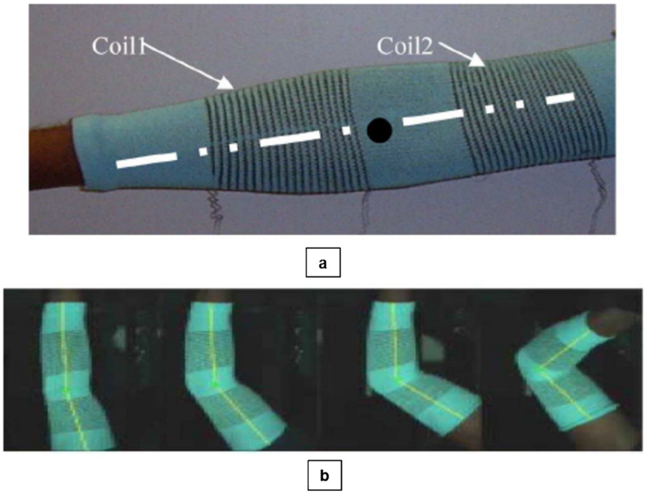

Fig. 32. Knitted inductive coil sensors. Images are © (2006) IEEE.
Reprinted, with permission, from [223].

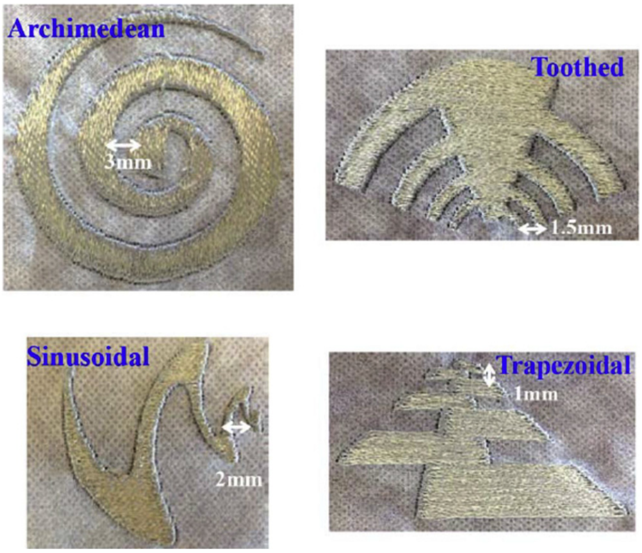

Fig. 33. Textile antennae – embroidery of conducting threads allows for flexible patterns of almost any shape. Images are © (2014) IEEE.
Reprinted, with permission, from [224].

where the switching component is developed by the natural formation of a thin Al_2O_3 layer on the aluminium [9]. Bae et al. [193] also used cotton yarns as the starting material; these were dip-coated with aluminium followed by oCVD (cf. Section 3.5) of poly(ethylene glycol dimethacrylate) (pEGDMA) as the active component. Combined with uncoated cotton yarns for selective insulation, these yarns formed a wearable woven architecture, which retained functionality after laundry in a commercial washing machine with detergent. The mechanism of resistive switching in this case is shown to result from local pyrolysis of the pEGDMA layer due to Joule heating (cf. Eq. (6)). The effect of pyrolysis could be reversed by a 'reset' voltage exceeding the 'set' voltage. This architecture could be used to realise logic-in-memory devices including basic Boolean functions and a half adder (Fig. 25).

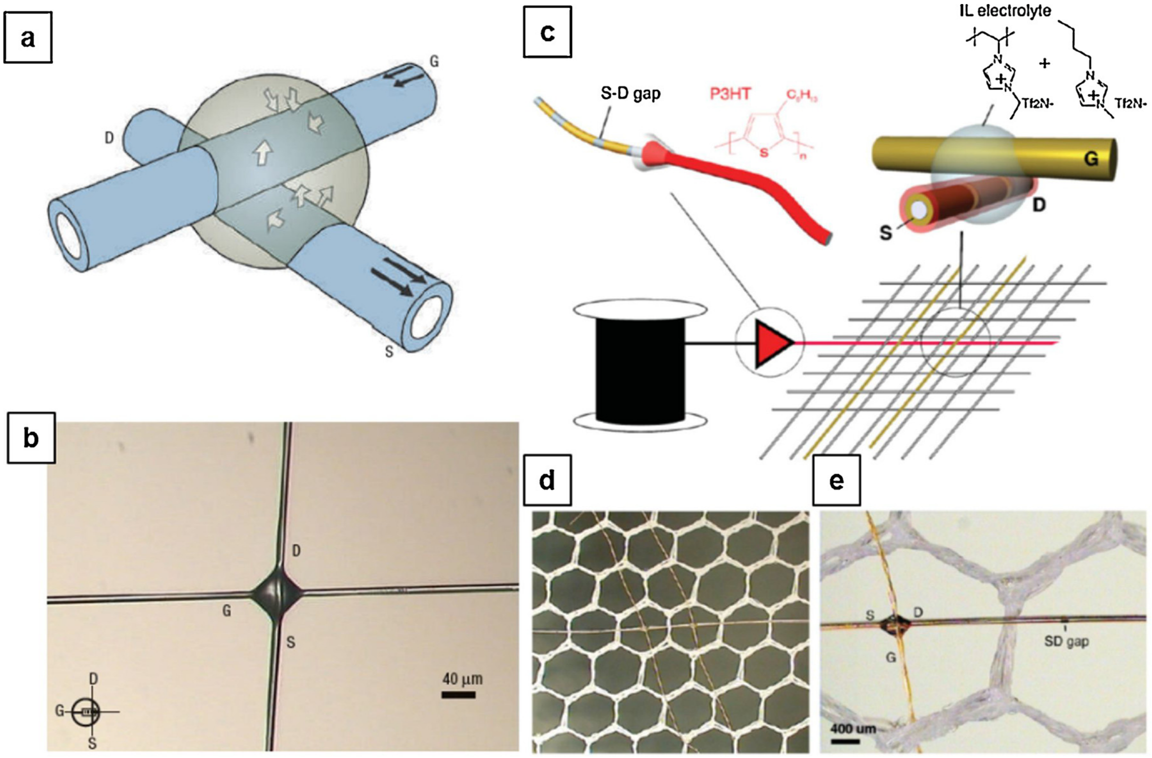

Fig. 34. Textile transistors: (a) schematic of a fibre-based OECT which was realised (b) by placing a drop of electrolyte at the junction of two PEDOT:PSS coated fibres (Reprinted from [7] by permission from Springer Nature © 2007). (c) Schematic of an EG-OFET constructed from P3HT-coated (red) fibres with pre-patterned source-drain (S-D) gaps and an ionic liquid (IL) placed at the junction with a gold fibre. (d) Two EG-OFETs woven into a tulle fabric, and (e) a close up of the left side fibre transistor. (For interpretation of the references to colour in this figure legend, the reader is referred to the web version of this article.)
Reproduced from [236] with permission from Wiley.

4.8. The transistor and logic circuits

The crossing of two conducting lines can be bridged by an active material to form transistors as well as other devices. Organic Field-effect transistors (OFETs) have been realised at the crossing of textile fibres [228–233]. When a voltage is applied between the source and gate of an OFET, majority carriers are generated at the insulator/semiconductor interface, which lead to the formation of a conducting channel between the source (S) and drain (D). In fibre OFETs the channel, the insulator and the gate are patterned on a single fibres for example by evaporation. The Gate, or the S-D contacts are subsequently contacted using other conducting fibres that create the Ohmic connections at the crossings.

Probably the most interesting type of transistors that can be realised at the crossing of organic electronic fibres are those that rely on electrochemical reactions. These components can easily be fabricated by connecting two fibre electrodes at the crossing with an electrolyte, and more preferably a solid polymer electrolyte [234,235]. The biggest advantage of fibre based electrochemical components is that their operation voltage does not depend on the thickness of the dielectric insulator (the electrolyte in this case), but rather on the electrochemical potential of the system, which is around one volt. This means that the shape of the solid polymer electrolyte and the distances between the fibres can vary substantially without affecting the low operation voltage. The fabrication of electrochemical components is therefore compatible with the rough precision of textile manufacturing.

Two types of electrochemical fibre-based devices have been realised: (1) organic electrochemical transistors (OECTs) [7,8,231], and (2) electrolyte gated organic field-effect transistors (EG-OFETs) [236]. In the case of OECTs, the channel and gate are in electrolytic contact and the modulation of the channel conductivity is a result of an electrochemical redox reaction between the gate and the channel (e.g. PEDOT:PSS). Instead, in EG-OFETs an electric double layer is formed at the interface of the electrolyte/semi-conductor, which causes a field-effect modulation of the channel (e.g. a P3HT coating).

The fabrication of individual components at the crossings of textile fibres opens up possibilities for designing and fabricating textile circuit boards, such as digital logic circuits, or active matrix panels, using textile manufacturing methods [7,232]. In one example, Hamedi et al. constructed logic elements such as an inverter and a binary tree multiplexer by selectively fabricating Ohmic contacts, or fibre OECTs at different crossings of a textile [7] (Fig. 34).

A further interesting application area for integrated textile transistors, especially electrochemical transistors, is biosensing [237–239]. Some groups have demonstrated textile biosensors where fibre based electrochemical transistors have been used for sensing of glucose and hemoglobin [239] found in blood, and for the detection of various analytes from artificial blood [237]. Textile based biosensors are particularly interesting for wearables, or for large-scale/low-cost devices.

4.9. Devices for energy harvesting and storage

One intriguing concept is to equip textiles with the ability to both harvest and store electricity, which could then be used to power other electronic devices such as for instance sensors and logic circuits. A number of physical phenomena exist that permit to generate electrical power, including piezoelectrics, thermoelectrics and triboelectrics, as well as photovoltaics. The power density of many energy harvesting concepts is on the order of microwatts, which is not sufficient to continuously power most electronic devices. Therefore, it will be necessary to integrate energy harvesting and storage devices (supercapacitors, batteries) into the same textile. For instance, an energy harvesting device could be used to gradually charge a supercapacitor, followed by rapid discharge of the latter to briefly power an otherwise idle sensor, transmitter, etc. Several fabrics have been demonstrated that combine triboelectric generators and/or solar cells with (super)capacitors [12,22,240–242]. An extensive body of literature on textile based energy harvesting and storage devices exists and we refer the reader to several recent reviews for a complete overview [21,24,243–246]. We here focus on piezoelectric and thermoelectric textiles to provide the reader with a flavour of the type of devices that can be realised with conducting fibres.

Piezoelectric materials respond to a mechanical stress with the build-up of charge, and hence an electrical potential, that can be used to drive a current (energy harvesting) or as a means to detect the impact of a force (cf. piezoelectric sensing in Section 4.5). The most widely studied piezoelectric polymer is poly(vinylidene fluoride) (PVDF), which displays a considerable piezoelectric effect provided the right crystal polymorph (e.g. β-phase PVDF) is present [247,248]. Soin et al. have demonstrated knitted piezoelectric 3D-spacer fabrics, which consist of meltspun PVDF monofilaments that form the spacer layer, and silver coated polyamide yarns that form the top and bottom electrode [17] (Fig. 35a). These devices were able to generate a peak power of up to 5 μW cm^{-2}. Alternatively, core-shell monofilaments can be prepared that comprise a conducting core (based on a carbon black/PE composite with a conductivity of 0.2 S cm^{-1}), which can be used as the inner electrode, and a piezoelectric PVDF shell. We prepared woven piezoelectric textiles that generate a continuous power of 4 μW by combining these core-shell fibres (in the warp direction) with silver-coated polyamide yarns (in the weft direction), which acted as the outer electrode [14] (Fig. 35b). Intriguingly, these woven piezoelectric textiles continued to function when submerged under water, which indicates that truly resilient e-textiles are indeed feasible. We anticipate that further gains in output power can be achieved if more conducting electrode materials are used, which is of course limited by the need to retain a certain degree of pliability desired for most practical textile applications (cf. Section 2.1).

Thermoelectric devices permit to convert heat directly into electricity [55]. An electrical potential ΔV develops across any (semi)conducting material that is exposed to a temperature gradient ΔT, with its magnitude defined by the Seebeck coefficient α:

$$\alpha = -\frac{\Delta V}{\Delta T} \tag{8}$$

Doped conjugated polymers feature a Seebeck coefficient of tens to hundreds of μV K^{-1}, depending on the degree of doping. The thermoelectric efficacy of a material can be described by the figure of merit that combines the Seebeck coefficient α, the absolute temperature T, as well as the electrical and thermal conductivity, c and κ, into a dimensionless quantity:

$$ZT = \frac{\alpha^2 c}{\kappa} T \tag{9}$$

To build thermoelectric generators many *legs* consisting of alternating p- and n-type materials must be connected electrically in series but thermally in parallel, leading to meander-like structures that can be realised with a wide range of in-plane and out-of-plane textile architectures. In case of carbon nanotubes, both efficient p- and n-type materials with a figure of merit (Eq. (9)) $ZT > 0.1$ have been realised [249,250], and modules with a power output of 2.5 μW for a temperature difference of $\Delta T = 27.5$ K have been demonstrated [250]. Whereas similar figures of merit can be achieved with p-type conjugated polymers based on e.g. PEDOT:PSS [251,252], stable n-type conjugated polymers with a competitive ZT are still lacking. Several examples of prototype thermoelectric textiles exist that are based on PEDOT:PSS coated fabrics or dyed yarns, although further integration and downscaling is needed to improve the generated power of currently not more than about 10 nW [18,20] (Fig. 35c–e). In contrast, woven thermoelectric textiles based on PAN yarns [19] decorated with inorganic materials (Sb_2Te_3 and Bi_2Te_3) reach a considerably higher power output of up to 1 μW for $\Delta T = 55$ °C, which indicates that there is further room for improvement once better carbon-based thermoelectric

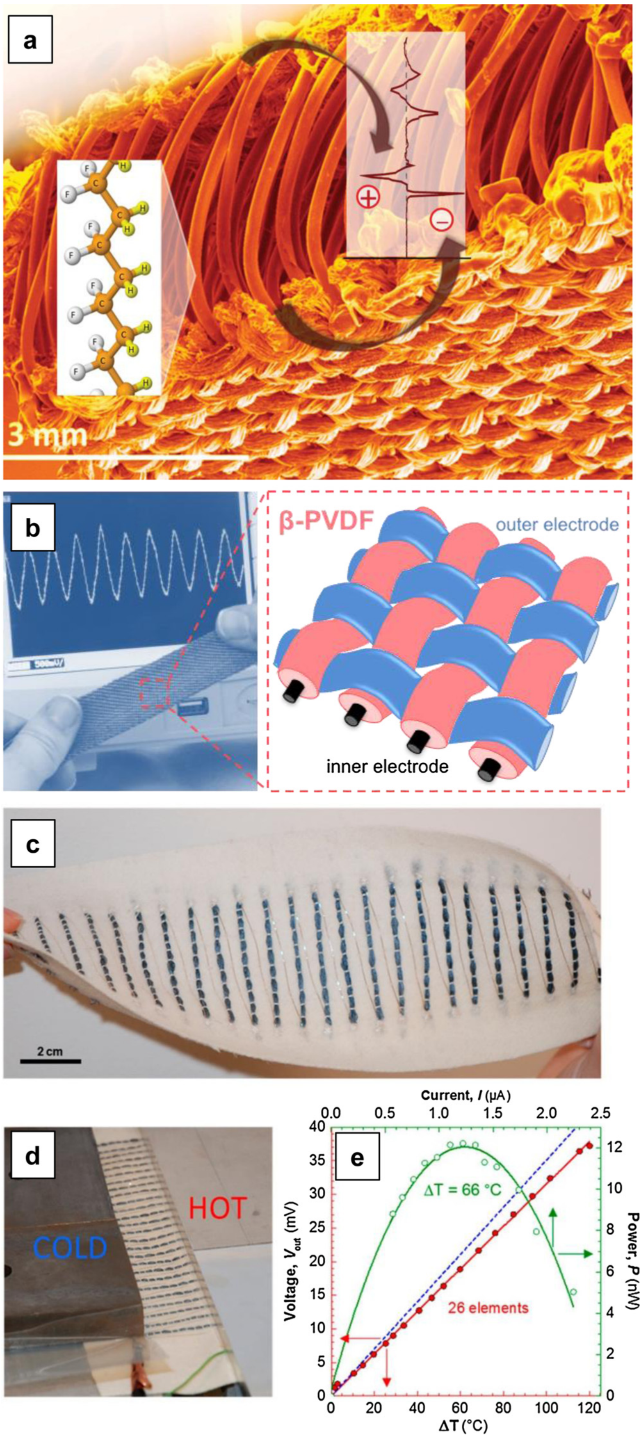

Fig. 35. Textiles for energy harvesting: (a) A piezoelectric 3D-spacer fabric that generates a voltage upon compression (Reproduced from [17] with permission of The Royal Society of Chemistry); (b) a strain-sensitive woven fabric with bicomponent piezoelectric yarns (Reprinted from [14] – Published by Springer Nature), and (c) an embroidered 26-leg thermoelectric device which, when (d) subjected to an in-plane thermal gradient produces (e) up to 37 mV and 12 nW. Reproduced from [20] – Published by The American Chemical Society.

materials have been developed. The power factor $\alpha^2 c$ of both carbon nanotubes and conjugated polymers tends to increase with the conductivity c [249,253], and therefore we postulate that the most efficient thermoelectric textiles will ultimately be produced with highly conducting (but somewhat pliable) fibres or yarns, possibly on the order of 10^2–$10^3\,\mathrm{S\,cm^{-1}}$. Despite a compromise between conductivity and stiffness (cf. Fig. 1) it is also important to consider the impact of orientation on the thermal conductivity (Eq. (9)). Doped conjugated polymers and carbon nanotube/polymer nanocomposites tend to display a relatively low thermal conductivity of $\kappa \sim 0.5$–$1.5\,\mathrm{W\,m^{-1}\,K^{-1}}$ [254–256]. However, high modulus fibres of e.g. UHMWPE reach values of $\kappa > 10\,\mathrm{W\,m^{-1}\,K^{-1}}$ [257], and thus we anticipate that the concomitant increase in thermal and electrical conductivity ultimately limits the thermoelectric figure of merit of carbon-based conducting fibres.

5. Environmental aspects of E-textiles

In this section we discuss the environmental aspects of e-textiles associated with their life cycle phases. Materials are generally designed towards a final application in a product, which will go through a lifecycle of materials extraction, manufacturing, use phase and finally the end-of-life (Fig. 36). Cradle to gate approaches will only include the impact of the first two lifecycle phases. This can provide insights in the environmental performance of materials as such and facilitate an objective comparison to other materials, but will not account for the overall footprint of the final product. For example, the environmental impact of polyester fibres is lower than that of nylon fibres. Still, because the process of weaving requires about twenty times as much energy as the process of knitting, the impact of a knitted garment made from nylon fibres might be lower than the footprint of a polyester garment manufactured by weaving [258,259]. Indeed, we want to emphasize the importance of taking the whole lifecycle into account for environmental assessment. Consequently, designers of e-textiles must include life cycle thinking in the early stages of the design process [260].

The first generation of e-textiles, as developed in the early years of this century, merely consisted of electric components e.g. lighting elements, sensors, conductive wires, printed wire boards, switches and batteries, that were added onto textile substrates (cf. Section 4.1). These materials could be used to enhance the functionality of sports and outdoor clothing, for example for heart rate monitoring and to control mobile devices, but also for fashionable applications such as integrated light emitting panels in shirts and shoes [261]. For these kind of "semi-integrated" e-textile products a combination of life cycle assessment (LCA) and eco-design can provide guidelines to lower the eco-costs of the final product, by means of awareness in materials selection already during the early design stage [262]. The rapid developments in the field, however, are already resulting in new types of e-textiles, with a higher degree of integration of electronics and electrical materials, including nanoscale components. Carrying out an accurate LCA of these products is challenging, because of non-conventional material combinations and manufacturing processes not included in contemporary LCA databases. A future approach might be the integration of LCA and risk assessment, but this visionary method is yet to be implemented [263].

5.1. Eco-design of e-textiles

From an eco-design point of view, and focusing on the first life cycle phase – material extraction – the trend towards smaller parts and less material is a positive one. As the component size decreases and their efficiency increases, the same functionality can be achieved with use of less material. Also, the recent developments in conductive fibre materials and the shift towards bio based and non-metallic solutions for e-textiles, do fit well with the eco-design approach. For example, silver is known as a scarce material, which is difficult to mine and has a much higher environmental impact than carbon black. The eco-cost (a single-unit prevention based indicator for environmental burden [264,265]), for silver trade mix is 162.00 €/kg while the eco-cost of carbon black is 0.31 €/kg [266]. The diminution up to a nanoscale, however, may lead to hitherto unknown environmental problems and health issues

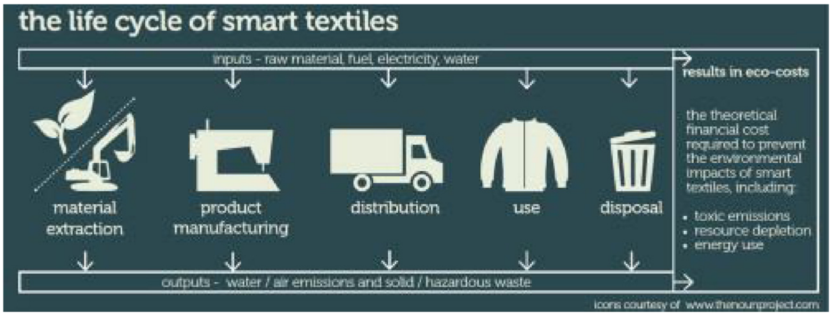

Fig. 36. Outline of the life cycle of textiles.
Reprinted from [262], Copyright (2015), with permission from Elsevier.

[260,267]. Certainly there may be consequences of manufactured nanoparticles entering the soil, the air and organisms and at present it is not well known how the already applied nanotechnological solutions in daily products affect the environment [263].

The environmental impact of the manufacturing stages of textiles in general and specifically for e-textiles is dominated by the energy use (measured in terms of *embodied* energy), the use of (sometimes toxic) materials, chemicals and additives. The release of the latter and the leakage of base materials can harm the environment already during processing, but also during the next use-phase. In the fashion and textile industry, microfibre leakage during manufacturing and consumer laundry gains a lot of attention [268,269] and research for the replacement of microfibres shedding materials and preventative solutions has been initiated [270,271]. It is known that for e-textiles containing silver particles, the leakage of the silver during laundry can be considerable [272]. In non-metallic e-textile materials, concerns from this perspective might arise around the effects on human health due to dopant release from conjugated polymers or carbon materials, or the CNTs/graphene themselves [273]. Here it is interesting to note that initial studies on the wash and wear resistance of conducting fibres is encouraging. For instance, Ryan et al. studied PEDOT:PSS dyed silk fibres and found that the conductivity was unaffected by several washing cycles [20] indicating that the conducting material, which is considered to be biocompatible [274], does not wear off (Fig. 37). Moreover, washable e-textiles comprising GO [164], PANI [154] or PEDOT:PSS in a PU binder [171] have been reported.

5.2. To recycle or to not recycle

With reference to the end-of-life of e-textiles the topic of circularity comes to the fore. The ultimate goal is to make fashion circular by keeping products and materials in the loop as much and as long as possible. In the fashion and textiles industry, methods for post-consumer waste collection are under development and current textile recycling and collecting schemes are being up-scaled. Recycling of textile materials can be done in several ways, at different levels including fabric recycling (cutting and re-sewing the product while the fibres remain intact), yarn recycling (unravelling the yarns used to make the product), fibre recycling (the textiles are shredded and reprocessed into fibres), polymer recycling (after melting or dissolving the polymers new fibres are spun) and chemical recycling (disintegrating the polymers into individual monomers to form new building blocks) [275]. The practice of textile recycling today concentrates on mechanical recycling, mainly for PET. Although the textile industry is making progress and processes to separate materials to the neat materials are being developed, in general composite textile materials and blends are challenging to recycle. The introduction of unknown and unrecognised blends and materials into these recycling schemes, as will be the case for e-textile products, may obstruct the currently available processes.

Conjugated polymers, for example, can in principle be recycled through melting, but this would require de-doping. Chemical recycling on the other hand might be a potential route to separate the fibre components into monomeric material streams that can be used again as feedstock materials. Finally, there is always the possibility to incinerate the materials at the end of life, with or without energy recovery and in controlled facilities, but this way of waste treatment is only common practice in a few places in the world such as the Nordic countries. It has been observed that e-textile designers are concerned about the sustainability of wearable electronics, and that the issue is a topic on the design agenda [276–278]. On the other hand, designers are intrigued by the possibilities that new materials offer and eager to explore the open playground. As long as the uncertainty about the impact of newly developed materials remains, it is advised to start as early as possible in the (material) design process with the exploration of (1) the toxicity and scarcity of the basic materials, (2) the prospective impact of the manufacturing processes, (3) the durability of the product during the use phase, and (4) the impact of a possible unintended end of life stadium.

In relation to the growing concerns about the exponential rise of textile production volumes [279] it would be desirable if e-textiles are able to replace a part of the growing clothing mountain rather than adding to the current portfolio of clothing products [280]. This again underlines the importance of retained textile qualities in electronically functionalised textiles, i.e. the material should still have an attractive appearance and feel, resistance to wash and wear as well as relevant mechanical properties. It is envisioned that the most promising type of material, from an environmentally friendly point of view, is a material that allows the variation of mechanical and electrical properties without changing the type of components, but only their stoichiometry and composition (e.g. coated and dyed fibres and textiles, as well as those based on blends and nanocomposites; cf. Sections 3.2, 3.4 and 3.5).

We expect that the complexity of this issue requires close collaborations in perhaps novel constellations across both industrial sectors (such as textiles, fashion, electronics and waste recycling) and scientists of several disciplines (such as biotechnologists, toxicological specialists and material engineers). While the penetration of e-textile products to the market is already ongoing and possible harmful effects are still unknown it is advised, as a first step, to remain transparent with reference to the materials composition of the products. This could be done by electronic tracking of textiles and their components throughout the whole lifecycle, as well as adequate labelling of the final products, which will ease end-of-use recycling. In the foreseeable future, an agreement of the e-textiles sector to select one type or a convenient set of types of materials that can be used for a wide range of applications, would be beneficial. Alongside this initiative, ongoing research towards the least toxic carbon nanoparticles [281,282], biodegradable and nontoxic electronic polymers [274,283,284] and materials for transient electronics, which degrade over time [285–287] could steer the harmonisation process over time. We refer the reader to the aforementioned interesting studies and reviews that cover these topics in detail.

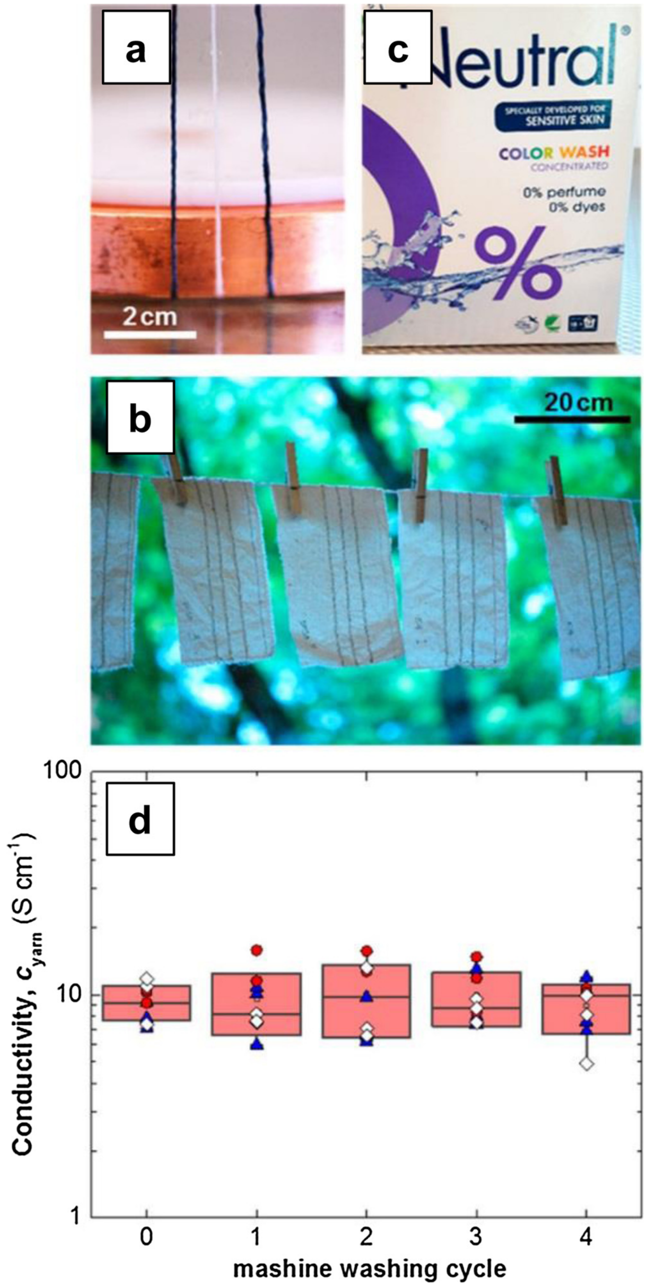

Fig. 37. Washable conducting PEDOT:PSS/silk yarns (a) submerged in distilled water (uncoated yarn in centre); (b) drying of the yarns on carrier swatches after machine washing with a (c) standard detergent. The electrical conductivity (d) was measured after each washing cycle for the yarns dyed with PEDOT:PSS and a secondary dopant (MeOH (white diamond), EG (blue triangle), DMSO (red circle)). (For interpretation of the references to colour in this figure legend, the reader is referred to the web version of this article.) Reproduced from [20] – Published by The American Chemical Society.

6. Conclusions and outlook

We conclude that conducting fibres with a wide range of highly intriguing properties can be prepared with conjugated polymers and carbon nanomaterials, resulting in textile materials with a broad spectrum of electrical and mechanical properties. Generally, the electrical conductivity and Young's modulus both increase with the degree of alignment of the fibre forming material, and hence scale with each other (see Fig. 1). Very conducting (and stiff) fibres, with a conductivity exceeding 1000 S cm^{-1}, have been realised with conjugated polymers and in particular carbon nanotubes (as well as in at least one case graphene). More pliable conducting fibres with a modulus of less than 0.1 GPa have been prepared with polymer blends and nanocomposites, although the conductivity appears to be limited to about 10 S cm^{-1} (and less in case of the latter). One type of fibre that has proven elusive are highly elastic, low-modulus fibres (Young's modulus < 0.1 GPa) with a very high electrical conductivity of 100 S cm^{-1} or more. We anticipate that the realisation of such fibres would certainly open up new application areas.

To develop conducting fibres based on carbon materials for *practical* use a number of developments are necessary. Currently, many types of conjugated polymers and grades of carbon nanotubes and graphene are only available in exceedingly small amounts, which hinders the exploration of bulk processing schemes, such as the fibre spinning processes described in Section 2. In this review only a few types of conjugated polymers such as polythiophenes and PEDOT based materials were discussed. Many others, including high-mobility polymers, are not available in sufficiently large quantities that are required for fibre spinning. Likewise, in case of carbon nanotubes and graphene, larger amounts of high quality materials (e.g. SWNTs with a specific chirality) must become available so that scalable and, crucially, continuous fibre/yarn processing schemes can be developed. Further, progress hinges on the development of more stable doping schemes, since many commonly used dopants are either too volatile (cf. doping of conjugated polymers with iodine) or not environmentally stable (e.g. n-type dopants).

Even though the in this review discussed types of conducting fibres are still at an early stage of development, it is paramount that sustainability aspects are already considered now, since otherwise many lessons learned will have to be rethought latter on. Factors that should be taken into account include (1) an ample supply of high-quality materials, (2) toxicity, (3) the embodied energy of fibre/yarn and textile production, and (4) ease of recycling. Conducting fibres and yarns should be suitable for weaving, knitting and/or embroidery/stitching, which largely rules out very stiff and hence the most conducting fibres. Instead, a compromise must be sought between a high electrical conductivity and an adequate portfolio of mechanical properties that satisfy both the demands imposed by textile manufacturing and later by the desired application. Further, development should focus on a limited class of materials that can be easily recycled, either by separation or melting. Ideally, the selected class(es) of materials will be versatile so that a wide range of electrical and mechanical properties can be realised without changing the ingredients. Once the here outlined hurdles have been overcome, carbon based e-textiles are poised to play their part in advancing the next generation of wearable electronics.

Funding

This work was supported by the Knut and Alice Wallenberg Foundation through a Wallenberg Academy Fellowship, and the European Research Council (ERC) under grant agreement no. 637624.

References

[1] E.R. Post, M. Orth, P.R. Russo, N. Gershenfeld, IBM Syst. J. 39 (2000) 840–860.
[2] S. Takamatsu, T. Lonjaret, E. Ismailova, A. Masuda, T. Itoh, G.G. Malliaras, Adv. Mater. 28 (2016) 4485–4488.
[3] K. Cherenack, L. van Pieterson, J. Appl. Phys. 112 (2012).
[4] S. Seyedin, J.M. Razal, P.C. Innis, A. Jeiranikhameneh, S. Beirne, G.G. Wallace, ACS Appl. Mater. Interfaces 7 (2015) 21150–21158.
[5] Z. Zhao, C. Yan, Z. Liu, X. Fu, L.M. Peng, Y. Hu, Z. Zheng, Adv. Mater. 28 (2016) 10267–10274.
[6] M. Zirkl, A. Sawatdee, U. Helbig, M. Krause, G. Scheipl, E. Kraker, P.A. Ersman, D. Nilsson, D. Platt, P. Bodö, S. Bauer, G. Domann, B. Stadlober, Adv. Mater. 23 (2011) 2069–2074.
[7] M. Hamedi, R. Forchheimer, O. Inganäs, Nat. Mater. 6 (2007) 357–362.
[8] C. Müller, M. Hamedi, R. Karlsson, R. Jansson, R. Marcilla, M. Hedhammar, O. Inganäs, Adv. Mater. 23 (2011) 898–901.
[9] A. Jo, Y. Seo, M. Ko, C. Kim, H. Kim, S. Nam, H. Choi, C.S. Hwang, M.J. Lee, Adv. Funct. Mater. 27 (2017) 1605593.

[10] R. Salvado, C. Loss, R. Gonçalves, P. Pinho, Sensors-Basel 12 (2012) 15841–15857.
[11] W. Weng, P. Chen, S. He, X. Sun, H. Peng, Angew. Chem. Int. Ed. 55 (2016) 6140–6169.
[12] J. Chen, Y. Huang, N. Zhang, H. Zou, R. Liu, C. Tao, X. Fan, Z.L. Wang, Nat. Energy 1 (2016) 16138.
[13] K.N. Kim, J. Chun, J.W. Kim, K.Y. Lee, J.-U. Park, S.-W. Kim, Z.L. Wang, J.M. Baik, ACS Nano 9 (2015) 6394–6400.
[14] A. Lund, K. Rundqvist, E. Nilsson, L. Yu, B. Hagström, C. Müller, NPJ Flex. Electron. 2 (2018) 9.
[15] J. Chang, M. Dommer, C. Chang, L. Lin, Nano Energy 1 (2012) 356–371.
[16] L. Persano, C. Dagdeviren, Y. Su, Y. Zhang, S. Girardo, D. Pisignano, Y. Huang, J.A. Rogers, Nat. Commun. 4 (2013) 1633.
[17] N. Soin, T.H. Shah, S.C. Anand, J. Geng, W. Pornwannachai, P. Mandal, D. Reid, S. Sharma, R.L. Hadimani, D.V. Bayramol, E. Siores, Energy Environ. Sci. 7 (2014) 1527–1794.
[18] Y. Du, K. Cai, S. Chen, H. Wang, S.Z. Shen, R. Donelson, T. Lin, Sci. Rep. 5 (2015) 6411.
[19] J.A. Lee, A.E. Aliev, J.S. Bykova, M.J. de Andrade, D. Kim, H.J. Sim, X. Lepró, A.A. Zakhidov, J.B. Lee, G.M. Spinks, S. Roth, S.J. Kim, R.H. Baughman, Adv. Mater. 28 (2016) 5038–5044.
[20] J.D. Ryan, D.A. Mengistie, R. Gabrielsson, A. Lund, C. Müller, ACS Appl. Mater. Interfaces 9 (2017) 9045–9050.
[21] H. Peng, Fiber-Shaped Energy Harvesting and Storage Devices, Springer-Verlag, Berlin Heidelberg, 2015.
[22] Z. Wen, M.-H. Yeh, H. Guo, J. Wang, Y. Zi, W. Xu, J. Deng, L. Zhu, X. Wang, C. Hu, L. Zhu, X. Sun, Z.L. Wang, Sci. Adv. 2 (2016) e1600097.
[23] Y. Fu, H. Wu, S. Ye, X. Cai, X. Yu, S. Hou, H. Kafafy, D. Zou, Energy Environ. Sci. 6 (2013) 805–812.
[24] K. Jost, G. Dion, Y. Gogotsi, J. Mater. Chem. A 2 (2014) 10776.
[25] X. Pu, M. Liu, L. Li, S. Han, X. Li, C. Jiang, C. Du, J. Luo, W. Hu, Z.L. Wang, Adv. Energy Mater. 6 (2016) 1601254.
[26] J. Zhu, S. Tang, J. Wu, X. Shi, B. Zhu, X. Meng, Adv. Energy Mater. 7 (2016) 1601234.
[27] F.G. Emmerich, Carbon 79 (2014) 274–293.
[28] J. Moulton, P. Smith, J. Polym. Sci. Polym. Phys. 30 (1992) 871–878.
[29] A. Ziabicki, Fundamentals of Fibre Formation, John Wiley & Sons, Bath, 1976.
[30] V.B. Gupta, V.K. Kothari, Manufactured Fibre Technology, Springer Science + Business Media, Dordrecht, Bristol, 1997.
[31] Z. Tadmor, C.G. Gogos, Principles of Polymer Processing, John Wiley & Sons, Hoboken, 2006.
[32] H. Eberle, M. Hornberger, D. Menzer, H. Hermeling, R. Kilgus, W. Ring, Clothing Technology, Verlag Europa-Lehrmittel, Haan-Gruiten, 2002.
[33] E.P.G. Gohl, L.D. Vilensky, Textile Science, Longman Cheshire, Melbourne, 1983.
[34] A.K. Sen, Coated Textiles: Principles and Applications, CRC, Press, Boca Raton, 2007.
[35] A. Wynne, Textiles, Macmillan Education Ltd., London, 1997.
[36] J.P. O'Brien, S.R. Fahnestock, Y. Termonia, K.H. Gardner, Adv. Mater. 10 (1998) 1185–1195.
[37] J.B. Quig, Text. Res. J. 23 (1953) 280–288.
[38] J.H. Park, G.C. Rutledge, Macromolecules 50 (2017) 5627–5642.
[39] R. Séguéla, Macromol. Mater. Eng. 292 (2007) 235–244.
[40] S.L. Kwolek, Optically Anisotropic Aromatic Polyamide Dopes, U.S. Patent No. 3 671 542, 1972.
[41] M. Panar, P. Avakian, R.C. Blume, K.H. Gardner, T.D. Gierke, H.H. Yang, J. Polym. Sci. Polym. Phys. 21 (1983) 1955–1969.
[42] P. Smith, P.J. Lemstra, J. Mater. Sci. 15 (1980) 505–514.
[43] J. Foroughi, G.M. Spinks, G.G. Wallace, Conducting polymer fibers, in: X. Tao (Ed.), Handbook of Smart Textiles, Springer Science + Business Media, Singapore, 2015, pp. 31–62.
[44] L. Allison, S. Hoxie, T.L. Andrew, Chem. Commun. 53 (2017) 7182–7193.
[45] A. Mirabedini, J. Foroughi, G.G. Wallace, RSC Adv. 6 (2016) 44687–44716.
[46] L. Liu, W. Ma, Z. Zhang, Small 7 (2011) 1504–1520.
[47] W. Lu, M. Zu, J.-H. Byun, B.-S. Kim, T.-W. Chou, Adv. Mater. 24 (2012) 1805–1833.
[48] Z. Xu, C. Gao, Mater. Today 18 (2015) 480–492.
[49] A. Andreatta, S. Tokito, P. Smith, A.J. Heeger, Mol. Cryst. Liq. Cryst. 189 (1990) 169–182.
[50] D.S. Pearson, P.A. Pincus, G.W. Heffner, S.J. Dahman, Macromolecules 26 (1993) 1570–1575.
[51] E.M. Pérez, N. Martín, Chem. Soc. Rev. 44 (2015) 6425–6433.
[52] T.A. Skotheim, J. Reynolds, Conjugated Polymers: Theory, Synthesis, Properties and Characterization, Kluwer Academic Publishers, Dordrecht, 2006.
[53] F.P.V. Koch, J. Rivnay, S. Foster, C. Müller, J.M. Downing, E. Buchaca-Domingo, P. Westacott, L. Yu, M. Yuan, M. Baklar, Z. Fei, C. Luscombe, M.A. McLachlan, M. Heeney, G. Rumbles, C. Silva, A. Salleo, J. Nelson, P. Smith, N. Stingelin, Prog. Polym. Sci. 38 (2013) 1978–1989.
[54] X.F. Zhang, Q.W. Li, T.G. Holesinger, P.N. Arendt, J.Y. Huang, P.D. Kirven, T.G. Clapp, R.F. DePaula, X.Z. Liao, Y.H. Zhao, L.X. Zheng, D.E. Peterson, Y.T. Zhu, Adv. Mater. 19 (2007) 4198–4201.
[55] R. Kroon, D.A. Mengistie, D. Kiefer, J. Hynynen, J.D. Ryan, L. Yu, C. Müller, Chem. Soc. Rev. 45 (2016) 6147–6164.
[56] R. Xie, R.H. Colby, E.D. Gomez, Adv. Electron. Mater. (2017) 1700356.
[57] J. Moulton, P. Smith, M. Lewin, J. Preston (Eds.), High Technology Fibers, Part C, Marcel Dekker Inc., New York, 1993, pp. 275–315.
[58] Y. Cao, P. Smith, A.J. Heeger, Polymer 32 (1991) 1210–1218.
[59] Y. Nogami, H. Kaneko, T. Ishiguro, A. Takahashi, J. Tsukamoto, N. Hosoito, Solid State Commun. 76 (1990) 583–586.
[60] I.E. Jacobs, A.J. Moulé, Adv. Mater 29 (2017) 1703063.
[61] A.J. Heeger, P. Smith, J.L. Brédas, R. Silbey (Eds.), Conjugated Polymers, Kluwer Academic Publishers, Dordrecht, 1991, pp. 141–210.
[62] D.R. Gagnon, J.D. Capistran, F.E. Karasz, R.W. Lenz, Polym. Bull. 12 (1984) 293–298.
[63] I. Murase, T. Ohnishi, T. Noguchi, M. Hirooka, Synthetic Met. 17 (1987) 639–644.
[64] S.Z. Tokito, P. Smith, A.J. Heeger, Synthetic Met. 36 (1990) 183–194.
[65] S. Tokito, P. Smith, A.J. Heeger, Polymer 32 (1991) 464–470.
[66] A. Andreatta, Y. Cao, J.C. Chiang, A.J. Heeger, P. Smith, Synthetic Met. 26 (1988) 383–389.
[67] Y. Cao, P. Smith, A.J. Heeger, Synthetic Met. 48 (1992) 91–97.
[68] A. Elschner, S. Kirchmeyer, W. Lövenich, U. Merker, K. Reuter, PEDOT − Principles and Applications of an Intrinsically Conductive Polymer, CRC Press, Boca Raton, 2011.
[69] F. Motamedi, K.J. Ihn, Z. Ni, G. Srdanov, F. Wudl, P. Smith, Polymer 33 (1992) 1102–1104.
[70] J. Moulton, P. Smith, Polymer 33 (1992) 2340–2347.
[71] C. Müller, Chem. Mater. 27 (2015) 2740–2754.
[72] J. Fanous, M. Schweizer, D. Schawaller, M.R. Buchmeiser, Macromol. Mater. Eng. 297 (2012) 123–127.
[73] S. Savagatrup, A.D. Printz, T.F. O'Connor, A.V. Zaretski, D. Rodriquez, E.J. Sawyer, K.M. Rajan, R.I. Acosta, S.E. Root, D.J. Lipomi, Energy Environ. Sci. 8 (2015) 55–80.
[74] S. Savagatrup, A.D. Printz, H. Wu, K.M. Rajan, E.J. Sawyer, A.V. Zaretski, C.J. Bettinger, D.J. Lipomi, Synthetic Met. 203 (2015) 208–214.
[75] M. Ito, A. Tsuruno, S. Osawa, K. Tanaka, Polymer 29 (1988) 1161–1165.
[76] D. Kiefer, L. Yu, E. Fransson, A. Gómez, D. Primetzhofer, A. Amassian, M. Campoy-Quiles, C. Müller, Adv. Sci. 4 (2017) 1600203.
[77] R. Jalili, J.M. Razal, P.C. Innis, G.G. Wallace, Adv. Funct. Mater. 21 (2011) 3363–3370.
[78] D. Yuan, B. Li, J. Cheng, Q. Guan, Z. Wang, W. Ni, C. Li, H. Liu, B. Wang, J. Mater. Chem. A 4 (2016) 11616–11624.
[79] J. Zhou, E.Q. Li, R.P. Li, X.Z. Xu, I.A. Ventura, A. Moussawi, D.H. Anjum, M.N. Hedhili, D.M. Smilgies, G. Lubineau, S.T. Thoroddsen, J. Mater. Chem. C 3 (2015) 2528–2538.
[80] A. Andreatta, P. Smith, Synthetic Met. 55–57 (1993) 1017–1022.
[81] H. Okuzaki, Y. Harashina, H. Yan, Eur. Polym. J. 45 (2009) 256–261.
[82] H. Okuzaki, M. Ishihara, Macromol. Rapid Commun. 24 (2003) 261–264.
[83] J. Moulton, P. Smith, Synthetic Met. 40 (1991) 13–22.
[84] J. Li, P.C. Ma, W.S. Chow, C.K. To, B.Z. Tang, J.K. Kim, Adv. Funct. Mater. 17 (2007) 3207–3215.
[85] A. Andreatta, A.J. Heeger, P. Smith, Polym. Commun. 31 (1990) 275.
[86] M. Reghu, C.O. Yoon, C.Y. Yang, D. Moses, P. Smith, A.J. Heeger, Y. Cao, Phys. Rev. B 50 (1994) 13931–13941.
[87] A.J. Granero, P. Wagner, K. Wagner, J.M. Razal, G.G. Wallace, M. in het Panhuis, Adv. Funct. Mater 21 (2011) 955–962.
[88] M.Z. Seyedin, J.M. Razal, P.C. Innis, G.G. Wallace, Adv. Funct. Mater. 24 (2014) 2957–2966.
[89] X. Wang, M.-Q. Ge, G.-Y. Feng, Fiber. Polym. 16 (2016) 2578–2585.
[90] M.F. Yu, O. Lourie, M.J. Dyer, K. Moloni, T.F. Kelly, R.S. Ruoff, Science 287 (2000) 637–640.
[91] P. Avouris, Z.H. Chen, V. Perebeinos, Nat. Nanotechnol. 2 (2007) 605–615.
[92] L.M. Ericson, H. Fan, H.Q. Peng, V.A. Davis, W. Zhou, J. Sulpizio, Y.H. Wang, R. Booker, J. Vavro, C. Guthy, A.N.G. Parra-Vasquez, M.J. Kim, S. Ramesh, R.K. Saini, C. Kittrell, G. Lavin, H. Schmidt, W.W. Adams, W.E. Billups, M. Pasquali, W.F. Hwang, R.H. Hauge, J.E. Fischer, R.E. Smalley, Science 305 (2004) 1447–1450.
[93] Z. Xu, H. Sun, X. Zhao, C. Gao, Adv. Mater. 25 (2013) 188–193.
[94] M. Motta, A. Moisala, I.A. Kinloch, A.H. Windle, Adv. Mater. 19 (2007) 3721–3726.
[95] R. Jalili, S.H. Aboutalebi, D. Esrafilzadeh, R.L. Shepherd, J. Chen, S. Aminorroaya-Yamini, K. Konstantinov, A.I. Minett, J.M. Razal, G.G. Wallace, Adv. Funct. Mater. 23 (2013) 5345–5354.
[96] M. Zu, Q.W. Li, Y.T. Zhu, M. Dey, G.J. Wang, W.B. Lu, J.M. Deitzel, J.W. Gillespie Jr., J.H. Byun, T.W. Chou, Carbon 50 (2012) 1271–1279.
[97] S.H. Aboutalebi, R. Jalili, D. Esrafilzadeh, M. Salari, Z. Gholamvand, S.A. Yamini, K. Konstantinov, R.L. Shepherd, J. Chen, S.E. Moulton, P.C. Innis, A.I. Minett, J.M. Razal, G.G. Wallace, ACS Nano 8 (2014) 2456–2466.
[98] V.A. Davis, A.N. Parra-Vasquez, M.J. Green, P.K. Rai, N. Behabtu, V. Prieto, R.D. Booker, J. Schmidt, E. Kesselman, W. Zhou, H. Fan, W.W. Adams, R.H. Hauge, J.E. Fischer, Y. Cohen, Y. Talmon, R.E. Smalley, M. Pasquali, Nat. Nanotechnol. 4 (2009) 830–834.
[99] Z. Xu, C. Gao, Nat. Commun. 2 (2011) 571.
[100] S. Zhang, K.K. Koziol, I.A. Kinloch, A.H. Windle, Small 4 (2008) 1217–1222.
[101] K. Jiang, Q. Li, S. Fan, Nature 419 (2002) 801.
[102] M. Zhang, K.R. Atkinson, R.H. Baughman, Science 306 (2004) 1358–1361.
[103] X. Zhang, Q. Li, Y. Tu, Y. Li, J.Y. Coulter, L. Zheng, Y. Zhao, Q. Jia, D.E. Peterson, Y. Zhu, Small 3 (2007) 244–248.
[104] K. Liu, Y.H. Sun, X.Y. Lin, R.F. Zhou, J.P. Wang, S.S. Fan, K.L. Jiang, ACS Nano 4 (2010) 5827–5834.
[105] W.J. Ma, L.Q. Liu, Z. Zhang, R. Yang, G. Liu, T.H. Zhang, X.F. An, X.S. Yi, Y. Ren, Z.Q. Niu, J.Z. Li, H.B. Dong, W.Y. Zhou, P.M. Ajayan, S. Xie, Nano Lett. 9 (2009) 2855–2861.
[106] J.J. Vilatela, A.H. Windle, Adv. Mater. 22 (2010) 4959–4963.
[107] C. Xiang, C.C. Young, X. Wang, Z. Yan, C.C. Hwang, G. Cerioti, J. Lin, J. Kono,

M. Pasquali, J.M. Tour, Adv. Mater. 25 (2013) 4592–4597.
[108] E. Muñoz, D.S. Suh, S. Collins, M. Selvidge, A.B. Dalton, B.G. Kim, J.M. Razal, G. Ussery, A.G. Rinzler, M.T. Martínez, R.H. Baughman, Adv. Mater. 17 (2005) 1064–1067.
[109] M.E. Kozlov, R.C. Capps, W.M. Sampson, V.H. Ebron, J.P. Ferraris, R.H. Baughman, Adv. Mater. 17 (2005) 614–617.
[110] Z. Xu, Z. Liu, H. Sun, C. Gao, Adv. Mater. 25 (2013) 3249–3253.
[111] H.P. Cong, X.C. Ren, P. Wang, S.H. Yu, Sci. Rep. 2 (2012) 613.
[112] L. Chen, Y. He, S. Chai, H. Qiang, F. Chen, Q. Fu, Nanoscale 5 (2013) 5809–5815.
[113] W. Bauhofer, J.Z. Kovacs, Compos. Sci. Technol. 69 (2009) 1486–1498.
[114] L. Peponi, D. Puglia, L. Torre, L. Valentini, J.M. Kenny, Mat. Sci. Eng. R 85 (2014) 1–46.
[115] T. Gkourmpis, G.R. Mitchell, A. Tojeira (Eds.), Controlling the Morphology of Polymers Multiple Scales of Structure and Processing, Springer International Publishing, Switzerland, 2016, pp. 209–236.
[116] J.-B. Donnet, R. Chand Bansal, M.-J. Wang, Carbon Black: Science and Technology, Marcel Dekker Inc, New York, 1993.
[117] G. Mazzanti, M. Marzinotto, Extruded Cables for High-Voltage Direct-Current Transmission, John Wiley & Sons Inc, Hoboken, 2013.
[118] Z. Wang, J.K. Nelson, H. Hillborg, S. Zhao, L.S. Schadler, Adv. Mater. 24 (2012) 3134–3137.
[119] R. Jain, Y.H. Choi, Y. Liu, M.L. Minus, H.G. Chae, S. Kumar, J.-B. Baek, Polymer 51 (2010) 3940–3947.
[120] M. Abdel-Goad, P. Pötschke, J. Non-Newtonian Fluid Mech. 128 (2005) 2–6.
[121] R. Shvartzman-Cohen, E. Nativ-Roth, E. Baskaran, Y. Levi-Kalisman, I. Szleifer, R. Yerushalmi-Rozen, J. Am. Chem. Soc. 126 (2004) 14850–14857.
[122] C. Bounioux, P. Díaz-Chao, M. Campoy-Quiles, M.S. Martín-González, A.R. Goñi, R. Yerushalmi-Rozen, C. Müller, Energy Environ. Sci. 6 (2013) 918–925.
[123] K.C. See, J.P. Feser, C.E. Chen, A. Majumdar, J.J. Urban, R.A. Segalman, Nano Lett. 10 (2010) 4664–4667.
[124] C. Yu, K. Choi, L. Yin, J.C. Grunlan, ACS Nano 5 (2011) 7885–7892.
[125] S. Seyedin, J.M. Razal, P.C. Innis, G.G. Wallace, Smart Mater. Struct. 25 (2016) 035015.
[126] F. Du, R.C. Scogna, W. Zhou, S. Brand, J.E. Fischer, K.I. Winey, Macromolecules 37 (2004) 9048–9055.
[127] A. Lund, C. Jonasson, C. Johansson, D. Haagensen, B. Hagström, J. Appl. Polym. Sci. 126 (2012) 490–500.
[128] E. Nilsson, M. Rigdahl, B. Hagström, J. Appl. Polym. Sci. 132 (2015) 42255.
[129] M. Strååt, S. Toll, A. Boldizar, M. Rigdahl, B. Hagström, J. Appl. Polym. Sci. 119 (2011) 3264–3272.
[130] H.M. Laun, H. Schuch, J. Rheol. 33 (1989) 119–175.
[131] C. Zhu, J. Chen, K.K. Koziol, J.W. Gilman, P.C. Trulove, S.S. Rahatekar, Express Polym. Lett. 8 (2014) 154–163.
[132] L. Härdelin, B. Hagström, J. Appl. Polym. Sci. 132 (2015) 41417.
[133] H. Qi, B. Schulz, T. Vad, J. Liu, E. Mäder, G. Seide, T. Gries, ACS Appl. Mater. Interfaces 7 (2015) 22404–22412.
[134] P. Pötschke, H. Brünig, A. Janke, D. Fischer, D. Jehnichen, Polymer 46 (2005) 10355–10363.
[135] F. Du, J.E. Fischer, K.I. Winey, Phys. Rev. B. 72 (2005) 121404.
[136] H. Deng, T. Skipa, E. Bilotti, R. Zhang, D. Lellinger, L. Mezzo, Q. Fu, I. Alig, T. Peijs, Adv. Funct. Mater. 20 (2010) 1424–1432.
[137] S.H. Foulger, J. Appl. Polym. Sci. 72 (1999) 1573–1582.
[138] X. Gao, S. Zhang, F. Mai, L. Lin, Y. Deng, H. Deng, Q. Fu, J. Mater. Chem. 21 (2011) 6401.
[139] C. Mercader, V. Denis-Lutard, S. Jestin, M. Maugey, A. Derré, C. Zakri, P. Poulin, J. Appl. Polym. Sci. 125 (2012) E191–E196.
[140] A.-T. Chien, S. Cho, Y. Joshi, S. Kumar, Polymer 55 (2014) 6896–6905.
[141] A. Soroudi, M. Skrifvars, Synthetic Met. 160 (2010) 1143–1147.
[142] N. Piri, V. Mottaghitalab, S. Arbab, e-Polymers 13 (2013) 67–81.
[143] X. Jin, C.F. Xiao, W.Y. Wang, Mater. Sci. Tech. -Lond. 26 (2010) 1453–1458.
[144] X. Jin, C. Xiao, S. An, G. Jia, J. Mater. Sci. 42 (2007) 4384–4389.
[145] S. Seyedin, J.M. Razal, P.C. Innis, R. Jalili, G.G. Wallace, Adv. Mater. Interfaces 3 (2016) 1500672.
[146] D. Esrafilzadeh, R. Jalili, E.M. Stewart, S.H. Aboutalebi, J.M. Razal, S.E. Moulton, G.G. Wallace, Adv. Funct. Mater. 26 (2016) 3105–3117.
[147] S.A. Gordeyev, J.A. Ferreira, C.A. Bernardo, I.M. Ward, Mater. Lett. 51 (2001) 32–36.
[148] A. Schwarz, L. Van Langenhove, P. Guermonprez, D. Deguillemont, Text. Prog. 42 (2010) 99–180.
[149] C. Müller, R. Jansson, A. Elfwing, G. Askarieh, R. Karlsson, M. Hamedi, A. Rising, J. Johansson, O. Inganäs, M. Hedhammar, J. Mater. Chem. 21 (2011) 2909–2915.
[150] M.R. Moraes, A.C. Alves, F. Toptan, M.S. Martins, E.M.F. Vieira, A.J. Paleo, A.P. Souto, W.L.F. Santos, M.F. Esteves, A. Zille, J. Mater. Chem. C 5 (2017) 3807–3822.
[151] Z. Lu, C. Mao, H. Zhang, J. Mater. Chem. C 3 (2015) 4265–4268.
[152] J. Eom, R. Jaisutti, H. Lee, W. Lee, J.-S. Heo, J.-Y. Lee, S.K. Park, Y.-H. Kim, ACS Appl. Mater. Interfaces 9 (2017) 10190–10197.
[153] K.H. Hong, K.W. Oh, T.J. Kang, J. Appl. Polym. Sci. 97 (2005) 1326–1332.
[154] Y. Xia, L. Yun, Compos. Sci. Technol. 68 (2008) 1471–1479.
[155] R.V. Gregory, W.C. Kimbrell, H.H. Kuhn, Synthetic Met. 28 (1989) C823–C835.
[156] R.V. Gregory, W.C. Kimbrell, H.H. Kuhn, J. Coat. Fabr. 20 (1991) 167–175.
[157] H.H. Kuhn, A.D. Child, W.C. Kimbrell, Synthetic Met. 71 (1995) 2139–2142.
[158] H.H. Kuhn, W.C. Kimbrell, J.E. Fowler, C.N. Barry, Synthetic Met. 55–57 (1993) 3707–3712.
[159] A. Varesano, L. Dall'Acqua, C. Tonin, Polym. Degrad. Stab. 89 (2005) 125–132.
[160] A. Varesano, A. Belluati, D.O. Sanchez Ramirez, R.A. Carletto, C. Vineis, C. Tonetti, M. Bianchetto Songia, G. Mazzuchetti, J. Appl. Polym. Sci. 133 (2016) 42831.
[161] S. Garg, C. Hurren, A. Kaynak, Synthetic Met. 157 (2007) 41–47.
[162] J. Molina, A.I. del Río, J. Bonastre, F. Cases, Eur. Polym. J. 45 (2009) 1302–1315.
[163] J. Molina, J. Fernández, A.I. del Río, R. Lapuente, J. Bonastre, F. Cases, Polym. Degrad. Stab. 95 (2010) 2574–2583.
[164] X. Tang, M. Tian, L. Qu, S. Zhu, X. Guo, G. Han, K. Sun, X. Hu, Y. Wang, X. Xu, Synthetic Met. 202 (2015) 82–88.
[165] T. Bashir, M. Skrifvars, N.-K. Persson, Polym. Adv. Technol. 22 (2011) 2214–2221.
[166] P. Kovacik, G. del Hierro, W. Livernois, K.K. Gleason, Mater. Horiz. 2 (2015) 221–227.
[167] L. Zhang, M. Fairbanks, T.L. Andrew, Adv. Funct. Mater. 27 (2017) 1700415.
[168] N. Cheng, L. Zhang, J. Joon Kim, T.L. Andrew, J. Mater. Chem. C 5 (2017) 5787–5796.
[169] M. Åkerfeldt, M. Strååt, P. Walkenström, Text. Res. J. 83 (2013) 618–627.
[170] M. Åkerfeldt, M. Strååt, P. Walkenström, Text. Res. J. 83 (2013) 2164–2176.
[171] M. Åkerfeldt, A. Lund, P. Walkenström, Text. Res. J. 85 (2015) 1789–1799.
[172] Y. Guo, M.T. Otley, M. Li, X. Zhang, S.K. Sinha, G.M. Treich, G.A. Sotzing, ACS Appl. Mater. Interfaces 8 (2016) 26998–27005.
[173] Z. Stempien, T. Rybicki, E. Rybicki, M. Kozanecki, M.I. Szynkowska, Synthetic Met. 202 (2015) 49–62.
[174] E. Steven, W.R. Saleh, V. Lebedev, S.F. Acquah, V. Laukhin, R.G. Alamo, J.S. Brooks, Nat. Commun. 4 (2013) 2435.
[175] M.D. Irwin, D.A. Roberson, R.I. Olivas, R.B. Wicker, E. MacDonald, Fiber. Polym. 12 (2011) 904–910.
[176] T.J. Kang, A. Choi, D.-H. Kim, K. Jin, D.K. Seo, D.H. Jeong, S.-H. Hong, Y.W. Park, Y.H. Kim, Smart Mater. Struct. 20 (2011) 015004.
[177] Y. Ding, M.A. Invernale, G.A. Sotzing, ACS Appl. Mater. Interfaces 2 (2010) 1588–1593.
[178] T. Lin, L. Wang, X. Wang, A. Kaynak, Thin Solid Films 479 (2005) 77–82.
[179] J. Wu, D. Zhou, C.O. Too, G.G. Wallace, Synthetic Met. 155 (2005) 698–701.
[180] S. Takamatsu, T. Kobayashi, N. Shibayama, K. Miyake, T. Itoh, Sens. Actuators A-Phys. 184 (2012) 57–63.
[181] A.F. Abouraddy, M. Bayindir, G. Benoit, S.D. Hart, K. Kuriki, N. Orf, O. Shapira, F. Sorin, B. Temelkuran, Y. Fink, Nat. Mater. 6 (2007) 336–347.
[182] M. Bayindir, F. Sorin, A.F. Abouraddy, J. Viens, S.D. Hart, J.D. Joannopoulus, Y. Fink, Nature 431 (2004) 826–829.
[183] S. Egusa, Z. Wang, N. Chocat, Z.M. Ruff, A.M. Stolyarov, D. Shemuly, F. Sorin, P.T. Rakich, J.D. Joannopoulos, Y. Fink, Nat. Mater. 9 (2010) 643–648.
[184] S. Park, Y. Guo, X. Jia, H.K. Choe, B. Grena, J. Kang, J. Park, C. Lu, A. Canales, R. Chen, Y.S. Yim, G.B. Choi, Y. Fink, P. Anikeeva, Nat. Neurosci. 20 (2017) 612–619.
[185] T. Nguyen-Dang, A.G. Page, Y. Qu, M. Volpi, W. Yan, F. Sorin, J. Phys. D: Appl. Phys. 50 (2017) 144001.
[186] L. Hu, Y. Cui, Energy Environ. Sci. 5 (2012) 6423–6435.
[187] L.M. Castano, A.B. Flatau, Smart Mater. Struct. 23 (2014) 053001.
[188] W. Zeng, L. Shu, Q. Li, S. Chen, F. Wang, X.M. Tao, Adv. Mater. 26 (2014) 5310–5336.
[189] J. Di, X. Zhang, Z. Yong, Y. Zhang, D. Li, R. Li, Q. Li, Adv. Mater. 28 (2016) 10529–10538.
[190] Q. Huang, D. Wang, Z. Zheng, Adv. Energy Mater. 6 (2016) 1600783.
[191] L. Guo, T. Bashir, E. Bresky, N.-K. Persson, V. Koncar (Ed.), Smart Textiles and Their Applications, Elsevier Ltd., Duxford, 2015.
[192] T. Kirstein, D. Cottet, J. Grzyb, G. Tröster, X. Tao (Ed.), Wearable Electronics and Photonics, Woodhead Publishing Ltd., Cambridge, 2005, pp. 177–197.
[193] H. Bae, B.C. Jang, H. Park, S.H. Jung, H.M. Lee, J.Y. Park, S.B. Jeon, G. Son, I.W. Tcho, K. Yu, S.G. Im, S.Y. Choi, Y.K. Choi, Nano Lett. 17 (2017) 6443–6452.
[194] K. Jost, D. Stenger, C.R. Perez, J.K. McDonough, K. Lian, Y. Gogotsi, G. Dion, Energy Environ. Sci. 6 (2013) 2698.
[195] A. Maziz, A. Concas, A. Khaldi, J. Stålhand, N.-K. Persson, E.W.H. Jager, Sci. Adv. 3 (2017) 1–11.
[196] T.K. Ghosh, A. Dhawan, J.F. Muth, H. Mattila (Ed.), Intelligent Textiles and Clothing, Woodhead Publishing Ltd, Cambridge, 2006, pp. 239–282.
[197] T. Bashir, M. Ali, N.-K. Persson, S.K. Ramamoorthy, M. Skrifvars, Text. Res. J. 84 (2014) 323–334.
[198] X. Wu, Y. Han, X. Zhang, C. Lu, ACS Appl. Mater. Interfaces 8 (2016) 9936–9945.
[199] H. Zhao, Y. Zhang, P.D. Bradford, Q. Zhou, Q. Jia, F.G. Yuan, Y. Zhu, Nanotechnology 21 (2010) 305502.
[200] S. Wang, S. Xuan, M. Liu, L. Bai, S. Zhang, M. Sang, W. Jiang, X. Gong, Soft Matter 13 (2017) 2483–2491.
[201] J. Foroughi, G.M. Spinks, S. Aziz, A. Mirabedini, A. Jeiranikhameneh, G.G. Wallace, M.E. Kozlov, R.H. Baughman, ACS Nano 10 (2016) 9129–9135.
[202] Y.-H. Lee, Y. Kim, T.-I. Lee, I. Lee, J. Shin, H.S. Lee, T.-S. Kim, J.W. Choi, ACS Nano 9 (2015) 12214–12223.
[203] J. Wang, P. Xue, X. Tao, T. Yu, Adv. Eng. Mater. 16 (2014) 565–570.
[204] A. Tognetti, F. Lorussi, R. Bartalesi, S. Quaglini, M. Tesconi, G. Zupone, D. De Rossi, J. Neuroeng. Rehabil. 2 (2005) 8.
[205] E. Gunnarsson, M. Karlsteen, L. Berglin, J. Stray, Text. Res. J. 85 (2015) 499–511.
[206] M. Catrysse, R. Puers, C. Hertleer, L. Van Langenhove, H. van Egmond, D. Matthys, Sens. Actuators A-Phys. 114 (2004) 302–311.
[207] H. Miura, Y. Fukuyama, T. Sunda, B. Lin, J. Zhou, J. Takizawa, A. Ohmori, M. Kimura, Adv. Eng. Mater. 16 (2014) 550–555.
[208] D. Pani, A. Achilli, P.P. Bassareo, L. Cugusi, G. Mercuro, B. Fraboni, A. Bonfiglio, Comput. Cardiol. 43 (2016) 373–376.
[209] S.K. Sinha, Y. Noh, N. Reljin, G.M. Treich, S. Hajeb-Mohammadalipour, Y. Guo, K.H. Chon, G.A. Sotzing, ACS Appl. Mater. Interfaces 9 (2017) 37524–37528.

[210] S. Takamatsu, T. Lonjaret, D. Crisp, J.M. Badier, G.G. Malliaras, E. Ismailova, Sci. Rep. 5 (2015) 15003.

[211] I.G. Trindade, F. Martins, P. Baptista, Synthetic Met. 210 (2015) 179–185.

[212] M.T. Otley, F.A. Alamer, Y. Guo, J. Santana, E. Eren, M. Li, J. Lombardi, G.A. Sotzing, Macromol. Mater. Eng. 302 (2017) 1600348.

[213] C. Yeon, G. Kim, J.W. Lim, S.J. Yun, RSC Adv. 7 (2017) 5888–5897.

[214] L. Zhang, M. Baima, T.L. Andrew, ACS Appl. Mater. Interfaces 9 (2017) 32299–32307.

[215] A. Laforgue, J. Mater. Chem. 20 (2010) 8233.

[216] A. Laforgue, G. Rouget, S. Dubost, M.F. Champagne, L. Robitaille, ACS Appl. Mater. Interfaces 4 (2012) 3163–3168.

[217] J. Meyer, B. Arnrich, J. Schumm, G. Tröster, IEEE Sens. J. 10 (2010) 1391–1398.

[218] Y. Meng, Y. Zhao, C. Hu, H. Cheng, Y. Hu, Z. Zhang, G. Shi, L. Qu, Adv. Mater. 25 (2013) 2326–2331.

[219] S. Takamatsu, T. Yamashita, T. Murakami, A. Masuda, T. Itoh, Sens. Mater. 26 (2014) 559–570.

[220] E. Nilsson, A. Lund, C. Jonasson, C. Johansson, B. Hagström, Sens. Actuators A-Phys. 201 (2013) 477–486.

[221] E. Yang, Z. Xu, L.K. Chur, A. Behroozfar, M. Baniasadi, S. Moreno, J. Huang, J. Gilligan, M. Minary-Jolandan, ACS Appl. Mater. Interfaces 9 (2017) 24220–24229.

[222] A. Ainla, M.M. Hamedi, F. Güder, G.M. Whitesides, Adv. Mater. 29 (2017) 1702894.

[223] R. Wijesiriwardana, IEEE Sens. J. 6 (2006) 571–579.

[224] A. Kiourti, J.L. Volakis, IEEE Antenn. Wirel. Pr. 14 (2015) 1474–1477.

[225] J. Zhong, A. Kiourti, T. Sebastian, Y. Bayram, J.L. Volakis, IEEE Antenn. Wirel. Pr. 16 (2017) 230–233.

[226] J.M. Tour, T. He, Nature 453 (2008) 42–43.

[227] G. Sun, J. Liu, L. Zheng, W. Huang, H. Zhang, Angew. Chem. 125 (2013) 13593–13597.

[228] A. Bonfiglio, D. DeRossi, T. Kirstein, I.R. Locher, F. Mameli, R. Paradiso, G. Vozzi, IEEE T. Inf. Technol. B 9 (2005) 319–324.

[229] J.B. Lee, V. Subramanian, IEEE T. Electron. Dev. 52 (2005) 269–275.

[230] M. Maccioni, E. Orgiu, P. Cosseddu, S. Locci, A. Bonfiglio, Appl. Phys. Lett. 89 (2006) 143515.

[231] G. Mattana, P. Cosseddu, B. Fraboni, G.G. Malliaras, J.P. Hinestroza, A. Bonfiglio, Org. Electron. 12 (2011) 2033–2039.

[232] X. Tao, V. Koncar, C. Dufour, J. Electrochem. Soc. 158 (2011) H572–H577.

[233] G. Tarabella, M. Villani, D. Calestani, R. Mosca, S. Iannotta, A. Zappettini, N. Coppedè, J. Mater. Chem. 22 (2012) 23830–23834.

[234] D.A. Bernards, G.G. Malliaras, Adv. Funct. Mater. 17 (2007) 3538–3544.

[235] D.T. Simon, E.O. Gabrielsson, K. Tybrandt, M. Berggren, Chem. Rev. 116 (2016) 13009–13041.

[236] M. Hamedi, L. Herlogsson, X. Crispin, R. Marcilla, M. Berggren, O. Inganäs, Adv. Mater. 21 (2009) 573–577.

[237] I. Gualandi, M. Marzocchi, A. Achilli, D. Cavedale, A. Bonfiglio, B. Fraboni, Sci. Rep. 6 (2016) 33637.

[238] A. Modali, S.R.K. Vanjari, D. Dendukuri, Electroanalysis 28 (2016) 1276–1282.

[239] T. Choudhary, G.P. Rajamanickam, D. Dendukuri, Lab Chip 15 (2015) 2064–2072.

[240] K. Dong, Y.C. Wang, J. Deng, Y. Dai, S.L. Zhang, H. Zou, B. Gu, B. Sun, Z.L. Wang, ACS Nano 11 (2017) 9490–9499.

[241] Y.H. Lee, J.S. Kim, J. Noh, I. Lee, H.J. Kim, S. Choi, J. Seo, S. Jeon, T.S. Kim, J.Y. Lee, J.W. Choi, Nano Lett. 13 (2013) 5753–5761.

[242] X. Pu, L. Li, M. Liu, C. Jiang, C. Du, Z. Zhao, W. Hu, Z.L. Wang, Adv. Mater. 28 (2016) 98–105.

[243] V. Kaushik, J. Lee, J. Hong, S. Lee, S. Lee, J. Seo, C. Mahata, T. Lee, Nanomaterials-Basel 5 (2015) 1493–1531.

[244] M. Ha, J. Park, Y. Lee, H. Ko, ACS Nano 9 (2015) 3421–3427.

[245] A. Proto, M. Penhaker, S. Conforto, M. Schmid, Trends Biotechnol. 35 (2017) 610–624.

[246] Y. Wang, Y. Yang, Z.L. Wang, NPJ Flex. Electron. 1 (2017) 10.

[247] I. Katsouras, K. Asadi, M. Li, T.B. van Driel, K.S. Kjaer, D. Zhao, T. Lenz, Y. Gu, P.W. Blom, D. Damjanovic, M.M. Nielsen, D.M. de Leeuw, Nat. Mater. 15 (2016) 78–84.

[248] A.J. Lovinger, Science 220 (1983) 1115–1121.

[249] B.A. MacLeod, N.J. Stanton, I.E. Gould, D. Wesenberg, R. Ihly, Z.R. Owczarczyk, K.E. Hurst, C.S. Fewox, C.N. Folmar, K. Holman Hughes, B.L. Zink, J.L. Blackburn, A.J. Ferguson, Energy Environ. Sci. 10 (2017) 2168–2179.

[250] W. Zhou, Q. Fan, Q. Zhang, L. Cai, K. Li, X. Gu, F. Yang, N. Zhang, Y. Wang, H. Liu, W. Zhou, S. Xie, Nat. Commun. 8 (2017) 14886.

[251] D.A. Mengistie, C.H. Chen, K.M. Boopathi, F.W. Pranoto, L.J. Li, C.W. Chu, ACS Appl. Mater. Interfaces 7 (2015) 94–100.

[252] O. Bubnova, Z.U. Khan, A. Malti, S. Braun, M. Fahlman, M. Berggren, X. Crispin, Nat. Mater. 10 (2011) 429–433.

[253] A.M. Glaudell, J.E. Cochran, S.N. Patel, M.L. Chabinyc, Adv. Energy Mater. 5 (2015) 1401072.

[254] B. Dörling, J.D. Ryan, J.D. Craddock, A. Sorrentino, A. El Basaty, A. Gomez, M. Garriga, E. Pereiro, J.E. Anthony, M.C. Weisenberger, A.R. Goñi, C. Müller, M. Campoy-Quiles, Adv. Mater. 28 (2016) 2782–2789.

[255] D. Kim, Y. Kim, K. Choi, J.C. Grunlan, C. Yu, ACS Nano 4 (2010) 513–523.

[256] J. Liu, X. Wang, D. Li, N.E. Coates, R.A. Segalman, D.G. Cahill, Macromolecules 48 (2015) 585–591.

[257] X. Wang, V. Ho, R.A. Segalman, D.G. Cahill, Macromolecules 46 (2013) 4937–4943.

[258] N.M. van der Velden, M.K. Patel, J.G. Vogtländer, J. Int, Life Cycle Ass. 19 (2014) 331–356.

[259] S. Roos, G. Sandin, B. Zamani, G. Peters, Environmental Assessment of Swedish Fashion Consumption. Five Garments − Sustainable Futures, Mistra Future Fashion Reports, (2015).

[260] N.M. van der Velden, Making Fashion Sustainable The Role of Designers, Delft University of Technology, Delft, 2016 (PhD Thesis).

[261] A.R. Köhler, L.M. Hilty, C. Bakker, J. Ind. Ecol. 15 (2011) 496–511.

[262] N.M. van der Velden, K. Kuusk, A.R. Köhler, Mater. Des. 84 (2015) 313–324.

[263] J.B. Guinée, R. Heijungs, M.G. Vijver, W. Peijnenburg, Nat. Nanotechnol. 12 (2017) 727–733.

[264] N.M. van der Velden, J.G. Vogtländer, J. Clean. Prod. 153 (2017) 320–330.

[265] J.G. Vogtländer, H.C. Brezet, C.F. Hendriks, J. Int, Life Cycle Ass. 6 (2001) 157–166.

[266] Database Idematapp published by Delft University of Technology http://www.ecocostsvalue.com/EVR/model/theory/subject/5-data.html. (Accessed 17 November 2017).

[267] A.K. Yetisen, H. Qu, A. Manbachi, H. Butt, M.R. Dokmeci, J.P. Hinestroza, M. Skorobogatiy, A. Khademhosseini, S.H. Yun, ACS Nano 10 (2016) 3042–3068.

[268] I.E. Napper, R.C. Thompson, Mar. Pollut. Bull. 112 (2016) 39–45.

[269] F. Salvador Cesa, A. Turra, J. Baruque-Ramos, Sci. Total Environ. 598 (2017) 1116–1129.

[270] Microfiber release from clothes after washing: Hard facts, figures and promising solutions. Position Paper, MERMAIDS, Consortium, EU Life+ (2017).

[271] S. Roos, O. Levenstam Arturin, A.-C. Hanning, Microplastics Shedding from Polyester Fabrics, Mistra Future Fashion Reports, (2017).

[272] T. Walser, E. Demou, D.J. Lang, S. Hellweg, Environ. Sci. Technol. 45 (2011) 4570–4578.

[273] A.R. Köhler, C. Som, A. Helland, F. Gottschalk, J. Clean. Prod. 16 (2008) 927–937.

[274] M. Irimia-Vladu, E.D. Głowacki, G. Voss, S. Bauer, N.S. Sariciftci, Mater. Today 15 (2012) 340–346.

[275] A New Textiles Economy: Redesigning Fashion's Future, Ellen MacArthur Foundation, 2017.

[276] A. McLaren, D.A. Hardy, T. Hughes-Riley, C. Bakker, R. Mugge (Eds.), PLATE Conference, Delft, 2017, pp. 473–476.

[277] A. Prahl, Design for circularity: material innovation for wearable technology, in: R. Earley, K. Godsworthy (Eds.), Circular Transitions Conference, London, 2016, pp. 285–302.

[278] M. Toeters, Wearables designer, Personal communication on Nov. 7th (2017).

[279] I. Maldini, A.R. Balkenende, Reducing clothing production volumes by design: a critical review of sustainable fashion strategies, in: C. Bakker, R. Mugge (Eds.), PLATE Conference, Delft, 2017, pp. 233–237.

[280] I. Maldini, On paradigm shifts and industrial revolutions: tracing prevalent dressmaking practices and apparel production systems in the Netherlands and northwest Europe, IFFTI Conference, Amsterdam, 2017.

[281] L. Ma-Hock, V. Strauss, S. Treumann, K. Küttler, W. Wohlleben, T. Hofmann, S. Gröters, K. Wiench, B. van Ravenzwaay, R. Landsiedel, Part. Fibre Toxicol. 10 (2013) 1–19.

[282] M.V.D.Z. Park, E.A.J. Bleeker, W. Brand, F.R. Cassee, M. van Elk, I. Gosens, W.H. de Jong, J.A.J. Meesters, W.J.G.M. Peijnenburg, J.T.K. Quik, R.J. Vandebriel, A.J.A.M. Sips, ACS Nano 11 (2017) 9574–9593.

[283] M. Irimia-Vladu, Chem. Soc. Rev. 43 (2014) 588–610.

[284] M.J. Tan, C. Owh, P.L. Chee, A.K.K. Kyaw, D. Kai, X.J. Loh, J. Mater. Chem. C 4 (2016) 5531–5558.

[285] C.J. Bettinger, Z. Bao, Polym. Int. 59 (2010) 563–567.

[286] J.-K. Chang, H. Fang, C.A. Bower, E. Song, X. Yu, J.A. Rogers, PNAS 114 (2017) E5522–E5529.

[287] K.K. Fu, Z. Wang, J. Dai, M. Carter, L. Hu, Chem. Mater. 28 (2016) 3527–3539.

[288] P.A. Irvine, P. Smith, Macromolecules 19 (1986) 240–242.